THE VISCOELASTIC PROPERTIES OF DNA; EFFECT OF A TOPOLOGY CONTROLLING ENZYME AND ITS TARGETING INHIBITORS

BINU KUNDUKAD

NATIONAL UNIVERSITY OF SINGAPORE

2010

THE VISCOELASTIC PROPERTIES OF DNA; EFFECT OF A TOPOLOGY CONTROLLING ENZYME AND ITS TARGETING INHIBITORS

BINU KUNDUKAD

(M.Sc., University of Kerala)

A THESIS SUBMITTED FOR

THE DEGREE OF DOCTOR OF PHILOSOPHY

DEPARTMENT OF PHYSICS

FACULTY OF SCIENCE

NATIONAL UNIVERSITY OF SINGAPORE

2010

Acknowledgements

I would like to express my deep and sincere gratitude to my supervisor, Prof. Johan R C van der Maarel, Associate Professor, Department of Physics, National University of Singapore, for his support, encouragement and guidance from the initial to the final stage of my research, without which this thesis would not have been possible. His wide knowledge of polymer physics and his logical thinking has helped me in having a better understanding of the subject.

I am grateful to Prof. Sow Chorng Haur, for his support and guidance at the initial stages of my research.

I would like to thank Jean-Louis Sikorav and Arach Goldar, Department of Physics, Institut de Physique Théorique (IPhT), CEA/ Saclay, for the their help in performing the gel electrophoresis experiments and discussions.

I owe my deepest gratitude to the Head of the physics department, Feng Yuan Ping, for giving me an opportunity to pursue my Ph.D. degree at the Department of Physics, National University of Singapore.

I would like to thank Mr. Teo Hwee Hoon, Laboratory Officer, Department of Physics, NUS, for all his help during the course of my research.

I am indebted to my colleagues for their support in a number of ways.

I would like to thank my family for their support and patience without which this work would not be possible.

Last, but not the least; I would like to thank the National University of Singapore, for the support of my research.

Contents

Synopsis

The flow properties of DNA are important for understanding cell division and, indirectly, cancer therapy. DNA topology controlling enzymes such as topoisomerase II are thought to play an essential role.

The viscoelastic moduli of phage λ-DNA through the entanglement transition were obtained with particle tracking microrheology. With increasing frequency, the viscous loss modulus first increases, then levels off, and eventually increases again. Concurrently, the elastic storage modulus monotonously increases and eventually levels off to a constant high frequency plateau value. Once the DNA molecules become entangled at about ten times the overlap concentration, the elastic storage modulus becomes larger than the viscous loss modulus in an intermediate frequency range. The number of entanglements per chain is obtained from the plateau value of the elasticity modulus. The longest, global relaxation time pertaining to the motion of the DNA molecules is obtained from the low shear viscosity as well as from the lowest crossover frequency of the viscous loss and elastic

storage moduli. The concentration dependencies of the low shear viscosity, the number of entanglements per chain, and the relaxation time agree with the relevant scaling laws for reptation dynamics of entangled polyelectrolytes in an excess of simple, low molecular weight salt with screened electrostatic interactions.

This methodology is used to show how double strand passage facilitated by topoisomerase II controls DNA rheology. For this purpose, elastic storage and viscous loss moduli of a model system comprising bacteriophage λ-DNA and human topoisomerase IIα are measured using video tracking of the Brownian motion of colloidal probe particles. It is found that the rheology is critically dependent on the formation of temporal entanglements among the DNA molecules with a relaxation time on the order of a second. It is observed that topoisomerase II effectively removes these entanglements and transforms the solution from an elastic physical gel to a viscous fluid depending on the consumption of adenosine-triphosphate (ATP). Another aspect of this thesis is the effect of the generic topoisomerase II inhibitor adenylyl-imidodiphosphate (AMP-PNP) and the anticancer drug bisdioxopiperazine ICRF-193. In mixtures of AMP-PNP and ATP, the double strand passage reaction gets blocked and progressively fewer entanglements are relaxed. A total replacement of ATP by AMP-PNP results in a temporal increase in elasticity at higher frequencies, but no transition to an elastic gel with fixed cross-links is observed. Addition of anticancer drugs results

in the inhibition of topoisomerase II.

List of Tables

List of Figures

List of Publications

1. Control of the flow properties of DNA by topoisomerase II and its targeting inhibitor, Binu Kundukad, Johan R C van der Maarel, *Biophysical Journal* 99: 1906 (2010).

2. Viscoelasticity of entangled λ-phage DNA solutions, Xiao Ying Zhu, Binu Kundukad and Johan R. C. van der Maarel, *The Journal of Chemical Physics* 129: 185103 (2008).

Chapter 1

Introduction

Deoxyribonucleic acid (DNA) is an important biopolymer that contains the genetic information and is present in the nucleus of cells. DNA are long polymers made of repeating units called deoxyribo nucleotides, which are made up of a phosphate group, a sugar moiety and four different nitrogenous bases. The sugar, (II)-deoxyribose links with the phosphate group through a diester bond and forms the repeat units of the DNA backbone. The nitrogen bases are of two types: purines and pyrimidines. The purines include Adenine (A) and Cytosine (C) and the pyrimidines include Thymine (T) and Guanine (G). These bases are attached to the sugar. The purines form hydrogen bonds with the pyrimidines, with A bonding to T and C bonding to G. These hydrogen bonds connect one chain to another in an antiparallel fashion. Since the hydrogen bonds are weak, they can be broken and rejoined relatively easily either by mechanical force or high temperature

[2]. Watson and Crick in 1953, proposed a double helical structure for DNA. The double stranded DNA chain in the B form is about 2.2 nm in diameter and the z-axis projected distance between the base pairs is 0.34 nm [3].

This double helical structure provides the twisting and bending rigidity, making the DNA a semi flexible, charged polymer chain. The dynamical properties of DNA have an impact on many biological processes such as the transcription of the genome and the segregation of the intertwined sister chromatids during mitosis. Hence the study of these properties is very important in understanding cell division and indirectly cancer therapy.

The local concentration of DNA within a cell depends on the stage of the cell in its life cycle. During mitosis, the local concentration is very high and is of the order of 1 to 10 g/L. At a sufficiently high concentration, DNA molecules become entangled and they form a transient dynamic network. Entanglements are topological constraints resulting from the fact that the DNA molecules cannot cross through each other. The motion of the DNA molecules is strongly hindered by the presence of the neighboring DNA molecules and the relaxation times may become very long. Polymer dynamics under entangled conditions can be described by the reptation model, in which the polymer is thought to move in a snake-like fashion along the axial line (primitive path) of an effective tube formed by the entanglements. As a result of these entanglements, concentrated solutions of DNA have a complex viscoelasticity, *i.e.*, they partially store and dissipate

energy.

The dynamics of DNA in an entangled solution is very different from the dynamics in a non-entangled DNA solution. The semi-dilute, non-entangled DNA solution exhibits Rouse behavior , *i.e.*, the molecules move as single dynamic units. In the entangled solution, the lateral displacement is hindered by the presence of the other chains and the dynamics can be described by the reptation model. The Rouse model at low DNA concentration and the reptation model at high concentration give specific scaling laws for the longest, global relaxation time, high frequency limiting value of the elastic storage modulus, and the zero shear limit of the viscosity of neutral polymers as well as polyelectrolytes with screened electrostatics. The transition from the non-entangled to entangled regime is dependent on the concentration and the molecular weight.

The cell is the basic unit of life which can perform metabolism, self reproduction and mutability. It is an open system; which permanently exchanges substances with the environment. Advances in the technology of electron microscopy have established a major morphological distinction between two groups of cells. They are prokaryotic and eukaryotic cells. The majority of the cells are eukaryotes. Eukaryotic cells have a well defined nucleus surrounded by the nuclear membrane whereas prokaryotes do not have a nucleus. Eukaryotes have DNA which forms a complex with proteins called histones. Prokaryotes have DNA without any histones attached to

it. Prokaryotic DNA is replicated in a similar manner as that of eukaryotic DNA. The only difference is that there are only two replication forks used in prokaryotes, while eukaryotes have many replication forks acting at the same time [1, 107].

One of the major biological processes that takes place in both prokaryotic and eukaryotic cells is cell division. Cell division is the process by which a cell replicates and divides into two daughter cells. This is very important for the growth of an organism. The cell division in eukaryotes takes place by mitosis and in prokaryotes by binary fission. Before the cell divides, the DNA must replicate itself so that the two daughter cells have the same genetic material as the parent cell. In DNA replication, each of the two DNA strands serves as a template for the formation of a new strand, so that the resulting double stranded DNA has one strand of the parental DNA and another newly constructed strand. For this reason, DNA replication is said to be 'semiconservative'.

Mitosis is a process which separates the sister chromosomes into two identical nuclei followed by cytokinesis to produce two daughter cells. The cell goes through different phases during cell division, namely, the interphase, prophase, prometaphase, metaphase, anaphase and telophase. Mitosis of eukaryotic cells involves processes like condensation of chromosomes during the prophase stage and the separation of sister chromosomes during the anaphase stage [1, 4, 5, 86].

The discovery of the double helical structure of DNA by Watson and Crick in 1953, led to the topological problem of disentanglement. In the 1960s, ring shaped, circular DNA was discovered. As the replication fork moves along the double stranded DNA, the entire DNA ahead of it has to rotate rapidly to avoid any problem of unwinding. For long chromosomes, this would require a large amount of energy. This problem was solved by a protein known as DNA topoisomerase. It was shown in the 1970s that the entire chromosome in a cell, made up of tens of millions of base pairs, consisted of a single DNA molecule with a length of several millimeters. During mitosis, the DNA molecule replicates and the local concentration of DNA is very high. During the anaphase stage of mitosis, the replicated DNA molecules are disentangled and pulled to the two poles of the cell with the help of the spindle fibers attached to the centromeres. Moreover, the segregation of the inter wound sister chromosomes takes place within 1 to 2 minutes. So during the separation of chromosomes, the DNA gets tangled or knotted, resulting in the breakage of chromosomes and leading to cell death [6, 7].

The solution to this topological problem is provided by a class of topology controlling enzymes called DNA topoisomerase type II. Topoisomerase II are thought to play an essential role in chromatid motion and the kinetics of chromosome condensation, but to date there are no quantitative measurements of the effect of disentanglement on the flow properties (viscoelastic-

ity) of DNA [8, 9]. Topoisomerase II binds a DNA segment, introduces a transient break in the duplex, captures another segment from the same or another molecule, transports the captured segment through the gap of the break, reseals the break, and releases the captured segment. This enzymatic reaction requires the hydrolysis of two molecules of adenosine-triphosphate (ATP) [10, 11, 12].

In 1971, Wang discovered the first DNA topoisomerase in $E-$coli [13]. He also proposed that enzymes may form covalent bonds between itself and the broken ends of DNA.

DNA topoisomerase II is a dimeric protein which opens and closes with the capture and hydrolysis of ATP. The transport of a double helix through another molecule takes place by the opening and closing of the jaws of the DNA topoisomerase II. In this catalytic cycle, the opening and closing of the pair of jaws can take place with or without the capture of the DNA strand. The mechanism is described in detail in the next chapter. Since topoisomerase II allows the passage of one double stranded DNA segment through another segment, it can be thought to relax the topological constraint. Concomitantly, the dynamics of the molecule is expected to change from reptation to Rouse.

DNA topoisomerase are of special interest due to their involvement in a large number of biological activities. They unlink DNA catenanes and resolve intertwined chromosome pairs and in their absence cause cell death

(reviewed by Wang, 1998). They are also known to be target for many anticancer drugs [14]. Thus, these enzymes are DNA-dependent ATPase which requires the binding and hydrolysis of ATP for the reaction to take place.

DNA topoisomerase II is found to be responsible for the breaking of the double stranded DNA and enabling strand passage. A decrease or increase in the amount of topoisomerase-DNA complex leads to either a slow or fast rate of double strand passage. In either case it leads to cell death. In some cases, the uncontrolled strand passage leads to a condition where the cells multiply uncontrollably. This condition is called cancer.

Nowadays, many anticancer drugs are known. These anticancer drugs have been found to act on topoisomerase II at different stages of its catalytic cycle to stop strand passage. Adenylyl-imidodiphosphate (AMP-PNP), which is a nonhydrolysable analog of ATP, act as a topoisomerase II inhibitor. AMP-PNP changes the conformation of topoisomerase II and holds it in a closed clamp conformation. With the replacement of ATP by AMP-PNP the DNA topoisomerase is able to capture a DNA strand, but cannot allow passage of the strand through the gap as the hydrolysis of AMP-PNP is impossible.

Another class of anticancer drug, bisdioxopiperazine (ICRF-193), have also been found to act on topoisomerase II in a similar fashion as that of AMP-PNP. It allows a second DNA strand to be captured, but does not al-

low strand passage, as it stabilizes the DNA-topoisomerase II complex. The action of the anticancer drugs are expected to affect the viscoelastic properties of DNA through the inhibition of topoisomerase II by the formation of cross-linking protein clamps [15].

1.1 Overview of the thesis

This thesis is divided into six chapters. The contents in each chapter are discussed briefly in this section.

Chapter one gives a general overview of the thesis.

Chapter two includes the theory and literature review. The theory includes the dynamics of DNA in the entangled and non-entangled regimes. The scaling laws for the flow properties of DNA as a salted polyelectrolyte are also discussed. A short description of microrheology with some of the passive microrheology techniques are included. The methodology of obtaining the viscous loss modulus and the elastic storage modulus from the Brownian motion of the microspheres dispersed in a solution of DNA is discussed. An overview of the topology controlling enzyme, DNA topoisomerase type II is given. Finally a brief introduction to topoisomerase II inhibitors is given, particularly AMP-PNP, which is an $\beta,\gamma-$imido analog of ATP and the anticancer drug, bisdioxopiperazine (ICRF-193).

Chapter three gives a brief description of the motivation and aim of

study.

Chapter four discusses the materials and methods used in this thesis in the order in which the experiments have been done. A brief description of sample preparation is presented. The materials include phage $\lambda-$DNA, DNA topoisomerase IIα, AMP-PNP, bisdioxopiperazine (ICRF-193), and the buffers Tris-EDTA and topoisomerase II reaction buffer. The different techniques used in the sample preparation, including freeze drying, dialysis, Ultra-Violet spectroscopy and microscopy, are also discussed.

Chapter five presents the results and discussions. It is divided into 3 sections. The first section includes the results and discussions of the viscoelasticity of entangled phage $\lambda-$DNA, the second section includes the effect of DNA topoisomerase on the viscoelastic properties of DNA and the third section includes the effect of topoisomerase targeting inhibitors.

Chapter six gives the conclusions for the thesis and the scope for future work.

Chapter 2

Theory and Literature Review

A polymer such as DNA can be described by a thin elastic filament obeying Hooke's law of elasticity under small deformation. Such a model of the polymer chain is called persistent or worm like chain model.

The persistence length, the length over which the stiffness of the polymer persists, of such a chain is found to be proportional to the bending rigidity, κ_b, *i.e.*,

$$L_p = \frac{\kappa_b}{kT} \tag{2.1}$$

with kT being the thermal energy. It can be shown that for a chain of contour length $L = L_p$, the thermally averaged bending energy is given by $\langle \Delta U \rangle = kT$. So, the persistence length of a worm like chain is the segment contour length over which the average bending energy is equal to kT. For DNA, the persistence length exceeds 50 nm, which corresponds with 150 base pairs and is dependent on the ionic strength of the solution. According

to the worm like chain model, the characteristic size of the molecule, radius of gyration,

$$\langle R_g^2 \rangle \propto L^2 \quad for \quad L \ll L_p \tag{2.2}$$

$$\langle R_g^2 \rangle \propto LL_p \quad for \quad L \gg L_p \tag{2.3}$$

where $L = lN$, with l the step length (0.34 nm per bp) and N the number of segments. Thus, it is seen from the above equation that the characteristic size of the coil scales as the square root of the contour length. It should be noted however that the size of the chain is modified by the so called excluded volume interaction.

2.1 Excluded volume interaction

Segments which are separated by a large distance along the contour can come close to each other in space. The worm like chain model ignores the effective interaction between segments which are separated by a large distance along the contour but are close together spatially. The interaction results from the balance of segment-segment and segment-solvent interactions. The affinity of the polymer for the good solvent results in an effective repulsion between the monomers. This effect is called the excluded volume effect. The chain segments are repelled from each other and the repulsive energy is counter balanced by the elastic energy which arises from the connectivity of the segments. This changes the static properties of the polymer

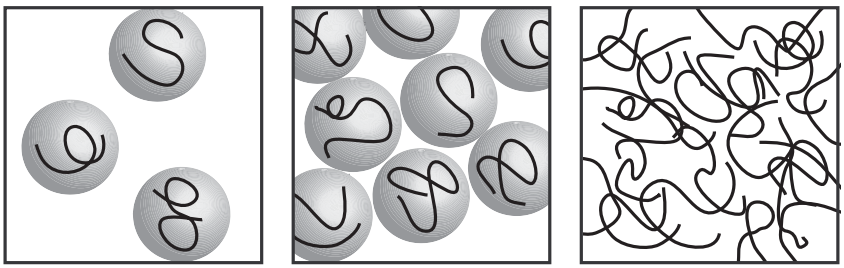

Figure 2.1: Dilute to semi-dilute regime. The overlap concentration is c*

entirely. This effect was discovered by Kuhn and later Flory showed that the average square of the polymer radius for the swollen chain is, $\langle R_F^2 \rangle \propto N^{2\nu}$, where ν=3/5 (precise calculation gives 0.588 for good solvent).

2.2 Dilute and concentrated regimes

DNA dissolved in a good solvent can be divided into at least three regimes: dilute, semi-dilute and concentrated. If the concentration is very low, then the molecules are widely separated from each other and the intercoil distance exceeds the size of the coil given by the Flory radius, R_F.

With increasing concentration, the coils are accommodated in a smaller volume and at a critical concentration called the overlap concentration, c^*, the molecules begin to overlap. The intercoil distance is the same as the size of the coil at the overlap concentration. The concentration, c^*, at which

the overlap starts is estimated as,

$$\frac{c^* N_A}{M} \frac{4}{3} \pi R_F^3 \simeq 1 \tag{2.4}$$

where $c^* N_A/M$ is the number of polymer coils per unit volume and R_F is proportional to M^ν, M being the molecular weight. When the concentration is increased above the overlap concentration, the chain begins to interpenetrate, and the individual coils are no longer discernible and we have the semi-dilute regime. The polymer solution can then be described by a system of closely packed blobs of decreasing size and decreasing number of links per blob with increasing monomer concentration.

2.3 Concept of blobs

If we consider a concentrated solution of long DNA molecules, there exists a certain characteristic length scale ξ, within which the statistics of the DNA segment is unperturbed by the presence of the other chains. We can consider domains of diameter ξ, which is much larger than the persistence length $\xi \gg L_P$, within which the chain is unperturbed by the presence of other chains and behave as an isolated chain. These domains are referred to as blobs. If there are g links inside each blob of diameter ξ ($g \ll N$) then,

$$\xi \simeq l g^\nu \tag{2.5}$$

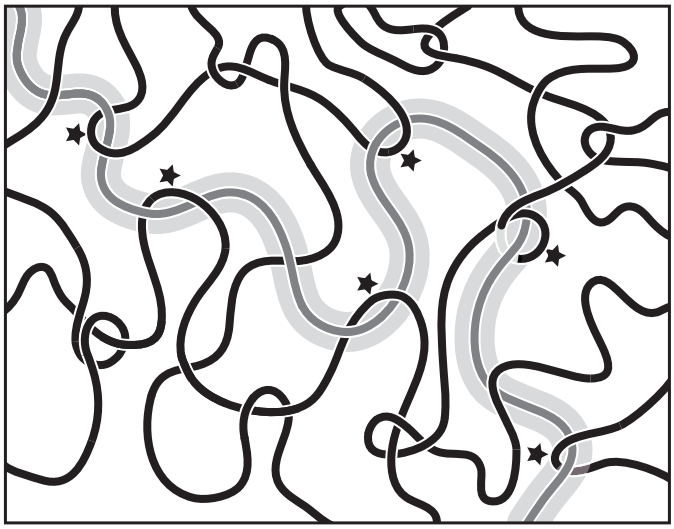

Figure 2.2: Entangled interactions

where l is the length of the segment and ν is the Flory exponent. The chain can be considered as a linear sequence of N/g blobs. It can also be considered as a renormalized chain with N/g segments of length ξ.

2.4 Effect of entanglements

The dynamics of DNA is very important in understanding biological processes like cell division. In humans DNA of length about 2 m is compacted into the cell nucleus with a cross sectional diameter of a few micrometers. During cell division, the concentration of DNA is of the order of 1 to 10 g/L. At such high concentrations, DNA becomes entangled and forms a dynamic transient network. Entanglements are topological constraints due to the fact that DNA cannot cross each other. In linear polymers, the

topological constraints do not affect the static properties, but seriously affect the dynamical properties. The dynamics of the entangled polymer is very different from that of the non-entangled polymer chain. The density of entanglements depends on the concentration of DNA, and they occur at a critical concentration called the entanglement concentration c^e. The dynamics of DNA pertaining to different concentration regimes are discussed below.

Entangled interactions are illustrated in Figure 2.2. The interactions marked by ($\star$) are entanglements. Due to these entanglements, the lateral displacements of the test chain shown in grey are not possible. The test chain can move only along the axial line of the effective tube formed by the entanglements in a snake like fashion. This snake like movement of the chains is called reptation [16].

2.5 Dynamics of DNA as a salted polyelectrolyte

Many biopolymers carry electric charges and can be ionized. In the case of DNA, every phosphate moiety connecting the nucleotides carries a negative charge. DNA which has a negative charge is soluble in water and is called a polyelectrolyte. The negative charges repel each other and the polymer chain stretches out, thereby increasing the viscosity of the solution . If salt is added to the solution the negative charges are screened by the ions

coming from the salt, which results in a change of the flow properties of the DNA solution. So, the flow properties may be different for salted and salt-free polyelectrolytes. The persistence length of DNA, which is 50 nm under salted condition, has been seen to increase significantly when the ionic strength is decreased. This stretching effect has been shown, among others, by Baumann et al. by using a single molecule manipulation technique and Sobel and Harpst by light scattering [26, 83].

Since the DNA solutions used in this research are salted, the scaling laws for the salted polyelectrolytes are briefly discussed here.

2.5.1 Rouse dynamics

The polymer chains can be represented by a set of beads connected along a chain. When considering the dynamics of polymers, these beads can be considered to be executing Brownian motion. This model was first proposed by Rouse and hence the dynamics of dilute and semi-dilute polymer solutions are referred to as Rouse dynamics. In the semi-dilute regime, the chains are considered to be a sequence of N/g blobs of size ξ. The chains are renormalized and the blobs are considered to be the basic units rather than the monomers. Since the blobs are closely packed, the fluctuation in blob density and the net force experienced by the blobs are considered to be vanishingly small. At distances exceeding the correlation length, the hy-

drodynamic interactions are screened and the chain of blobs follows Rouse dynamics.

The dynamics of DNA can be studied from the molecular transport properties like the diffusion coefficient, viscosity and elasticity modulus. The global relaxation time or the longest time scale over which the chain fluctuates owing to thermal motion is given by

$$\tau = \frac{\zeta}{K} \tag{2.6}$$

where ζ is the friction coefficient and K is the elasticity constant. The elasticity coefficient for a polymer coil in the Rouse model is given by

$$K^{-1} \simeq Nl^2/kT \tag{2.7}$$

The hydrodynamic friction is proportional to the number of links per chain

$$\zeta = \zeta_1 N \tag{2.8}$$

where the friction coefficient per link is given by Stokes law, $\zeta_1 = 6\pi\eta_s l$. Therefore, the relaxation time is given by

$$\tau \simeq N^2 l^3 \eta_s / kT \tag{2.9}$$

With the static scaling results for the blob size, ξ, and the number of links per blob, g, the relaxation time in the non-entangled regime is given by

$$\tau \simeq (N/g)^2 \tau_\xi \simeq l^{3/2} (L_p D_{eff})^{3/4} (cl^3)^{1/4} N^2 \eta_s / kT \quad \text{for} \quad (c^* < c < c^e) \tag{2.10}$$

where L_p and D_{eff} are the persistence length and effective diameter which depend on the ionic strength of the buffer. It can be seen that the relaxation time is proportional to the $(1/4)^{th}$ power of the concentration and to the square of the number of links. Here, c is the concentration of monomeric units.

In the non-entangled regime, the chains move as single dynamical units. So, the high frequency elasticity modulus is given by $G = c/NkT$. The viscosity increment is given by, $\Delta\eta/\eta_s \simeq G\tau$. Substituting the values of τ and G, we get

$$\Delta\eta/\eta_s \simeq l^{-3/2}(L_p D_{eff})^{3/4}(cl^3)^{5/4}N \quad \text{for} \quad (c^* < c < c^e) \tag{2.11}$$

From the above equations, it can be seen that the elasticity modulus G is directly proportional to the polymer concentration c/N. The viscosity increment is directly proportional to N and the $(5/4)^{th}$ power of the concentration c.

2.5.2 Reptation model

At even higher concentrations, $c > c_e$, the DNA molecules become entangled and they form a transient elastic network. The entanglement concentration can be shown to be $c_e \simeq n^{8/5}c^*$, where $c^* \simeq n^{-4/5}l^{-9/5}(L_p D_{eff})^{-3/5}$. n is the number of chains that have to overlap before the onset of the entanglements and depends on the chemical structure and the charge of the polymer.

At the entanglement concentration, the number of segments per entangled strand is given by

$$N_e \simeq n^2 g \simeq n^2 l^{3/2} (L_p D_{eff})^{-3/4} (cl^3)^{-5/4} \quad \text{for} \quad (c > c_e) \tag{2.12}$$

The dynamics of the salted polyelectrolyte is Zimm like up to the correlation length, ξ, Rouse like for a strand of N_e/g blobs of size ξ and reptation-like for N/N_e entangled strands, so that the relaxation time takes the form

$$\tau \simeq (N/N_e)^3 (N_e/g)^2 \tau_\xi \simeq (L_p D_{eff})^{3/2} (cl^3)^{3/2} (N^3/n^2) \eta_s / kT \quad \text{for} \quad (c > c_e) \tag{2.13}$$

and the high frequency elasticity modulus is given by

$$G \simeq \frac{c}{N_e} kT \simeq l^{-9/2} (L_p D_{eff})^{3/4} (cl^3)^{9/4} n^{-2} kT \quad \text{for} \quad (c > c_e) \tag{2.14}$$

from which we get the viscosity increment,

$$\Delta\eta/\eta_s \simeq G\tau \simeq l^{-9/2} (L_p D_{eff})^{9/4} (cl^3)^{15/4} N^3/n^4 \quad \text{for} \quad (c > c_e) \tag{2.15}$$

From the above equations it can be seen that the relaxation time is proportional to the 3/2 power of the concentration and to the cube of the number of links. The elasticity modulus G is directly proportional to $(9/4)^{th}$ power of the concentration c . The viscosity increment is directly proportional to the cube of N and $(15/4)^{th}$ power of the concentration c.

Table 2.1: Concentration scaling exponents for the viscosity increment $\Delta\eta$, high frequency elasticity modulus G, and relaxation time τ.

	non-entangled	entangled
$\Delta\eta$	$1/(3\nu-1)$	$3/(3\nu-1)$
G	1	$3\nu/(3\nu-1)$
τ	$(2-3\nu)/(3\nu-1)$	$(3-3\nu)/(3\nu-1)$

2.6 Microrheology

The measurement of the bulk viscoelastic properties of a fluid can be accomplished by means of a mechanical rheometer, where the stress response of the material to an applied oscillatory strain provides a measure of the storage and loss moduli. This technique probes the mechanical properties of the sample at the macroscopic level at frequencies up to tens of Hertz. They also require milliliters of sample.

Recently with increased interest in the study of biological systems, other complementary techniques have been developed which allows the measurement of the viscoelastic behavior of soft materials in a more efficient way. These techniques have allowed to probe the viscoelastic properties locally in a solution and also inside a cell. These techniques are known as microrheology which measures the rheological properties of a viscoelastic fluid by following the trajectory of a probe particle usually a few micrometers in size. The advantage of the microrheology technique is that it requires only a few microliters of sample compared to several milliliters needed for con-

ventional rheology. Hence, they are extremely useful for the measurement of the viscoelastic properties of expensive or rare biological materials.

There are two methods of microrheology -Active and Passive Microrheology. Active microrheology techniques involve the active manipulation of small probe particles by external forces like magnetic fields, electric fields, or micromechanical forces. It allows large stress to be applied to stiff materials in order to obtain detectable strain. This includes magnetic manipulation techniques like magnetic tweezers and twisting magnetometry, optical tweezer measurements also known as optical traps or laser traps and atomic force microscopy [95, 59].

In passive microrheology, no external force is applied to the colloidal particles dispersed in the sample. The movement of the probe particles are due to the thermal energy of the particles, given by k_BT. Hence, for passive measurements, in order to observe any detectable motion of the probe particles, the materials should be sufficiently soft. The size of the probe particles used depends on the resolution of the imaging device. This technique allows the use of probe particles with a size in the range from nano to micrometer. One of the advantages of passive microrheology is that the results obtained are within the linear viscoelastic regime as there is no external stress applied to the system. The passive microrheology includes techniques like laser deflection particle tracking, light scattering techniques, diffusion wave spectroscopy and video particle tracking [54]. Some of the

passive microrheology techniques are briefly discussed in the sections below.

2.6.1 Laser deflection particle tracking

Laser deflection particle tracking is a light scattering microscopy technique which can detect the colloidal spheres in 2 dimensions with sub nanometer resolution. In this technique, a laser is used to track the particles, but only less than 5 percent of the force is applied to the sphere compared to active microrheology. The deflection of the sphere from the beam axis will cause intensity fluctuation in the scattered light, which can be used to detect the position of the sphere. From this, the mean square displacement of the particles can be calculated. This technique has a high spatio-temporal resolution and the particle can be tracked with sub nanometer resolution at a frequency of 50 kHz. The limitation of this technique is in terms of the statistical accuracy. As a single bead is tracked at a time, it is difficult to obtain a trajectory for an ensemble of beads. Also, the beads can diffuse out of the beam in a few minutes and so it is difficult to track beads for longer time [53].

2.6.2 Dynamic light scattering

In this technique, laser light impinges on a sample and is scattered at a certain angle to the incident beam. As the spheres diffuse within the sample,

the intensity of the scattered beam fluctuates in time. From this fluctuation in intensity, the mean square displacement of the particles can be calculated. The frequency range is 0.01 to 10 Hz [51, 52].

2.6.3 Diffusion wave spectroscopy

Diffusion wave spectroscopy is a technique in which multiple scattering of light takes place. Since the measurements are obtained from multiple scattering, it is possible to extend the frequency range to higher values. Advantage of this technique is that an ensemble average over many particles can be performed. Mason et al. have pioneered this technique [53, 35].

2.6.4 Video particle tracking

Video particle tracking is a technique in which the particle embedded in a solution is imaged by video microscopy. This has the advantage of tracking a large number of particles at the same time. It hence gives a good statistics on the ensemble of the beads. One of the limitations of this technique is that the frequency range is limited to the speed of the camera. In this technique, simple optical microscopy, fluorescence microscopy or bright field microscopy can be used. A movie of the particle executing Brownian motion is recorded and a two dimensional trajectory is obtained for further analysis. This method has been employed in this thesis.

2.7 Viscoelasticity

One of the most fundamental properties of any material is its elastic susceptibility. According to the classical theory of elasticity, the mechanical properties of an elastic solid obeys Hooke's law, *i.e.*, the stress applied to a solid is directly proportional to strain. According to the classical theory of hydrodynamics, a viscous fluid obeys Newton's law, *i.e.*, the stress is directly proportional to the rate of strain. These are ideal cases as these behaviors are observed only for infinitesimal strain in case of Hooke's law and infinitesimal rate of strain in the case of the Newton's law.

Solids store mechanical energy and are elastic, whereas liquids dissipate energy and are viscous. Some materials have a mechanical property in between elastic and viscous behavior. These materials show viscoelastic behavior, *i.e.*, they partially store and dissipate energy, with relative proportions depending on frequency. If a sinusoidally oscillating stress is applied to a system, the strain is in phase with the stress in the case of a perfect elastic solid and the strain is 90^o out of phase with the stress for an perfectly viscous fluid, and somewhere in between for certain materials. Such materials are said to be viscoelastic.

The stress induced on a material is given by the complex shear modulus, $G^*(\omega)$, where the strain is applied at a frequency, ω. The complex shear modulus $G^*(\omega)$ has two components, the real part which is in phase with

the applied strain and the imaginary part which is out of phase with the applied strain and can be written as,

$$G^*(\omega) = G'(\omega) + iG''(\omega) \tag{2.16}$$

The real part of $G^*(\omega)$ is called the elastic storage modulus and the imaginary part is called the viscous loss modulus. $G'(\omega)$ and $G''(\omega)$ are not independent variables as they are connected by the Kramers-Kronig relations.

Concentrated solutions of DNA exhibit viscoelastic properties due to the large length of the molecules. The viscoelastic properties of entangled DNA solutions have been reported in the literature before. Musti et al. reported the low shear viscosity and relaxation times of solutions of T2-DNA (164 kbp, contour length of 56 μm). It was shown that the reduced zero shear viscosity obeys the same scaling law as the one for synthetic, linear polymers and that the entanglement concentration is 0.25 g/L of DNA. For solutions of 1 g/L, the relaxation times become very long on the order of 1000 s [61]. For phage λ-DNA (48.5 kbp, contour length of 16.3 μm) similar scaling behavior of the zero shear viscosity was observed, but the relaxation times are two orders of magnitude shorter because of the lower molecular weight [40]. Smith et al. showed that the self diffusion coefficient of phage λ-DNA follows the reptation prediction for concentrations exceeding 0.63 g/L [82]. The viscous loss and the elastic storage moduli of polydis-

perse calf thymus DNA (average molecular weight of 13 kbp) through the entanglement concentration were reported by Mason et al. [55, 24]. For concentrations exceeding the entanglement concentration, the viscous loss modulus is crossed by the elastic storage modulus at a crossover frequency, ω_c and the storage modulus levels off at a limiting high frequency plateau value. A region of weak dependence of the steady state shear stress of T4-DNA (166 kbp) on the shear rate has been reported by Jary et al. [44]. The concentration dependence of the lower boundary frequency scales as the reciprocal tube renewal or disengagement time, whereas the upper boundary corresponds with the Rouse relaxation time of the entire DNA molecule within the tube. Although these previous investigations are important in their own right, a comprehensive characterization of the viscoelasticity of solutions of rigorously monodisperse DNA with increasing concentration through the entanglement transition in terms of the viscous loss and elastic storage moduli is lacking.

2.8 Brownian motion and Einstein's theory

In 1827, Robert Brown, a Scottish Botanist, observed that small particles dispersed in a fluid move in a random manner. This phenomenon came to be known as 'Brownian motion'. In 1905, it was theoretically explained by Einstein, that this effect was due to the intrinsic thermal fluctuations

resulting from the random collision of the particles with the molecules of the liquid acting as a heat bath. The mean square displacement of the colloidal particles is the primary observable quantity [38]. Jean Baptiste Perrin used microscopic measurements on sub micron particles to show that Einstein's theory was in perfect agreement with reality for which he was awarded the Nobel prize in 1926 [72].

Einstein put forward the theory for the motion of the small particles suspended in a fluid in his paper published in 1905, titled, "On the movement of small particles suspended in a stationary liquid, as required by the molecular kinetic theory of heat". He wrote that,

"In this paper it will be shown that according to the molecular kinetic-theory of heat, bodies of microscopically- visible size suspended in a liquid will perform movements of such magnitude that they can be easily observed in a microscope".

He assumed that the suspended particle performed an irregular motion and this was due to the molecular movement of the liquid in which it was suspended. He explained that the movement of the particles under the influence of force is opposed by the diffusion of the particles and he derived ,

$$D = \frac{k_B T}{\mu} \tag{2.17}$$

where D is the diffusion constant. The mobility, μ is given by Stokes law, $\mu = 6\pi\eta a$, with η the low shear viscosity and a the radius of the particle.

Hence the diffusion of the particles is seen to depend on the viscosity of the fluid, the size of the particle and the temperature. This equation is called the Einstein-Sutherland equation as this equation was also derived by an Australian Physicist, William Sutherland, around the same time as Einstein [84, 85].

Einstein also derived the diffusion equation,

$$\frac{\partial P}{\partial t} = D\frac{\partial^2 P}{\partial x^2} \tag{2.18}$$

where $P(x,t)$ is the probability distribution for displacement x at time t [105, 74, 64]. The solution of the probability distribution is given by,

$$P(x,t) = \frac{1}{\sqrt{2\pi\langle\Delta x^2(t)\rangle}} exp(-\frac{|x-\bar{x}|^2}{2\langle\Delta x^2(t)\rangle}) \tag{2.19}$$

where $\langle\Delta x^2(t)\rangle$ is the mean square displacement. The viscoelastic properties of DNA solutions are probed by monitoring the one-dimensional mean square displacement $\langle\Delta x^2(t)\rangle$ over a time t, of an embedded colloidal and spherical bead of radius a. The mean square displacement as a function of time t is given by

$$\langle\Delta x^2(t)\rangle = \langle|x(t'+t) - x(t')|^2\rangle_{t'} \tag{2.20}$$

where the brackets denote an average over time, t'. The viscoelasticity of a complex fluid can be understood by considering a pure viscous fluid with probe particles embedded in it. From the Brownian motion of probe particles in a pure viscous fluid, it can be seen that they undergo simple

diffusion. The time dependent mean square displacement of the particles increases linearly with time t, with the rate of increase given by the diffusion constant D. The diffusion equation can be written as

$$\langle \Delta x^2(t) \rangle = 2Dt, \tag{2.21}$$

where D is given by the Stokes-Einstein-Sutherland equation,

$$D = k_B T / 6\pi\eta a. \tag{2.22}$$

In the case of an elastic fluid, the motion of the particles are locally constrained and the mean square displacement will reach a plateau value $\langle \Delta x^2 \rangle_p$ depending on the elastic moduli of the material. By equating the thermal energy $k_B T$, of the beads to its elastic energy $1/2\,\kappa\,\langle \Delta x^2 \rangle_p$, where κ is the spring constant that characterizes the elasticity of the medium, we can determine the elasticity modulus. Hence, the spring constant is given by $\kappa = k_B T / \langle \Delta x^2 \rangle_p$. The elasticity modulus $G'(\omega)$ is related to the spring constant by a factor of length which is the bead radius a. Hence, the relation between $G'(\omega)$ and the mean square displacement can be written as

$$G'(\omega) = \frac{k_B T}{a \langle \Delta x^2 \rangle_p}. \tag{2.23}$$

The elasticity modulus is found to be independent of time t.

A complex fluid exhibits both viscous and elastic behavior depending on the frequency which in turn depends on the time and length scale probed by the measurement. For such materials, both viscous and elastic contributions

can be derived from the mean square displacement of the thermally driven probe particles [51]. The mean square displacement of the tracer particles in the case of complex fluids will scale differently with time t, compared to the linear dependence in the case of viscous fluids. The mean square displacement can be written as

$$\langle \Delta x^2(t) \rangle \propto t^{\alpha} \tag{2.24}$$

For $\alpha = 1$, the behavior is diffusive and for α=0, the particle is locally constrained and shows elastic behavior. For $0 < \alpha < 1$, the particle exhibits sub-diffusive motion.

2.9 Generalized Stokes-Einstein equation

The Generalized Stokes-Einstein equation can be used to obtain the viscous loss modulus and the elastic storage modulus of a viscoelastic fluid by relating the mean square displacement of the probe particle to the complex shear modulus $G^*(\omega)$ [51]. The motion of a particle dispersed in a complex fluid with velocity $v(t)$ can be described by the generalized Langevin's equation,

$$m\dot{v}(t) = f_R(t) - \int_0^t dt' \, \zeta(t - t') \, v(t') \tag{2.25}$$

where m is the mass of the particle, $f_R(t)$ is the random force acting on the particle and the integral part represents the viscous damping of the fluid and incorporates a generalized time dependent memory function, $\zeta(t)$.

Due to causality, $\zeta(t)$=0 for $t < 0$. So the integral can be extended to infinity

$$m\dot{v}(t) = f_R(t) - \int_0^\infty \zeta(t - t')\, v(t')\, dt' \tag{2.26}$$

Taking the one sided Fourier transform of $v(t)$, $f_R(t)$ and $\zeta(t)$, we define

$$\int_0^\infty dt\, e^{-i\omega t} v(t) = \tilde{v}(\omega) \tag{2.27}$$

$$\int_0^\infty dt\, e^{-i\omega t} f_R(t) = \tilde{f}_R(\omega) \tag{2.28}$$

$$\int_0^\infty dt\, e^{-i\omega t} \zeta(t) = \tilde{\zeta}(\omega) \tag{2.29}$$

where $\tilde{f}_R(\omega)$, $\tilde{v}(\omega)$ and $\tilde{\zeta}(\omega)$ are the one sided Fourier transforms of the random force, velocity and the memory function, respectively.

Taking the one sided Fourier transform on both sides of equation 2.26, the left hand side becomes

$$m \int_{t=0}^\infty dt\, e^{-i\omega t} \dot{v}(t) = -mv(0) + mi\omega\tilde{v}(\omega) \tag{2.30}$$

The right hand side of equation 2.26 becomes

$$\begin{aligned} &\int_{t=0}^\infty dt\, e^{-i\omega t} \int_{t'=0}^\infty dt'\, \zeta(t - t') v(t') \\ &= \int_{t=0}^\infty dt \int_{t'=0}^\infty dt'\, e^{-i\omega(t-t')} \zeta(t - t')\, e^{-i\omega t'} v(t') \end{aligned} \tag{2.31}$$

Substituting, $t - t' = \tau$, and changing the order of integration, the above equation can be written as

$$= \int_{t'=0}^\infty dt' \int_{\tau=-t'}^\infty d\tau\, e^{-i\omega\tau} \zeta(\tau) e^{-i\omega t'} v(t') \tag{2.32}$$

Due to causality, $\zeta(\tau) = 0$ for $\tau < 0$. So, $\int_{\tau=-t'}^{\infty}$ can be replaced by $\int_{\tau=0}^{\infty}$

$$= \int_{t'=0}^{\infty} dt' \int_{\tau=0}^{\infty} d\tau\, e^{-i\omega\tau}\zeta(\tau)e^{-i\omega t'}v(t') \tag{2.33}$$

$$= \int_{\tau=0}^{\infty} d\tau\, e^{-i\omega\tau}\zeta(\tau) \int_{t'=0}^{\infty} dt'\, e^{-i\omega t'}v(t') \tag{2.34}$$

$$= \tilde{\zeta}(\omega)\tilde{v}(\omega) \tag{2.35}$$

Equation 2.26 hence takes the form

$$-mv(0) + mi\omega\tilde{v}(\omega) = \tilde{f}_R(\omega) + \tilde{v}(\omega)\tilde{\zeta}(\omega) \tag{2.36}$$

and the one sided Fourier transform of the velocity can be written as

$$\tilde{v}(\omega) = \frac{mv(0) + \tilde{f}_R(\omega)}{im\omega + \tilde{\zeta}(\omega)} \tag{2.37}$$

Multiplying both sides with $v(0)$ and taking the ensemble average gives

$$\langle v(0)\tilde{v}(\omega)\rangle = \frac{m\langle v(0)^2\rangle + \langle v(0)\tilde{f}_R(\omega)\rangle}{im\omega + \tilde{\zeta}(\omega)} \tag{2.38}$$

The first term in the numerator becomes equal to k_BT according to the equipartition theorem, $1/2m\langle v(0)^2\rangle = 1/2k_BT$. The second term in the numerator becomes zero, since we assume that there is no correlation between the velocity and the spectrum of the random force: $\langle v(0)\tilde{f}_R(\omega)\rangle = \langle v(0)\rangle\langle\tilde{f}_R(\omega)\rangle = 0$ and $\langle v(0)\rangle = 0$. The first term in the denominator represents the inertial effect of the probe particle and is neglected. Accordingly, we obtain

$$\langle v(0)\tilde{v}(\omega)\rangle = \frac{k_BT}{\tilde{\zeta}(\omega)} \tag{2.39}$$

or

$$\tilde{\zeta}(\omega) = \frac{k_B T}{\langle v(0)\tilde{v}(\omega)\rangle} \tag{2.40}$$

The complex Fourier transform of the memory function is hence inversely proportional to the complex Fourier transform of the velocity correlation function.

The displacement of a particle in a time t can be written as

$$\Delta x(t) = x(t) - x(0) = \int_0^t dt'\, v(t') \tag{2.41}$$

The square displacement can be written as

$$\Delta x^2(t) = [x(t) - x(0)]^2 = \int_{t'=0}^t dt' \int_0^t dt''\, v(t')v(t'') \tag{2.42}$$

The ensemble average can be written as

$$\langle \Delta x^2(t)\rangle = \langle [x(t) - x(0)]^2\rangle = \int_{t'=0}^t dt' \int_0^t dt'' \langle v(t')v(t'')\rangle \tag{2.43}$$

The above equation gives the mean square displacement $\langle \Delta x^2(t)\rangle$, where $\langle v(t')v(t'')\rangle$ is the velocity correlation function. As shown in Appendix A1, the mean square displacement can be written as the integral over the velocity correlation function,

$$\langle \Delta x^2(t)\rangle = 2t \int_0^t d\tau\, [1 - \tau/t]\, \langle v(\tau)v(0)\rangle \tag{2.44}$$

To derive the $G'(\omega)$ and $G''(\omega)$, we first take the one sided, complex Fourier transform of the mean square displacement

$$\langle \Delta \tilde{x}^2(\omega)\rangle = \int_0^\infty dt\, \exp(-i\omega t)\, \langle \Delta x^2(t)\rangle \tag{2.45}$$

As shown in Appendix A2, the one sided Fourier Transform of the mean square displacement is related to the one sided Fourier transform of velocity correlation function as

$$\langle \Delta\tilde{x}^2(\omega)\rangle = \frac{2}{(i\omega)^2}\langle v(0)\tilde{v}(\omega)\rangle \tag{2.46}$$

Therefore, the Fourier transform of the memory function in equation 2.40 can be written as

$$\tilde{\zeta}(\omega) = \frac{2k_BT}{(i\omega)^2\langle \Delta\tilde{x}^2(\omega)\rangle} \tag{2.47}$$

Assuming that we can generalize the Stokes friction to all the frequencies,

$$\tilde{\zeta}(\omega) = 6\pi a\tilde{\eta}(\omega), \tag{2.48}$$

we obtain for the complex viscosity

$$\tilde{\eta}(\omega) = \frac{kT}{3\pi a(i\omega)^2\langle \Delta\tilde{x}^2(\omega)\rangle}. \tag{2.49}$$

The viscoelastic moduli, $G^*(\omega) = i\omega\tilde{\eta}(\omega)$. So we derive the generalized Stokes-Einstein equation

$$G'(\omega) + iG''(\omega) = \frac{k_BT}{3\pi ai\omega\langle \Delta\tilde{x}^2(\omega)\rangle} \tag{2.50}$$

The generalized Stokes-Einstein equation is valid in the same conditions as the Stokes equation for the friction experienced by the bead, i.e., no slip boundary conditions on a sphere in an isotropic, incompressible fluid and neglect of the sphere's inertia. Furthermore, it has been assumed that the

Stokes drag for a viscous fluid may be extended to viscoelastic materials over all frequencies and that the fluid surrounding the bead can be treated as a continuum. The latter condition requires that the structures of the fluid, which give rise to the viscoelastic properties (e.g., the mesh size or correlation length of the semi dilute DNA solution), are much smaller than the size of the bead.

In order to evaluate the viscoelastic moduli, the one sided Fourier transform of the mean square displacement can be algebraically estimated by expanding $\ln \langle \Delta x^2(t) \rangle$ around the value of $\ln \langle \Delta x^2(t') \rangle$ at $t' = \omega^{-1}$, i.e., the value of $\ln \langle \Delta x^2(\omega^{-1}) \rangle$ in powers of $\ln \omega t$. In the double logarithmic representation of the mean square displacement vs time, the slope of the curve is linear for a viscous fluid and zero for an elastic body. Hence the slope for a viscoelastic fluid is between one and zero. The expansion of the power series of $\ln \omega t$ is carried out to the third order and is given by

$$\langle \Delta x^2(t) \rangle \approx \langle \Delta x^2(\omega^{-1}) \rangle (\omega t)^{\alpha + \beta \ln \omega t + \gamma \ln^2 \omega t} \tag{2.51}$$

The frequency dependent coefficients are defined by the first, second and the third order derivatives

$$\alpha = \left. \frac{\partial \ln \langle \Delta x^2(t') \rangle}{\partial \ln t'} \right|_{t'=\omega^{-1}} \tag{2.52}$$

$$\beta = \frac{1}{2} \left. \frac{\partial^2 ln \langle \Delta x^2(t') \rangle}{\partial \ln t'^2} \right|_{t'=\omega^{-1}} \tag{2.53}$$

$$\gamma = \frac{1}{6} \left. \frac{\partial^3 \ln \langle \Delta x^2(t') \rangle}{\partial \ln t'^3} \right|_{t'=\omega^{-1}} \tag{2.54}$$

However, since β and γ are small with respect to α, equation 2.51 can be expanded in powers of β and γ,

$$\langle \Delta x^2(t) \rangle \approx \langle \Delta x^2(\omega^{-1}) \rangle (\omega t)^{\alpha} (1 + \beta \ln^2 \omega t + \gamma \ln^3 \omega t + \beta^2/2 \ln^4 \omega t + \beta\gamma \ln^5 \omega t + \gamma^2/2 \ln^6 \omega t + ...) \quad (2.55)$$

The terms up to and including the second order in β and γ can be retained. Thus, the one sided Fourier transform of the mean square displacement equation (2.45) can then be evaluated in analytical form by transforming equation (2.55) term by term. This can be used to evaluate the elastic storage modulus, $G'(\omega)$ and the viscous loss modulus $G''(\omega)$, which are given by

$$G'(\omega) = G^*(\omega)\ \cos[\pi\alpha(\omega)/2] \quad (2.56)$$

$$G''(\omega) = G^*(\omega)\ \sin[\pi\alpha(\omega)/2] \quad (2.57)$$

So, the complex viscoelastic modulus can be written as

$$G^*(\omega) = \frac{k_B T(\cos(\alpha\pi/2) + i sin(\alpha\pi/2))}{3\pi a \langle \Delta x^2(\omega^{-1}) \rangle \Gamma(1+\alpha)(1 + c_1 + c_2 + c_3 + c_4 + c_5 + ...)} \quad (2.58)$$

where Γ denotes the gamma function. The complex coefficients c_1 through c_5 pertaining to the curvature in the mean square displacement up to and including the second order in β and γ are given in table 2.2. $\psi^{(n)}$ denotes the $n^{(th)}$ order polygamma function.

Table 2.2: The coefficients c_1 through c_5 in equation 2.58

c_1	$\beta/4(4\psi^{(1)}(\alpha+1) - (2i\psi^{(0)}(\alpha+1)+\pi)^2)$
c_2	$\gamma/8(i(2i\psi^{(0)}(\alpha+1)+\pi)^3 + 12(-i\pi + 2\psi^{(0)}(\alpha+1))\psi^{(1)}(\alpha+1)+ 8\psi^{(2)}(\alpha+1))$
c_3	$\beta^2/32(8(2\psi^{(0)}(\alpha+1)^4 - 4i\pi\psi^{(0)}(\alpha+1)^3 -3(\pi^2 - 4\psi^{(1)}(\alpha+1))\psi^{(0)}(\alpha+1)^2 + (i\pi(\pi^2 - 12\psi^{(1)} (\alpha+1)) + 8\psi^{(2)}(\alpha+1))\psi^{(0)}(\alpha+1) + 6\psi^{(1)}(\alpha+1)^2- -3\pi^2\psi^{(1)}(\alpha+1) - 4i\pi\psi^{(2)}(\alpha+1)) + \pi^4 + 16\psi^{(3)}(\alpha+1))$
c_4	$\beta\gamma/32\ (32\psi^{(0)}(\alpha+1)^5 - 80i\pi\psi^{(0)}(\alpha+1)^4- 80(\pi^2 - 4\psi^{(1)}(\alpha+1))\psi^{(0)}(\alpha+1)^3 + 40i(-12\pi\psi^{(1)}(\alpha+1) + \pi^3- 8i\psi^{(2)}(\alpha+1))\psi^{(0)}(\alpha+1)^2 + 10(-8(3\psi^{(1)}(\alpha+1)(\pi^2 - 2\psi^{(1)}(\alpha+1))+ 4i\pi\psi^{(2)}(\alpha+1)) + \pi^4 + 16\psi^{(3)}(\alpha+1))\psi^{(0)}(\alpha+1) - i(240\pi\psi^{(1)} (\alpha+1)^2 - 40(\pi^3 - 8i\psi^{(2)}(\alpha+1))\psi^{(1)}(\alpha+1) + \pi^5 + 80 \pi(\psi^{(3)}(\alpha+1) - i\pi\psi^{(2)}(\alpha+1)) + 32i\psi^{(4)}(\alpha+1)))$
c_5	$\gamma^2/128\ (4(16\psi^{(0)}(\alpha+1)^6 - 48i\pi\psi^{(0)}(\alpha+1)^5 - 60(\pi^2 - 4\psi^{(1)} (\alpha+1))\psi^{(0)}(\alpha+1)^4 + 40i(-12\pi\psi^{(1)}(\alpha+1) + \pi^3 - 8i\psi^{(2)} (\alpha+1))\psi^{(0)}(\alpha+1)^3 + 15(-8(3\psi^{(1)}(\alpha+1)(\pi^2 - 2\psi^{(1)}(\alpha+1))+ 4i\pi\psi^{(2)}(\alpha+1)) + \pi^4 + 16\psi^{(3)}(\alpha+1))\psi^{(0)}(\alpha+1)^2 - 3i(240\pi\psi^{(1)} (\alpha+1)^2 - 40(\pi^3 - 8i\psi^{(2)}(\alpha+1))\psi^{(1)}(\alpha+1) + \pi^5 + 80\pi(\psi^{(3)}(\alpha+1)- i\pi\psi^{(2)}(\alpha+1)) + 32i\psi^{(4)}(\alpha+1))\psi^{(0)}(\alpha+1) + 5(48\psi^{(1)}(\alpha+1)^3- 36\pi^2\psi^{(1)}(\alpha+1)^2 + 3(-32i\pi\psi^{(2)}(\alpha+1) + \pi^4 + 16\psi^{(3)}(\alpha+1)) \psi^{(1)}(\alpha+1) + 4(8\psi^{(2)}(\alpha+1)^2 + 2i\pi^3\psi^{(2)}(\alpha+1) - 3\pi^2\psi^{(3)} (\alpha+1))) - 48i\pi\psi^{(4)}(\alpha+1)) - \pi^6 + 64\psi^{(5)}(\alpha+1))$

2.10 Topological problem

In 1953, Watson and Crick discovered the double helical structure of DNA. This immediately led to the topological problem of separating the intertwined strands of DNA during replication. During replication, the two strands of the double helices are separated as the replication fork moves along the length of the DNA. During this process, the other end of the DNA must rotate rapidly, so as to avoid any problems of entanglements. The rate of replication of bacterial DNA is about a million base pairs per minute and about 500-5000 base pairs per minute in the case of eukaryotes. Since there are 10 base pairs per turn of the double helix, in order to replicate a DNA of 1,000,000 base pairs, the DNA strand must rotate at a speed of 100,000 rotations per minute. Even though this looked feasible during the early years, later discoveries regarding the length of DNA, fragile nature of DNA and most importantly the discovery of circular DNA made the topological problem more interesting (reviewed by Wang, 1998).

One of the major discoveries in 1963 was the ring shaped DNA. Dulbecco and Vogt (1963) and Weil and Vincograd (1963) discovered the ring shaped small DNA molecules in polyoma virus. The double stranded ring shaped DNA is considered to be 'covalently closed' as the two complimentary strands are topologically linked. During replication, the single strand of the DNA cannot be separated from one another without breaking at least

one of the strands. Hence the problem of separating a circular DNA is a topological one [6, 32, 33, 34].

Kavenoff et al., in 1974, discovered that an entire chromosome is made up of a single DNA which can be several millimeters long. This is a general assumption which is considered to be true for most eukaryotic cells and is known as the unineme hypothesis. According to this hypothesis, the degree of polymerization of chromosomal DNA is 10^5 - 10^9 base pairs. Inside the cell, this long linear DNA molecule is compacted in such a way that it forms multiple loops. So, the problem of separating a long linear strand of DNA is similar to that of the covalently closed circular DNA [10, 43, 22, 7].

Another topological problem arises during the anaphase stage of mitosis. During anaphase, the chromatids are pulled to the two poles of the cell by the mitotic spindle with a velocity of 0.005 to 0.1 μm/s (Mazia 1961). In normal anaphase, the metaphase chromosomes undergo a longitudinal fission which generate two daughter chromosomes. But if the daughter chromosomes are interlocked, they can cross each other and move to the two poles, still remaining intact (Bajer 1963). This was also observed in the case of interlocked ring chromosomes, that they cross each other without damaging either of them as illustrated in Figure 2.3 [57, 22, 23, 96].

Now it is well known that the topological problem of disentangling DNA strands occurs in almost all cellular activities of DNA, like transcription, chromosome condensation and decondensation and recombination.

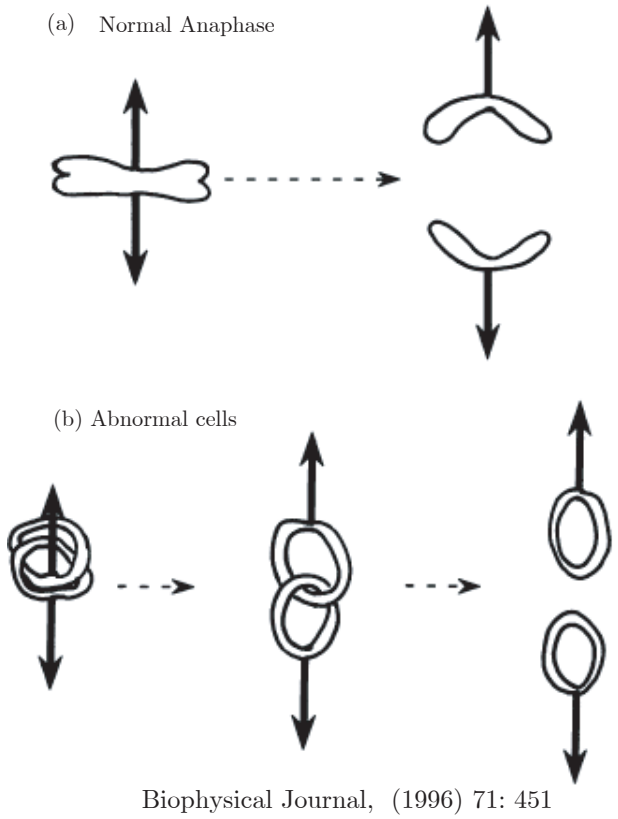

Figure 2.3: (a) Normal anaphase where chromosomes are separated by longitudinal fission. (b) Ring chromosomes in abnormal cells.

2.11 DNA Topoisomerase

The topological problems of disentangling DNA during different cellular activities are solved by an enzyme called topoisomerase [92]. They catalyze the passage of a DNA strand through another. This reaction often results in the interconversion between the topological isomers of DNA rings and hence the name topoisomerase.

DNA topoisomerase is of special interest due to their involvement in

a large number of biological activities. They unlink DNA catenanes and resolve intertwined chromosomes and in their absence cause cell death (reviewed by Wang, 1998). They are also target for many anticancer drugs [14]. These enzymes are also DNA-dependent ATPase. The binding and hydrolysis of ATP for the reaction to take place has been an area of fascinating research.

In 1971, Wang discovered the first DNA topoisomerase in *Escherichia–* coli. Gellert et al. in 1976 demonstrated that DNA gyrase catalyzed the formation of negative supercoils in double stranded DNA and this required the hydrolysis of ATP (reviewed by Chen and Liu) [20]. Liu et al. isolated T4 DNA topoisomerase in 1979 and showed that it catalyzed both negative and positive super coils [50].

DNA topoisomerase acts by introducing a transient break in one of the DNA strands, holds it there, captures another strand by using ATP and allows it to pass through the broken strand by the hydrolysis of ATP. The DNA enzymes are mainly classified into two categories based on the mechanism of action. They are the type I and the type II enzymes [93]. Type I enzymes introduce transient single stranded breaks into DNA, pass an intact single strand of DNA through the broken strand and then re-ligate the break. Type II enzymes make transient double-stranded breaks into one segment

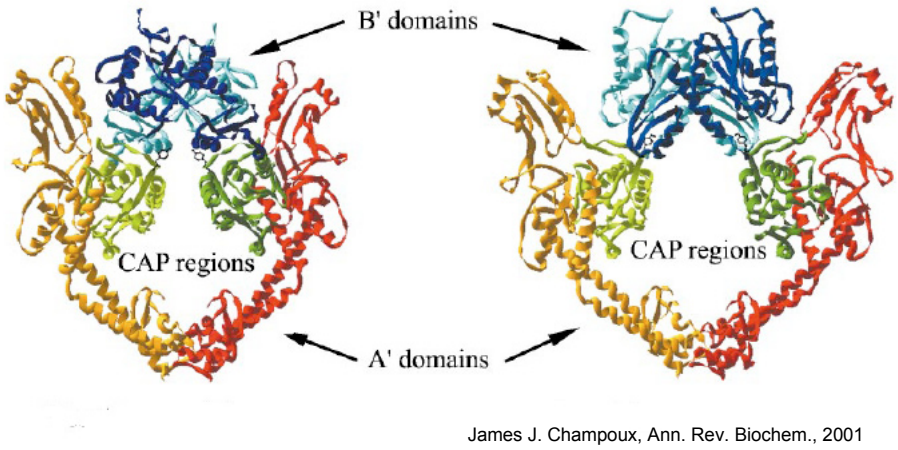

Figure 2.4: Representation of yeast topoisomerase II. The B' domain is shown in dark and light blue, the A' domain in red and orange and the active site tyrosine by black circles. The two structures shows different orientations of the B' and CAP domain, *i.e.*, partially opened 'gate' on the left and the fully opened 'gate' on the right.

of DNA and pass an intact duplex through the broken double stranded DNA, before resealing the break. The type I enzymes include, bacterial DNA topoisomerase I and III, eukaryotic DNA topoisomerase III, eukaryotic DNA topoisomerase I and pox virus DNA topoisomerase IV [93]. DNA type II topoisomerase II include topoisomerase IV, yeast and drosophila DNA topoisomerase II, mammalian DNA topoisomerase IIα and IIβ and T-even phage DNA topoisomerase. In 1971, Wang proposed that DNA strand breaking occurs by a transesterification process [13].

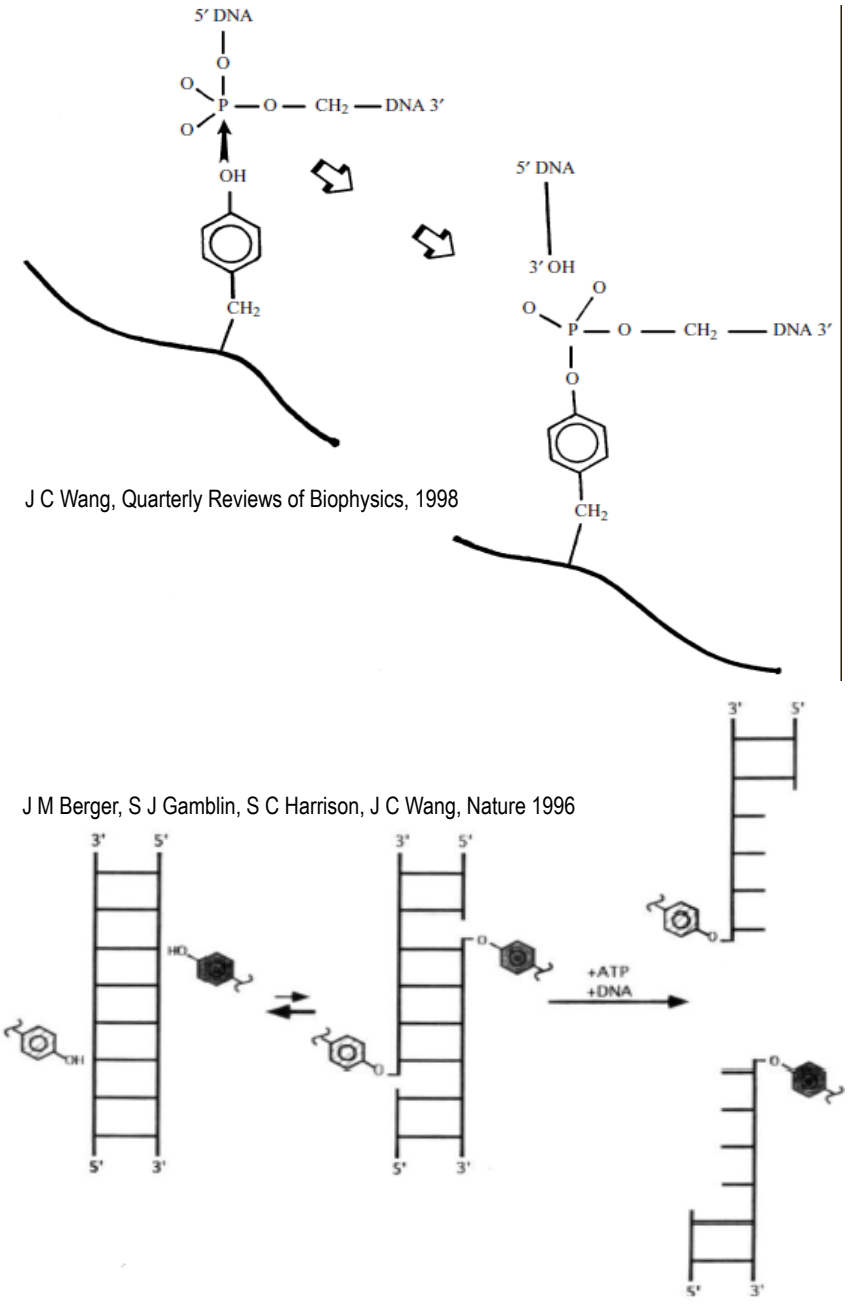

Figure 2.5: The formation of covalent intermediate between DNA and DNA topoisomerase and the cleavage of DNA molecule

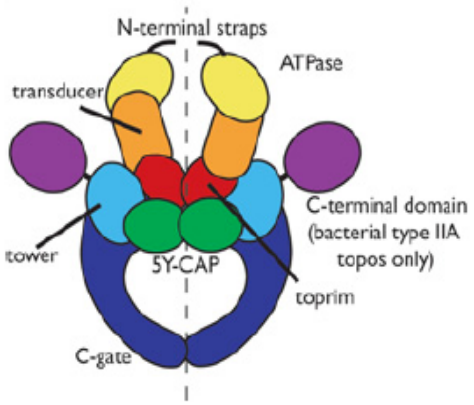

Figure 2.6: Model for the general arrangement of type II topoisomerase elements

2.11.1 Mechanism of action of DNA topoisomerase II

Topoisomerase II is a heart shaped dimeric protein with a large central hole of about 2-2.5 nm. The crystal structure of several type II topoisomerase has been determined Figure 2.4 [30, 28]. All the proteins possess an ATPase domain and DNA-binding domain. Pairs of like domains form dimer interfaces, which forms the gate for the passage of DNA [9]. Figure 2.6 shows the general arrangement of the elements in topoisomerase II. The yellow region represents the ATPase domain, which remains open until it gets an ATP. Once an ATP is bound to this domain, it dimerises trapping a DNA strand inside. The green region represents the 5Y-CAP domain which forms the DNA gate. The blue region is the C gate which remains closed until the hydrolysis of ATP.

The DNA cleavage by topoisomerase II is a transesterification process between a pair of tyrosyl residues, present on each half of the dimeric enzyme, and a pair of DNA phosphodiester bonds separated by four base pair (Figure 2.5) [60, 79, 48]. The phenolic oxygen of the tyrosines of the enzymes become covalently linked with the phosphoryl groups of the 5' ends of the transiently broken DNA leaving a pair of hydroxyl groups on the recessed 3'end of the DNA. The break is induced on both the strands of DNA separated by four base pairs. With the availability of ATP and another DNA double strand, the tyrosil-linked, 5' ends of DNA moves apart while the base pairs between them are separated. This opens a 'gate' for the second double stranded DNA to pass through, after which the two strands are sealed back again [28, 7, 30].

Figure 2.7 shows the mechanism of the topoisomerase II catalytic cycle. It was proposed by Roca and Wang that topoisomerase act by an ATP modulated clamp. The reaction of the topoisomerase II begins when a double stranded DNA segment called the gate segment or the G-segment (because it forms a gate for the other DNA segment to pass through) binds to the two catalytic sites, the 5Y-CAP (catabolite gene activator protein) and the toprim, that forms the DNA gate. The second double stranded DNA segment called the transfer segment or T-segment is captured by the dimerisation of the ATPase domain, induced by two molecules of ATP. The

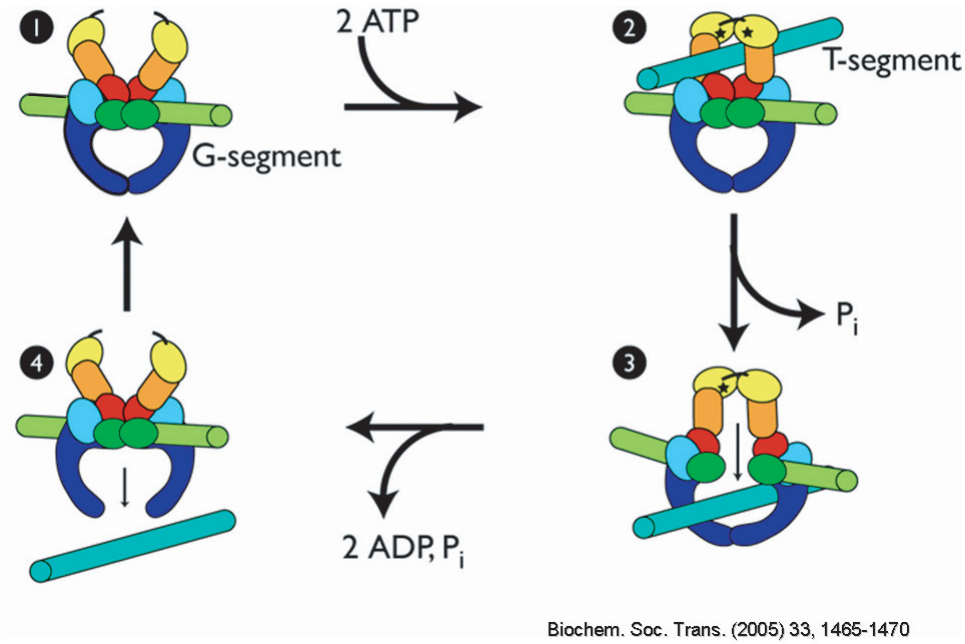

Figure 2.7: Mechanism of double strand passage by topoisomerase II

hydrolysis of one molecule of ATP leads to the cleavage of the G-segment followed by the passage of the T-segment through the gate. The hydrolysis of the second ATP and the release of ADP leads to the opening of a third gate called the C gate, through which the T segment is passed out and the G segment is sealed back. This is followed by the opening of the ATP gate, and the enzyme is ready for the next cycle of reaction.

Topoisomerase II requires two cofactors to carry out its catalytic double-stranded DNA passage reaction. First, it needs a divalent cation after the binding of the enzyme to DNA [65]. Mg^{2+} is the divalent cation that the enzyme uses *in vivo*. This can be replaced by Mn^{2+} or Ca^{2+} ions

in vitro[66, 67, 68]. Second, topoisomerase II uses the energy of adenosine triphosphate (ATP) to drive the overall DNA strand passage reaction [69]. The closing and opening of the ATP gate takes place regardless of the presence or absence of DNA. The binding of topoisomerase II to the DNA greatly stimulated the activity by about 20 folds. At low ATP concentration, about 2 ATP molecules are hydrolyzed during single DNA transport and at higher ATP concentrations, the transport is less efficient as about 7 ATP molecules are utilized per DNA transport event [47].

2.11.2 Models for disentangling DNA by type II topoisomerase

Studies on the binding of topoisomerase II to DNA show that DNA is cleaved only after two strands are bound. This suggests that the DNA topoisomerase act by recognizing the helix- helix juxtapositions in the entangled network.

Many models have been suggested regarding how the enzyme recognizes an entanglement and relaxes it. Some of these models include the 'three-binding-site model' which suggests that topoisomerase II binds to two strands of DNA and slide in the direction of an entangled third segment, to relax the entanglements [78]. Another model proposed is the 'phantom chain' model which says that self crossing of the polymer is possible [10].

These models were abandoned due to lack of experimental evidence. A kinetic proof reading model was proposed in which topoisomerase allows the DNA strand to pass through followed by two sequential collisions of topoisomerase II and DNA [63, 41, 97]. Some of the predictions of this model did not agree with experimental results (reviewed by Lui et al.) [98]. The authors who abandoned the three-binding-site model later came up with an 'active bending model'. According to this model, topoisomerase II introduces a sharp bend as it binds to the G segment and orients itself in a specific direction at the bend so that it allows the strand passage only in a specific direction [91]. The topoisomerase II is hence compared to Maxwell's demon. They also calculated the bending angle of DNA to be 130^o.

Buck and Zechiedrich [29] suggested that the active bending model considers topoisomerase II to be 'blind' which means that they do not allow the topoisomerase II to use the local information present in the substrate to figure out which is the best place to act. According to the model proposed by Buck and Zechiedrich, topoisomerase II uses local information to distinguish between two juxtaposed strands which are entangled from the strands which are juxtaposed but not entangled. The topoisomerase II will act only on hooked juxtapositions but not on free juxtapositions. The crystal structure determination of the binding of topoisomerase II to DNA have also shown a DNA bending angle of 150^o [37].

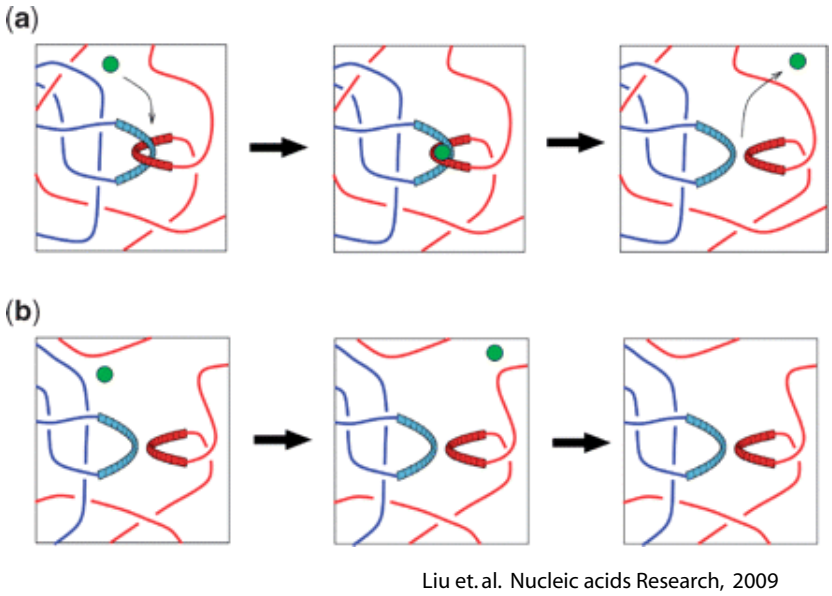

Figure 2.8: Topoisomerase II acts at the juxtapositions which are entangled (a) and does not act at the juxtapositions which are free (b)

Figure 2.8 shows the model by which topoisomerase II recognizes the entanglements as illustrated by Liu et al. Panel (a) shows two DNA juxtaposed strands which are entangled. Topoisomerase II identifies these positions and relax the entanglements. Panel (b) shows two DNA strands which are free and these positions are not recognized by topoisomerase II [98].

2.12 Topoisomerase II inhibitors

The fact that DNA topoisomerase are target for therapeutic agents was discovered soon after the discovery of DNA gyrase.

As seen in the previous sections topoisomerase II acts by breaking the

double stranded DNA. These breaks introduced in the DNA strand are transient, *i.e.*, they are short lived and within this time topoisomerase II does not cause any harm to the cells. However, any change in the conditions of the DNA-topoisomerase concentration leads to either inhibition of cell division or uncontrolled cell division [66]. This uncontrolled growth of cells leads to cancer.

Topoisomerase II have been found to be the target of many anticancer drugs. The mechanism by which anticancer drugs inhibit the action of topoisomerase II differ. It is known that they act by inhibiting at least one step of the catalytic cycle [21]. Based on their action, the anticancer drugs are classified into two classes. The agents that introduce a cytotoxic effect by stabilizing the covalent complex between DNA and topoisomerase II are called the cleavable complex. They introduce a double stranded break in the molecule leading to cell death and are referred to as topoisomerase poisons (classical inhibitors). Another important class of anticancer drugs act by inhibiting the activity of topoisomerase II at other stages of the catalytic cycle. They do not introduce a double stranded break in the DNA molecule. They act by stabilizing the non covalent complex. Hence they are referred to as catalytic inhibitors (non classical drugs) [89]. Examples of catalytic inhibitors include merbarone, fostriecin, aclarubicin, suramin, bisdioxipiperzines [49].

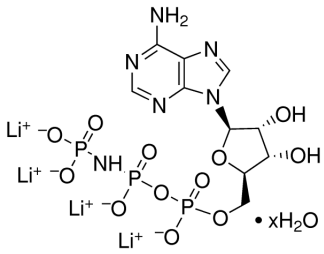

Figure 2.9: Molecular structure of AMP-PNP

2.12.1 Adenylyl-imidodiphosphate (AMP-PNP)

Adenylyl imidodiphosphate is a non-hydrolyzable ATP. It is an inhibitor of ATP-dependent systems. AMP-PNP can bind to the topoisomerase II to close the ATP domain and form an annulet [75, 77]. The closure of the jaws of the protein clamp is independent of the presence of the T-segment of DNA [94]. In such a conformation, the topoisomerase II can bind to linear molecules but not to circular molecules, as linear molecules can thread through the hole in the enzyme which is about 2 nm. The molecular structure of AMP-PNP is shown in Figure 2.9.

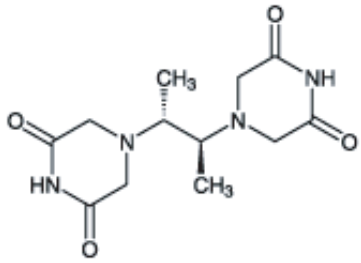

Figure 2.10: Molecular structure of ICRF-193

2.12.2 Bisdioxopiperazine (ICRF-193)

Bisdioxopiperazine derivatives belongs to a class of widely studied anti-cancer drugs. Several bisdioxopiperazine inhibit the action of topoisomerase II. ICRF-154 is a frequently studied drug. They have been shown to stabilize the noncovalent complex formed between topoisomerase II and the DNA molecule and to hold the topoisomerase in a closed clamp position [76]. ICRF-193, a dimethyl derivative of ICRF-154, has been shown to be most active towards topoisomerase II. Fattman et al. and Davies et al. have shown that topoisomerase IIα is sensitive to ICRF compounds suggesting that ICRF target topoisomerase II [39, 36]. Topoisomerase IIα is shown to be ten times more sensitive to ICRF compared to topoisomerase II β [73]. Hu et al. has shown that the formation of non covalent complex requires both ATP as well as ICRF-193 [42]. It is still not well established if the topoisomerase II inhibition is due to the inhibition of topoisomerase II itself or due to the stabilization of the non covalent complex [45].

Chapter 3

Aim of Study

The aim of study in this thesis is divided into three parts.

1. Viscoelasticity of entangled phage $\lambda-$DNA solutions.

   The dynamics of DNA depends on the concentration. At high concentrations, DNA molecules become entangled and follow reptation dynamics and at low concentration the dynamics of DNA follows Rouse behavior. Both the reptation and Rouse model gives specific scaling laws for the longest, global relaxation time, self-diffusion coefficient, high frequency limiting value of the elastic storage modulus, and the zero shear limit of the viscosity for salted polyelectrolytes. These scaling laws are dependent on the ionic strength of the buffer. The viscoelastic properties of phage $\lambda-$DNA at different ionic strengths are studied. Particle tracking microrheology is a convenient method to study the viscoelastic properties of DNA. The generalized Stokes-

Einstein equation is used to obtain the viscous loss modulus and the elastic storage modulus from the Brownian motion of particles embedded in a DNA solution.

2. Effect of DNA topoisomerase II on the viscoelastic properties of DNA.

   Topoisomerase type II binds to a DNA segment, introduces a transient break in the duplex, captures another segment from the same or another molecule, transports the captured segment through the gap of the break, reseals the break, and releases the captured segment. This enzymatic reaction requires the hydrolysis of two molecules of adenosine-triphosphate (ATP). Thus, topoisomerase II is expected to relax the entanglements in a concentrated solution of DNA. So, a concentrated solution of DNA changes its behavior from reptation to Rouse dynamics. This change of behavior from reptation to Rouse dynamics is studied. The relaxation of entanglements depends on the DNA, the topoisomerase and ATP concentrations. These effects are also studied.

3. Effect of topoisomerase II targeting inhibitors on the viscoelastic properties of DNA.

   Topoisomerase II are targets of many anticancer drugs. They act by either stabilizing the topoisomerase-DNA complex in the covalent form, non-covalent form or by introducing crosslinks in DNA

molecules. This would affect the behavior of topoisomerase II and prevent it from acting the way it is expected to do. The effect of different topoisomerase inhibitors on the relaxation of entanglements is studied.

Chapter 4

Materials and Methods

4.1 Materials

4.1.1 Phage λ-DNA

Bacteria phage λ-DNA was purchased from New England Biolabs, Ipswich, MA. The phage λ-DNA is a linear molecule which has 48,490 base pairs and 12 base, single-stranded overhangs at both sides that are complementary. The sequences of the overhangs are: 5' GGGCGGCGACCT 3' and 5' AGGTCGCCGCCC 3'. This makes a total of 48,502 base pairs. It has a contour length of 16.3 μm, persistence length of 50 nm and radius of gyration, R_g of approx. 500 nm. The overhangs could dimerize forming long DNA chains or both the complementary ends could meet each other forming circular molecules. In a concentrated DNA solution, the probability of one end of DNA meeting its other end is very small and hence it is expected that

DNA molecules dimerize to form longer molecules. To avoid this problem of dimerisation, a 12 base long oligonucleotide (single stranded DNA) with a sequence complementary to the right cohesive end of phage λ-DNA, 5' AGGTCGCCGCCC 3' was used. As received from the manufacturer, the phage λ- DNA stock solution has a concentration of 0.5 g/L in Tris-EDTA buffer.

4.1.2 Topoisomerase IIα

Mammalian cells have two isoforms of topoisomerase type II enzymes, namely topoisomerase IIα and IIβ differing in the pattern of expression. The levels of topoisomerase IIα have been seen to increase rapidly during cell division and hence topoisomerase IIα is believed to be the isoform that untangles chromosomes during mitosis. Many non dividing cells lack detectable topoisomerase IIα [12]. Topoisomerase IIα is a homodimeric protein with each subunit of $\approx$170 kDa. Shultz et al. have shown that human topoisomerase IIα has a three domain structure with a dense globular domain of size $\approx$ 9 nm and two smaller domains of about 5-6 nm [80]. Osheroff et al. have shown that the topoisomerase IIα requires a divalent cation in order to cleave DNA. They also proposed a two-metal-ion mechanism for the cleavage of DNA by human topoisomerase IIα [71]. Human topoisomerase IIα was purchased from Affymetrix. As supplied by the manufacturer, the

topoisomerase storage buffer contains 15 mM Na_2HPO_4, pH 7.1, 700 mM NaCl, 0.1 mM EDTA, 0.5 mM dithiothreitol (DTT), and 50% glycerol. One unit of topoisomerase is the amount of enzyme required to fully relax 0.3 μg of negatively supercoiled pBR322 plasmid DNA in 15 minutes at 303 K under the standard assay conditions. One unit is 20 ng of protein dimer. One unit per μg of $\lambda-$DNA corresponds with 1.9 dimers per DNA molecule.

4.1.3 Adenylyl-imidodiphosphate (AMP-PNP)

Adenosine 5'-($\beta\gamma-$imido) diphosphate (AMP-PNP) was purchased from Sigma-Aldrich [104]. It has a molecular weight of 529.9 g/mol. AMP-PNP being a non hydrolysable ATP, has been shown to change the conformation of topoisomerase II, upon binding to the ATPase domain. It changes the conformation of topoisomerase II from a three domain structure to a two domain structure of sizes 9 nm and 6 nm respectively. The smaller domain has a cavity of 2.5 nm and the larger domain has a cavity of 3 nm.

4.1.4 Bisdioxopiperazine (ICRF-193)

In 1984, it was recognized that mammalian DNA topoisomerases are targets for anti-cancer drugs (reviewed by Chen and Liu) [70]. Meso-4,4'-(2,3-butanediyl)-bis(2,6-piperazine) commonly known as ICRF-193 was purchased from Enzo Life Sciences. It has a molecular formula $C_{12}H_{18}N_4O_4$ and a

molecular weight of 282.3 g/mol. ICRF-193 is soluble only in dimethyl sulphoxide (DMSO). A stock solution of concentration 4 g/L was made.

4.1.5 TE buffer

Tris-EDTA is the solvent used for the first part of the experiments, *i.e*, the study of the viscoelastic properties of phage λ-DNA . TE buffer is composed of 10 mM tris-HCl, pH 8.0 and 1 mM EDTA. Tris is an organic compound known as tris(hydroxymethyl)aminomethane, with the formula $C_4H_{11}NO_3$ and a molecular weight of 121.14 g/mol. Tris is extensively used in biochemistry and molecular biology. It has a pKa of 8.1 and can buffer solutions from drastic pH changes. EDTA (ethylene di amine tetra acetic acid) has a molecular formula of $C_{10}H_{14}N_2O_8Na_2.2H_2O$ and a molecular weight of 372.24 g/mol. EDTA has the ability to chelate or complex metal ions in 1:1 metal-to-EDTA complexes. Water was de-ionized and purified by a Millipore system and has a conductivity less than $1 \times 10^{-6}\ \Omega^{-1}\mathrm{cm}^{-1}$. Samples were prepared with TE buffer which contains 10 mM Tris(1×) and 1 mM Tris (0.1×). The pH of the buffer was adjusted to 8 by the addition of concentrated HCl.

4.1.6 Topoisomerase reaction buffer

Topoisomerase II works only under specific buffer conditions. The standard reaction buffer is composed of 10 mM Tris-HCl, pH 7.9, 50 mM NaCl, 50 mM KCl, 5 mM $MgCl_2$, 0.1 mM EDTA, 1mM ATP and 15 mg/l bovine serum albumin (BSA). The divalent cations are required for the activity of topoisomerase II. Since experiments were performed at different concentrations of adenosine-triphosphate (ATP) and adenylyl-imidodiphosphate (AMP-PNP), they were purchased separately from Sigma-Aldrich.

4.2 Methods

4.2.1 Freeze drying

Phage λ-DNA solution, as it is purchased from the manufacturer has a concentration of 0.5 g/L. To study the viscoelastic behavior of entangled DNA solutions, the concentration of DNA has to be increased to at least 2 times higher. It can be seen in the later sections that DNA becomes entangled at a concentration of 0.5 g/L. The samples are concentrated using a freeze dryer.

Freeze drying is a process by which the sample temperature is lowered to the point where the solution is frozen and the solvent is removed by sublimation. Freeze drying is the most gentle way of drying biological samples.

The frozen product is placed in the vacuum chamber for drying. In order to start the sublimation process, heat must be supplied to the sample. The heat is taken from the warmer surroundings [102].

The DNA solution was first frozen rapidly by using liquid nitrogen, after which vacuum was applied so that the solvent can be removed by sublimation. For studying the viscoelasticity of phage $\lambda-$DNA, the DNA stock solution was freeze dried to a concentration of about 1 g/L. For experiments with topoisomerase and anticancer drugs, the DNA stock solution was concentrated to a concentration of about 1.8 g/L.

4.2.2 Dialysis

Dialysis is a procedure for removing excess salt from a sample and to have the sample in the desired buffer. The dialyzer used is a simple single-sided microdialyzer made of teflon, shown in Figure 4.1 [103]. It has a small well which can hold 200 μL or 50 μL of sample. Precut dialysis membrane of cellulose acetate with molecular weight cut off of 5000 Dalton was used to cover the sample, which was held in place by a tight cap. This was immersed in a beaker containing the desired buffer. For the study of the viscoelasticity of phage $\lambda-$DNA, the sample was dialyzed against $1\times$ and $0.1\times$ TE buffer. For the experiments with topoisomerase II and its inhibitors, the sample was dialyzed against the salts of the topoisomerase II reaction buffer (10

Figure 4.1: Microdialyzer

mM Tris-HCl, pH 7.9, 50 mM NaCl, 50 mM KCl, 5 mM $MgCl_2$, 0.1 mM EDTA). The concentration of the salts in the sample taken in the dialyzer equilibrates with the salts of the buffer in the beaker through the process of diffusion. The dialysis is carried out for 3-4 days by replacing the buffer a few times.

4.2.3 UV spectroscopy

After dialysis of the sample, the concentration of the stock is determined by ultraviolet spectrometry. Nucleic acids absorb light in the UV-visible region of the spectrum. Absorbance measurements are used for measuring concentrations of the DNA samples. Spectroscopy is a technique that measures the interaction of molecules with electromagnetic radiation. Light in the near-ultraviolet (UV) and visible range of the electromagnetic spectrum

is used to promote electrons from the ground state to an excited state. A spectrum is obtained when the absorption of light is measured as a function of frequency or wavelength. DNA has substantial absorbance in the UV region and hence UV absorption spectroscopy is the suitable device for determining the concentration of DNA.

Absorption spectroscopy is usually performed with molecules dissolved in a transparent solvent, such as in aqueous buffers. The absorbance of a solute depends linearly on its concentration and therefore absorption spectroscopy is ideally suited for quantitative measurements. Spectroscopic measurements are very sensitive and nondestructive, and require only small amounts of material for analysis.

The Beer-Lambert law gives the relation between the absorbance and concentration of the sample. The relation is written as.

$$A = \log(Io/I) = \varepsilon cl \tag{4.1}$$

where I and Io are the intensity of light from the reference cell and sample cell, ε is the absorptivity and l is the length of the cell (1 cm in most cases). The Beer-Lambert law is a limiting law since it can only be applied to solutions of relatively low analyte concentrations. At high concentrations (usually > 0.01 M), the average distance between the absorbing species is diminished and molecular interaction becomes significant. A similar effect is sometimes encountered in solutions containing low analyte concentrations

but high concentrations of other species, particularly electrolytes (salts). The close proximity of ions to the analyte molecule will alter the molar absorbance of the latter as a result of electrostatic interactions.

In order to obtain maximum sensitivity, measurements are usually made at a wavelength corresponding to the peak maximum λ_{max}, because the change in absorbance per unit of concentration is greatest at this point. For DNA, λ_{max} is 260 nm.

The freeze dried DNA after dialysis was concentrated and the approximate concentration is expected to be more than 1 g/L. A dilute solution of DNA was prepared by diluting the stock solution by a factor of 1000. The buffers used for absorbance measurements should not absorb light in the absorbance range of the analyte molecule. For DNA solution in reaction buffer, the dialysis was done only with reaction buffer salts. BSA was not added as λ_{max} of BSA is 280nm and hence interferes with the absorbance of DNA. The absorbance of the buffer was zeroed by loading a sample of the buffer alone. The absorbance, A_{260}, of the DNA solution was then obtained. The concentration is determined using Beer-Lambert's law. The value of the extinction coefficient, ε, for double stranded DNA is 0.020 (μ g/ml)$^{-1}$cm^{-1}. Using this value of the extinction coefficient, an absorbance, A_{260} of 1 corresponds to a ds DNA concentration of 50 μg/ml. Hence, from the absorbance the concentration of DNA can be obtained [106].

4.2.4 Sample preparation

The next step after dialysis and concentration determination is to add the oligo nucleotides to blunt the right sticky ends of the phage λ-DNA. For this purpose, the sample was heated to 338 K for 10 min and then cooled to 295 K by immersion in a water bath. The complementary oligonucleotide was hybridized to the right cohesive end with a 20% excess molar ratio. To check if this 20% excess of oligomer was sufficient, a solution of 100-fold excess oligomer was also prepared. This stock solution was then left in the refrigerator at 4 degree Celsius for 2 to 3 days to allow the DNA solution to homogenize.

Sample preparation for studying the viscoelasticity of phage λ-DNA

A series of samples with DNA concentrations in the range 0.2 - 0.8 g/L was subsequently prepared by dilution of the stock solution of 1 g/L with 1× TE buffer and 0.1× TE buffer. The samples were spiked with polystyrene microspheres (Polysciences, Warrington,PA) of 0.99±0.03 μm diameter with a final concentration of less than 0.1 wt%. To get an even distribution of microspheres in the sample, they are added to the buffer and vortexed well before preparing the samples. In order to check a possible bead size dependence of the viscoelastic moduli, samples were also prepared with a bead of 3.16±0.03 μm diameter. The samples were again left at 4 degree

Celsius for a day before the measurements were taken. Pipetting of the sample was done carefully and gently to avoid any breakage of the DNA strands. The solution was mixed by stirring gently and pipetting up and down with wide pipette tips.

To study the effect of topoisomerase II and its inhibitors

For the experiments to study the effect of the topoisomerase II and its inhibitors the following steps were done after dialysis with the reaction buffer salts.

BSA was added to the solution so that the final concentration of BSA in the DNA solution is 15 mg/L. A desired amount of ATP was also added. The final concentration of the stock solution is then calculated. The stock solution was left to equilibrate for at least 48 hours at 4 degree Celsius. No appreciable degradation or multimerization of hybridized λ-DNA was observed with field inversion gel electrophoresis (FIGE).

Figure 4.2 shows the image of the gel obtained using field inversion gel electrophoresis (FIGE). No significant dimerization of the molecules were observed. The field gel inversion electrophoresis was done at the Department of Physics, Institut de Physique Théorique, CEA Saclay by courtesy of Jean-Louis Sikorav.

Samples were prepared by dilution of the stock solution with reaction

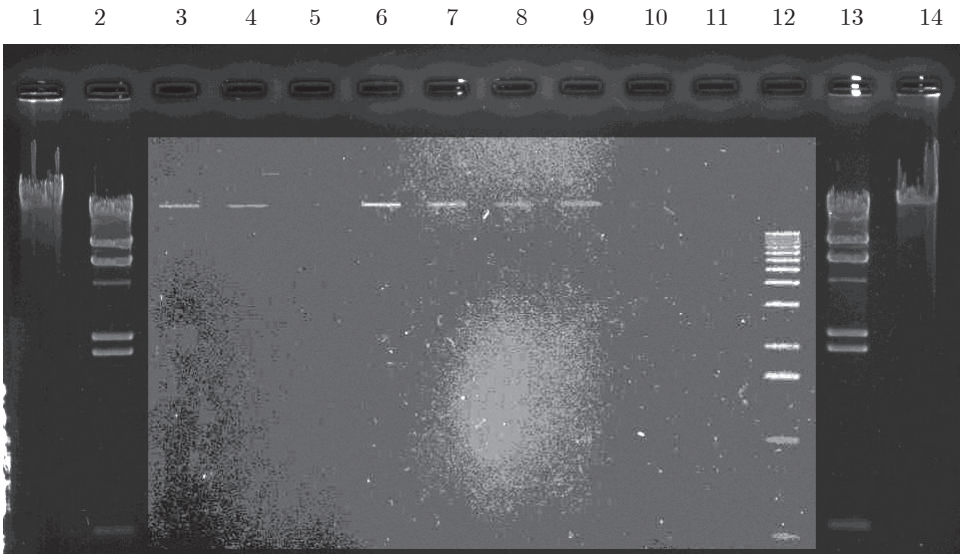

Figure 4.2: FIGE image of the phage λ-DNA before and after the experiments. The contrast of the middle portion has been adjusted for clarity. The lanes contain phage λ-DNA (1 and 14), λ Hind III (2 and 13), 100, 50 and 5 ng of the original DNA solution as purchased from the vendor (3, 4 and 5 respectively), 100, 50 and 5 ng of the stock solution of DNA used for the experiments (6, 7 and 8 respectively) and 100, 50 and 5 ng of DNA after the experiments (9, 10 and 11 respectively).

buffer. For the first series, ATP was added to solutions of 0.2, 0.4, 0.5, 0.7, 0.9, 1.0, and 1.2 g/L of DNA with a final concentration of 1 mM. These samples do not contain topoisomerase II. For the second series, topoisomerase II was added to solutions of 1.0 g/L of DNA in a ratio of 4 units per μg of DNA. The ATP concentrations are 0, 1.0, 2.5, or 4.0 mM. For the third series, topoisomerase II was added to solutions of 1.0 g/L of DNA in ratios of 1, 2, and 4 units per μg of DNA with an ATP concentration of 2.5 mM. For the fourth series, topoisomerase II was added to solutions of 0.5,

0.7, 0.9, 1.0, and 1.2 g/L of DNA in a ratio of 4 units per μg of DNA with ATP concentrations of 1.0, 1.0, 1.0, 2.5, and 4.0 mM, respectively.

4.2.5 Microscopy

The microscopic slide was prepared as shown in Figure 4.3. A droplet of solution was deposited on a microscopy slide and sealed with a cover slip separated by a spacer. The spacer has a thickness of 0.12 mm and a diameter of 13 mm. Around 10 to 13 μl of the sample was used so that it fills up the space surrounded by the spacer completely and prevent any evaporation of the sample.

For the experiments with topoisomerase II, 10 μL of solution was deposited on a microscopy slide. 2 μL of the enzyme in storage buffer is added to this DNA solution followed by mixing the solution through gentle stirring and pipetting up and down. Shear was minimized by using pipette tips that have wide openings. All samples were spiked with polystyrene microspheres (Polysciences, Warrington, PA) of 1.83$\pm$0.05 μm diameter with a final concentration of less than 0.1 wt %. For every experiment, done with topoisomerase II, a control experiment was also done without topoisomerase II. For the control experiments, an amount of buffer equal to the amount of topoisomerase II was added to account for dilution of the sample. For studying the viscoelasticity of phage λ-DNA, particle tracking experiments

were carried out at ambient temperature of 296 K with a Leica DM EP microscope or a Nikon microscope ECLIPSE 80i. The Leica microscope is equipped with a 50× long working distance and 100× oil immersion objectives. The Nikon microscope is equipped with a 50× and 100× long working distance and a 100× oil immersion objectives. The 50× and 100× objectives were used when imaging with Leica microscope and Nikon microscope respectively. It is not advisable to use the oil immersion objective as it exerts a slight pressure on the cover slip of the sample while focusing and affects the motion of the beads. In order to minimize hydrodynamic interactions, care was taken that the imaged beads are separated by at least 20 bead diameters (20 μm). Furthermore, the height level of the focal plane was adjusted so that it is situated right between slide and cover slip so that the imaged beads are not near the glass slide or the cover slip. Video was collected with a charge coupled device camera (JVC TK-C921EG) connected via an analog-to-digital video converter (Canopus, ADVC55) to a computer. For each sample, at least ten movies with a total duration exceeding 100 min of at least ten different beads were recorded with a rate of 25 frames per second and stored on hard disk. For studying the effect of topoisomerase II and its targeting inhibitors, particle tracking experiments were carried out at a temperature of 310 K. Each tracking experiment was started within one minute after addition of the enzyme. For samples without topoisomerase II, at least 1 movie with a total duration exceeding 100 minutes was recorded

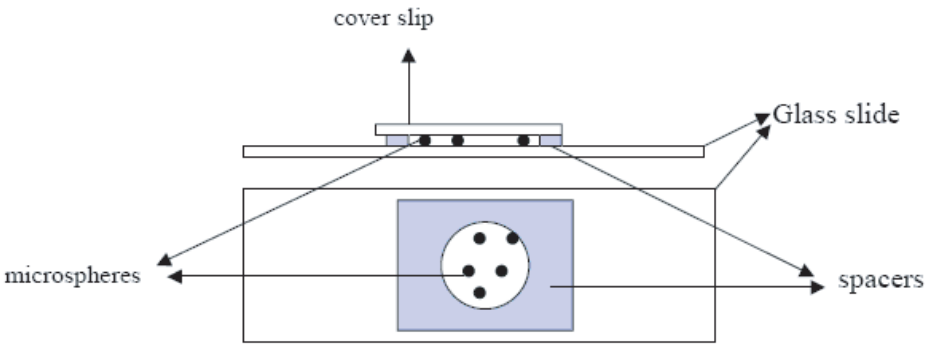

Figure 4.3: Sample with the microspheres on a glass slide covered with a cover slip separated by a spacer

with a rate of 25 frames per second and stored on hard disk. For samples with topoisomerase II , movies of shorter duration about 1-2 minutes were made for 100 minutes.

4.2.6 Particle tracking

The video was analyzed with MATLAB (Natick,MA) using an AVI file reader and the particle trajectories were obtained with public domain tracking software (http://physics.georgetown.edu/matlab/). All further data analysis was done with home developed software scripts written in MATLAB code. In order to monitor the time evolution of the viscoelasticity after the addition of topoisomerase II, the trajectories of the probe beads were binned over intervals of various durations. The pixel resolutions in the x- and y-directions were calibrated with the help of a metric ruler.

The set up was also checked by measuring the diffusion of colloidal beads dispersed in a concentrated solution of glycerol as well as by monitoring immobilized beads adsorbed at a glass slide.

Chapter 5

Results and discussions

5.1 Viscoelastic properties of entangled phage $\lambda-$DNA solutions

The effect of DNA concentration through the critical entanglement concentration on the viscoelastic properties was systematically explored. The number of entanglements per chain was derived from the limiting high frequency plateau value of the elastic storage modulus. The longest, global relaxation time was obtained from the lowest crossover frequency, ω_c, of the viscous loss and elastic storage modulus for entangled solutions as well as from the ratio of the low shear viscosity increment and the high frequency elasticity modulus for all samples. Finally, the results for the viscosity increment, number of entanglements per chain, and the longest relaxation time were compared with the relevant scaling laws for reptation dynamics

of salted polyelectrolytes. These properties of phage $\lambda-$DNA were studied at different buffer conditions like $1\times$ TE and $0.1\times$ TE buffer. The sample preparation and the movies of the particles executing Brownian motion were made as described in the previous chapter.

From the movies obtained, the mean square displacements of the particles are obtained. From the mean square displacement, the graph of the viscous loss modulus and the elasticity storage modulus versus frequency was obtained, from which the low shear viscosity, the plateau elasticity modulus and the relaxation time can be extracted. This can be compared with the scaling laws and it has been seen that they agree with the scaling laws for entangled DNA solutions. These are discussed in the sections below.

5.1.1 Particle trajectory and probability distribution

The matlab program to track the particles identifies the position of the particle based on the intensity and the diameter of the beads specified and records the x and the y coordinates of the particles in each frame. The trajectory of a bead plotted using the x and the y values are shown in Figure (5.1).

From the bead trajectories, the probability distributions for displacements in the x and y directions were extracted for a range of displacement

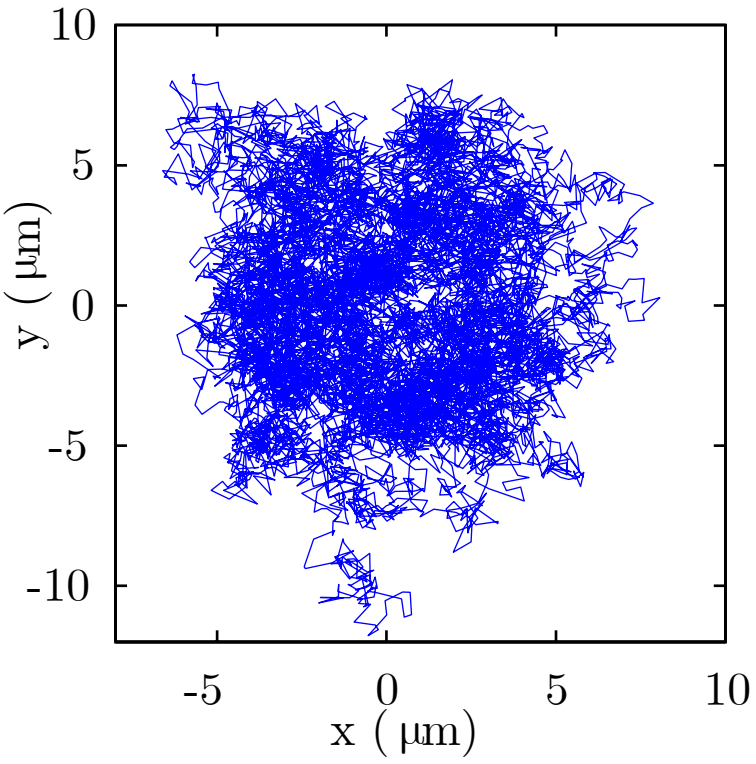

Figure 5.1: The trajectory of a microsphere executing Brownian motion

times, t. The minimum displacement time t=40 ms was determined from the frame rate of the video camera. The maximum time is in principle unbound, but in practice it is set by the rheological properties of the sample because the particles eventually diffuse out of the field of view or they are subjected to long time coherent flow. For the samples in this experiment, the practical upper limit of the displacement time was found to be about 100 s. The probability $P(x,t)$ of diffusing a given distance, x, in a given time interval, t , by an isolated sphere is given by,

$$P(x,t) = \frac{1}{\sqrt{2\pi\langle\Delta x^2(t)\rangle}} exp(-\frac{|x-\bar{x}|^2}{2\langle\Delta x^2(t)\rangle}) \tag{5.1}$$

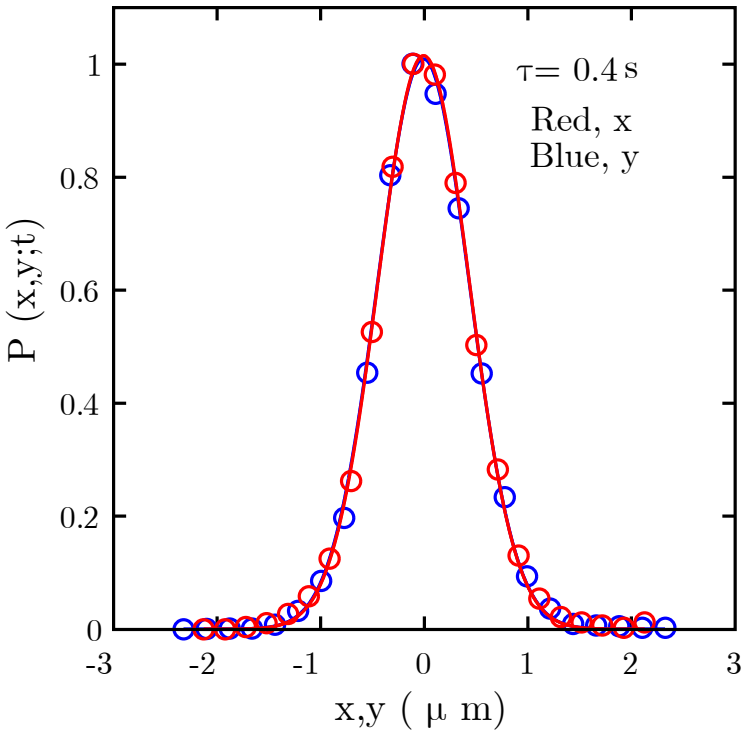

Figure 5.2: The probability distribution of microspheres diffusing in the x and the y direction for time τ=0.4 s

and this follows a Gaussian distribution. The probability distribution for the coordinates of the particles in both the x and the y direction are plotted. This is shown in Figure 5.2. The red and blue circles represent the probability distribution of the particles in the x and the y directions, respectively. A Gaussian was fitted to both probability distributions by optimizing the mean square displacements, shown by the solid line. The mean square displacements in the two orthogonal directions, x and y, were checked to be equal within experimental error, and henceforth the average value was

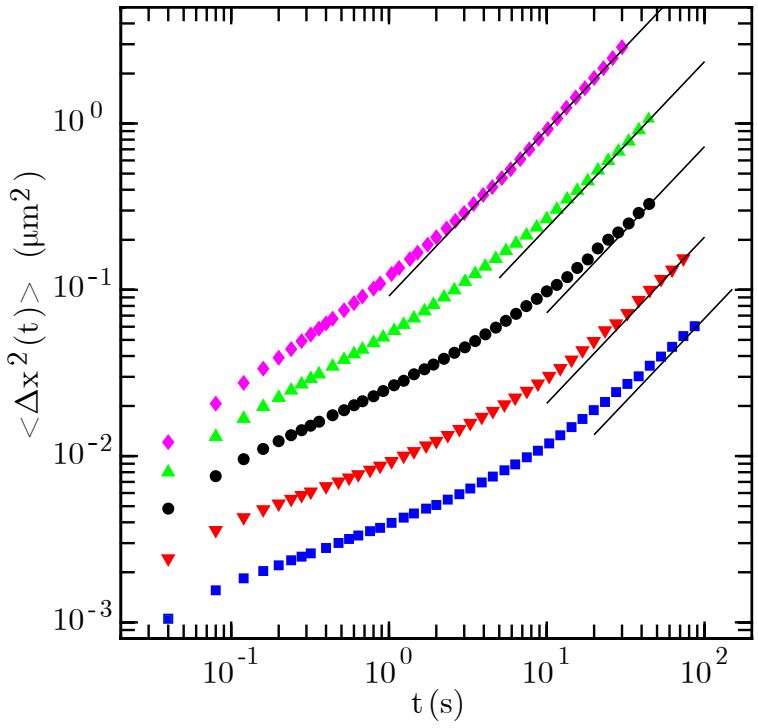

Figure 5.3: The mean square displacement, $\langle \Delta x^2(t) \rangle$ vs time, t for DNA concentrations of 0.8 g/L (□), 0.6 g/L (▽), 0.4 g/L (o), 0.3 g/L (△) and 0.2 g/L (◇) in 1× TE buffer.

taken.

5.1.2 Mean square displacement

Figure 5.3 shows the double logarithmic representation of the mean square displacement vs time, t. The symbol $\langle \Delta x^2(t) \rangle$ is used to stress that the mean square displacement referred to is in one dimension, albeit the experimental results are obtained by statistically averaging the widths of the distributions obtained in the x and y directions (these widths are identical

within experimental error because the fluid is isotropic, *i.e.*, the properties of the fluid does not depend on the direction).

It can be seen from Figure 5.3 that the mean square displacement first increases and then levels off to a certain extent and then increases again. As seen from equation (2.21) the graph of $\langle \Delta x^2(t) \rangle$ vs time t is a straight line for a viscous fluid and the slope of the curve gives the diffusion coefficient of the sphere in the solution. It can be seen from the graph that for a DNA concentration of 0.2 g/L, the graph begins to deviate from linear behavior. The deviation from linear behavior increases as the concentration of DNA is increased from 0.2 g/L to 0.8 g/L. The deviation from linear behavior is observed only for shorter times and this is due to the complex viscoelastic behavior of the DNA solution. It should also be noted that for very long times, the linear behavior is restored. This is because, due to the temporary entanglements formed by the DNA molecules, the solution exhibits an elastic response at short times. These entanglements will be relaxed in a time τ, which is the longest global relaxation times (the longest global relaxation times for lambda DNA is of the order of 1 s), i.e., the molecules can move over their molecular dimensions within this time, and the solution behaves as a viscous fluid for longer times.

With increasing DNA concentration, the mean square displacement decreases and the range of times with a subdiffusive scaling exponent less than one becomes wider. These phenomena are obviously related to changes in

the number of entanglements per chain, which can be conveniently discussed in terms of the viscous loss and the elastic storage moduli.

5.1.3 Viscoelastic moduli

The viscous loss modulus $G''(\omega)$ and the elastic storage modulus $G'(\omega)$ can be obtained from the mean square displacement using equation (2.58). For this purpose, it is important to determine α, β and γ defined in the equation (2.52). These values have been obtained by the fourth order polynomial fit to the data in Figure 5.3 and they describe the smooth variation of the mean square displacement well. The viscoelastic moduli are thus calculated and shown in Figure 5.4. Figure 5.4(a) shows $G'(\omega)$ and $G''(\omega)$ for different DNA concentrations in 1× TE buffer and Figure 5.4(b) shows the same in 0.1× TE buffer.

For a viscous fluid, the mean square displacement is given by Einstein's law $\langle \Delta x^2(t) \rangle = 2Dt$, with D being the diffusion coefficient. With the Stokes-Einstein equation $D = k_B T/(6\pi\eta a)$, the low shear viscosity of the DNA solution from the limiting long-time diffusive behavior of the mean square displacement can be derived. The measured viscosity increments $\Delta\eta = \eta - \eta_s$ with respect to the one of the solvent $\eta_s = 0.001$ Pa s are displayed in Figure 5.5. The viscosity increment increases by more than two orders of

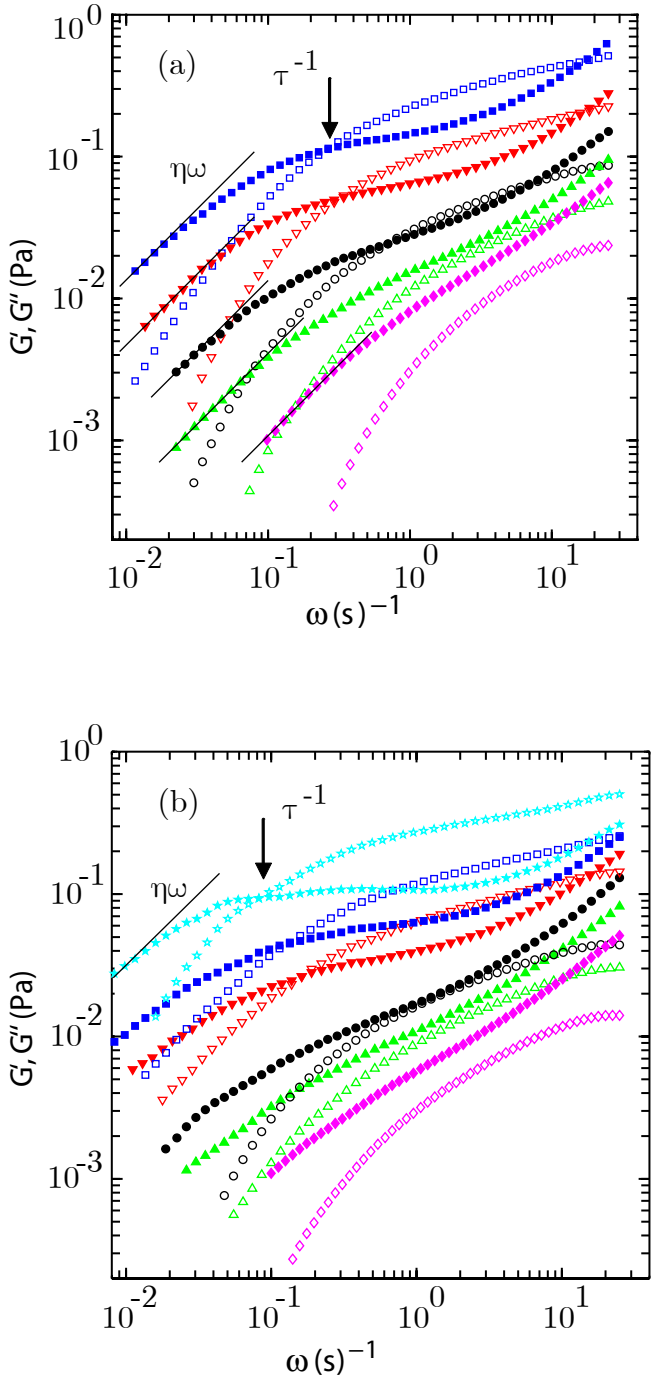

Figure 5.4: Elastic storage modulus G' and viscous loss modulus G'' versus frequency ω in (a) 1× and (b) 0.1× TE buffer. The concentrations shown are 0.2 g/L (◊), 0.3 g/L (△), 0.4 g/L (o), 0.6 g/L (▽), 0.8 g/L (□) and 1.0 g/L (⋆). The filled symbols represent the viscous loss modulus $G''(\omega)$ and the open symbols represent the elastic storage modulus $G'(\omega)$ for the different DNA concentrations.

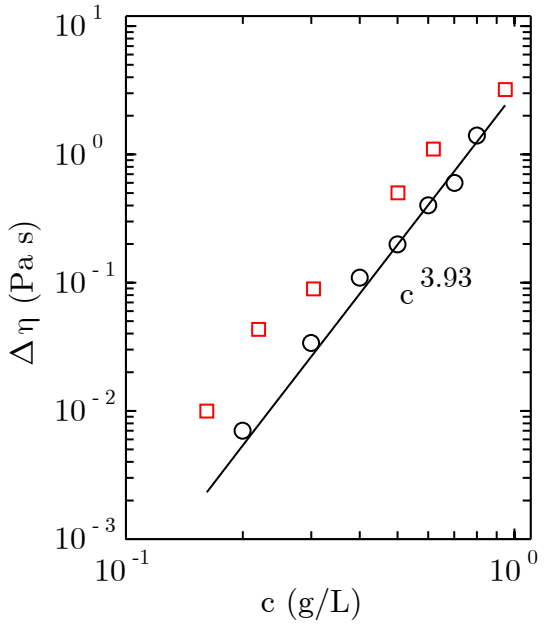

Figure 5.5: Low shear viscosity increment $\Delta\eta$ vs DNA concentrations, c, in 0.1× (□) and 1× (o) TE buffer. The line indicates the scaling law for the low shear viscosity of DNA solutions in the entangled regime.

magnitude if the DNA concentration increases from 0.2 to 0.8 g/L. For both the buffer concentrations the relaxation times follow a power law $\Delta\eta \simeq c^{3.93}$ pertaining to an entangled polyelectrolyte solution in an excess of simple salt and derived with a Flory exponent ν =0.588 [18, 61].

Viscous loss Modulus, $G''(\omega)$

In the double logarithmic representation, the viscous loss modulus first increases linearly with frequency, then deviates from linear behavior with a decreased value of the slope in the intermediate frequency range and then increases again for higher frequencies. This effect becomes more prominent

as the DNA concentration increases. The linear behavior of $G''(\omega)$ at low frequencies corresponds to the linear behavior of the mean square displacement at long times in Figure 5.3. The low shear viscosity, η, can be derived from the behavior of the viscous loss modulus at low frequencies. If the mean square displacement is given by $\langle \Delta x^2(t) \rangle = 2Dt$, an analytical calculation of the one sided Fourier transform gives for the viscoelastic moduli $G'' = \eta\omega$ and $G' = 0$. As seen in the Figure 5.4 the viscoelastic moduli approaches the linear scaling law $\eta\omega$ for low frequencies as shown by the solid lines. Qualitatively similar behavior has been reported in the shear stress versus shear rate of T4 DNA at comparable concentrations [44].

Elastic storage modulus, $G'(\omega)$

Concurrent to the behavior of the viscous loss modulus, the elasticity modulus monotonously increases and eventually levels off to a constant plateau value at high frequency. For a DNA concentration of 0.2 g/L, the viscous loss modulus is higher than the elasticity storage modulus implying that the DNA solution behaves as a viscous fluid. As the concentration of DNA increases, the elastic storage modulus increases with respect to the viscous loss modulus and the two curves meet each other for a concentration of about 0.3 g/L. This indicates the onset of entanglements. This transition concentration is about 10 times the overlap concentration. For concentrations exceeding 0.3 g/L, the elastic storage modulus become larger than the

viscous loss modulus in the intermediate frequency range. Also, the range of frequencies for which the elastic storage modulus exceeds the viscous loss modulus increases as the DNA concentration increases. The same behavior is observed for the DNA solution in a buffer of low ionic strength (0.1 mM TE). From self-diffusion experiments of fluorescence labeled phage λ−DNA in TE buffer, Smith et al. have estimated the entanglement concentration of DNA to be around 0.6 g/L [82].

The development of plateau elasticity for high frequencies and a crossing of the viscous loss by the elastic storage modulus at a crossover frequency, ω_c, for concentrations exceeding a critical entanglement concentration have been reported before for calf thymus DNA of poly disperse length [55]. The viscous loss modulus shows dispersion at two different frequency scales. One process is characterized by a relaxation time on the order of a second, which becomes longer with increasing concentration. This process is the reptation dynamics of the DNA molecules in the entangled solution. Its correlation time can be considered as an entanglement disengagement time or tube renewal time. For T2 or T4-DNA at comparable concentrations, the corresponding relaxation times are two orders of magnitude longer, in agreement with the higher molecular weight (164 or 166 versus 48.5 kbp) [61, 44]. The other process occurs at higher frequencies with a correlation time on the order of 0.1 s and is relatively insensitive to the DNA concentration. The high frequency dispersion is related to the Rouse dynamics of the entire

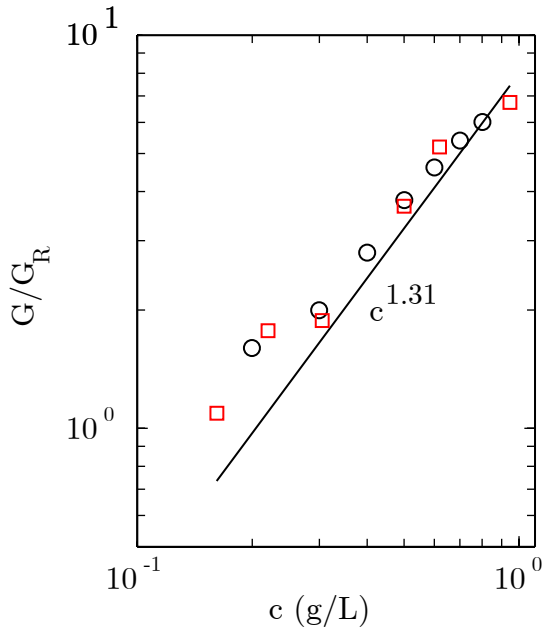

Figure 5.6: High frequency elasticity modulus over Rouse modulus G/G_R vs DNA concentration, c, in 0.1× (□) and 1× (o) TE buffer. The line indicates the scaling law for the high frequency elasticity modulus of DNA solutions in the entangled regime.

DNA molecule inside the tube formed by the entanglements. Similar high frequency dispersion has been observed in the shear stress versus shear rate of T4-DNA [44].

5.1.4 Entanglements and reptation dynamics

The number of entanglements and the longest global relaxation times can be obtained from the moduli in Figure 5.4. They follow specific scaling laws as described in section 2.5.

Number of entanglements

The number of entanglements can be derived from the ratio of the plateau elasticity modulus, G and the elasticity modulus pertaining to the non-entangled Rouse chain $G_R = \rho kT$ evaluated at the same molecular density ρ. The ratio G/G_R is proportional to the number of segments per chain divided by the average number of segments between entanglements, so that the number of entanglements per chain is given by $G/G_R - 1$ [16, 18, 17]. As seen from Figure 5.4, the elasticity storage modulus increases and reaches a constant value G. The ratio G/G_R is shown in Figure 5.6. It can be seen that the decrease in the ionic strength of the buffer from 1× to 0.1× TE, does not affect the number of entanglements for different concentrations of DNA. The experimental values can be considered as under limits because the elastic storage moduli might increase a bit for even higher frequencies outside our observation window. At low concentration, G/G_R is around unity which is in agreement with non-entangled dynamics. For concentrations exceeding 0.3 g/L of DNA, G/G_R increases and follows the scaling law for an entangled polyelectrolyte with screened electrostatics, *i.e.* $G/G_R \simeq c^{1.31}$ ($\nu = 0.588$) [18, 61]. The number of entanglements per chain at a concentration of 0.8 g/L of DNA is about 7. For a sample of phage λ− DNA of concentration 2 g/L, approximately 22 entanglements per chain has been reported in the literature based on bulk rheology measurements [87]. This

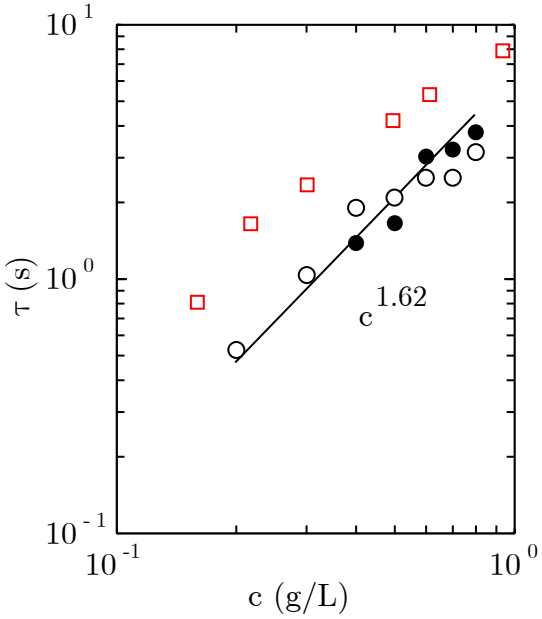

Figure 5.7: Relaxation time τ vs DNA concentration, c, in 0.1× (□) and 1× (o) TE buffer. The open circles are the relaxation times derived from the low shear viscosity and the high frequency limiting value of elastic storage modulus. The filled circles are the relaxation times obtained from the lowest cross over frequency. The line indicates the scaling law for the relaxation times of DNA solutions in the entangled regime.

value agrees with the observed number of entanglements per chain, if they are extrapolated to the relevant concentration according to $c^{1.31}$ scaling.

Relaxation time

The longest, global relaxation time can be obtained from the lowest crossover frequency of the viscous loss and elastic storage moduli $\omega_c = \tau^{-1}$ indicated by the arrows in Figure 5.4. The results are displayed in

Figure 5.7. As an alternative, τ can be derived from the increment in the low shear viscosity and the high frequency limiting value of the elastic storage modulus, according to the equation, $\Delta\eta = \pi^2/12\ G\tau$ [17]. The corresponding results are also displayed in Figure 5.7. The values of the relaxation times obtained from the DNA solutions in 1× TE buffer by both procedures agree within experimental accuracy. The crossover frequency is only observed for entangled solutions, *i.e.*, for concentrations exceeding 0.3 g/L of DNA, whereas the method based on the low shear viscosity is general and can also be used to derive the global relaxation of DNA molecules in the dilute and non-entangled semi dilute regimes. In 1× TE, the relaxation time increases by about an order of magnitude from 0.4 s for non-entangled DNA to about 4 s at the highest concentration in the entangled regime. In 0.1× TE, the relaxation times are longer by a factor of two. It is seen that the relaxation time increases with a decrease in the ionic strength of the buffer. The reduced screening of the electrostatic charges in the polymer causes the DNA to move slower. Furthermore, the relaxation time follow the scaling law for reptation dynamics of a salted polyelectrolyte $\tau \simeq c^{1.62}$ ($\nu = 0.588$) [18, 61]. For concentrations below the entanglement concentration, we do not observe the transition to Rouse dynamics with a much weaker concentration dependence $\tau_R \simeq c^{0.31}$.

5.1.5 Effect of depletion

The viscoelastic moduli derived here is based on the assumption that the DNA solution is homogeneous. In particular, the depletion in DNA concentration is neglected in an interfacial region surrounding the bead with a thickness on the order of the mesh size. For concentrations in the range 0.03-0.4 g/L of λ-DNA, Chen et al. have quantified the submicron scale variation in the viscoelastic response by using one and two-point tracking microrheology [31]. It was shown that the viscoelastic moduli, as measured by the single-particle method, are somewhat underestimated due to this depletion effect. This effect becomes progressively less important with increasing DNA concentration (smaller mesh size) and/or larger bead diameter. This can be understood on the basis of the small values of the correlation length less than 100 nm for concentrations exceeding 0.3 g/L of DNA [90]. It is possible to correct for the effect of depletion by using the shell model of Levine and Lubensky [46]. It is observed that the moduli obtained from the tracking of the 1.0 and 3.2 μm sized beads collapse to single curves by assuming a layer of water surrounding the beads with a thickness of the correlation length. In principle, all the viscoelasticity data can be corrected according this procedure. It is found that the correction does not result in a change in qualitative behavior of the viscoelastic response, including the scaling behavior of the low shear viscosity, the number of

entanglements per chain, and the relaxation time. Furthermore, the correction becomes vanishingly small due to the decrease in correlation length to a value around the persistence length for higher DNA concentrations in the entangled regime. Under the present experimental conditions, the effect of depletion is hence relatively unimportant and is not further pursued.

5.1.6 Conclusions

Particle tracking microrheology is used to study the viscoelastic properties of phage λ−DNA through the entanglement transition. Particle tracking microrheology is found to be very useful and effective in studying the dynamics of DNA as it uses minute samples of no more than 15 μL and does not involve excessive shearing of the sample. The mean square displacement of the particle executing Brownian motion is obtained. The generalized Stokes-Einstein relation is used to derive the viscous loss modulus and the elastic storage modulus from the mean square displacements. With increasing frequency, the viscous loss modulus first increases, then levels off, and eventually increases again. Concurrently, the elastic storage modulus monotonously increases and eventually levels off to a constant high frequency plateau value. Once the DNA molecules become entangled at about ten times the overlap concentration, the elastic storage modulus becomes larger than the viscous loss modulus in an intermediate frequency range.

The number of entanglements per chain is obtained from the plateau value of the elasticity modulus. A range of concentrations from the non-entangled, semi-dilute to the moderately entangled regime with about seven entanglements per chain have been studied. The longest, global relaxation time pertaining to the motion of the DNA molecules is obtained from the low shear viscosity as well as from the lowest crossover frequency of the viscous loss and elastic storage moduli. In the entangled regime, both relaxation times agree and can be identified with the entanglement disengagement time or tube renewal time. The concentration dependencies of the low shear viscosity, the number of entanglements per chain, and the relaxation time agree with the relevant scaling laws for reptation dynamics of entangled polyelectrolytes with screened electrostatic interactions. The high frequency dispersion in the viscous loss modulus is relatively insensitive to the DNA concentration and is related to the Rouse dynamics of the DNA molecule inside the tube formed by the entanglements.

5.2 Effect of DNA topoisomerase II on the viscoelasticity of DNA

The genome is highly compacted and concentrated, yet the time scales for replication and transcription are unexpectedly fast. For instance, the segregation of the intertwined sister chromatids in the anaphase of dividing cells occurs within a minute. Topology controlling enzymes (topoisomerases) are thought to play an essential role in chromatid motion and the kinetics of chromosome condensation, but to date there are no quantitative measurements of the effect of disentanglement on the properties of the flow (viscoelasticity) [10, 81, 11, 12].

The flow properties of DNA are important for understanding cell division and, indirectly, cancer therapy. This section is about how double strand passage facilitated by topoisomerase II controls the viscoelasticity of an entangled DNA solution. The elastic storage and viscous loss moduli of a model system comprising bacteriophage $\lambda-$DNA and human topoisomerase IIα have been measured using video tracking of the Brownian motion of colloidal probe particles. In particular, how the disentanglement of linear DNA molecules by topoisomerase II is coupled to the dissipation of energy through the hydrolysis of ATP has been explored. It has been found that the viscoelasticity is critically dependent on the formation of entanglements among the DNA molecules with a relaxation time on the order of a

second. It has also been observed that topoisomerase II effectively removes these entanglements and transforms the solution from an elastic physical gel to a viscous fluid depending on the consumption of adenosine-triphosphate (ATP). It has also been shown that for the complete relaxation of the entanglements, at least an equal number of dimers as that of the entanglements are required.

5.2.1 Entanglements and reptation dynamics

Topoisomerase II has specific requirements for its functioning in terms of buffer composition and temperature. The reaction buffer contains a mixture of different salts as mentioned in section 4.1.7 including $MgCl_2$ as well as protein and the optimal temperature for the double strand passage reaction is 310 K. Hence, the viscoelasticity of our model system and the critical concentration of DNA for the formation of entanglements in the relevant experimental conditions without the presence of the enzyme was first explored. For this purpose, the mean square displacement $\langle \Delta x^2(t) \rangle$ of the colloidal probe beads for a series of samples with increasing concentration of DNA in reaction buffer including 1.0 mM ATP was measured. The results are shown in Figure (5.8). The results for 0.5 g/L and 1.2 g/L of DNA are not shown for the sake of clarity, but they fall perfectly between the marks set by the other solutions. As discussed in the previous section

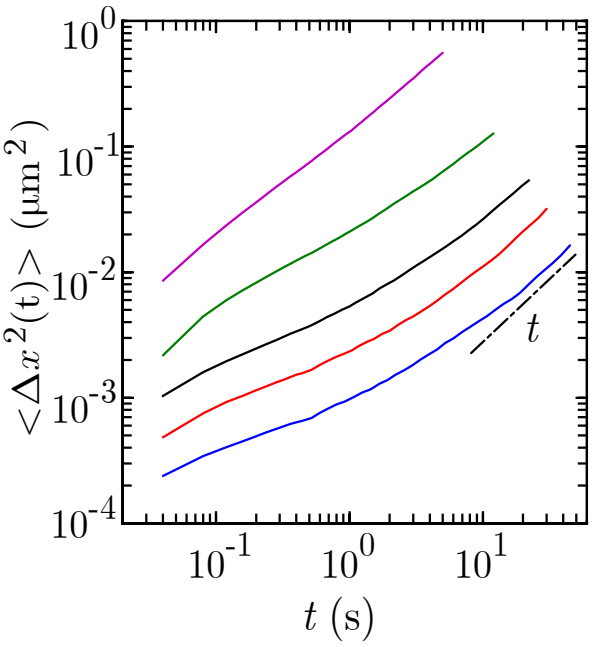

Figure 5.8: Mean square displacement$\langle \Delta x^2(t) \rangle$ versus time, t in reaction buffer at 310 K. The DNA concentrations shown are 0.2 g/L (magenta), 0.4 g/L (green), 0.7 g/L (black), 1.0 g/L (red) and 1.4 g/L (blue)

for a DNA solutions in TE buffer, diffusive behavior with $\langle \Delta x^2(t) \rangle \propto t$ is only observed for low DNA concentrations and for very long times in the case of higher DNA concentration. With increasing concentration of DNA, $\langle \Delta x^2(t) \rangle$ decreases and the range of times with a subdiffusive scaling exponent less than one becomes wider. This behavior is typical for a viscoelastic fluid and is more conveniently discussed in terms of the elastic storage and viscous loss moduli, G' and G'', respectively.

Following the procedure as described in chapter (2) [27], $G'(\omega)$ and $G''(\omega)$ were obtained from the one-sided, complex Fourier transform of $\langle \Delta x^2(t) \rangle$

and the generalized Stokes-Einstein equation.

$$G(\omega) = \frac{k_B T}{3\pi a i\omega \Delta\langle \tilde{x}^2(\omega)\rangle} \tag{5.2}$$

The formalism requires that the fluid can be treated as an incompressible continuum, no slip boundary conditions, and that the Stokes drag can be extended over all frequencies [56]. The typical mesh sizes or correlation lengths of our semi-dilute DNA solutions are less than 100 nm and on the order of the DNA persistence length. The structures of the fluid, which give rise to the properties of the flow, are hence much smaller than the bead size used which is 1.8 μm [90]. A larger bead as compared to that in the previous experiments is used to minimize the effect of a depletion layer surrounding the bead. Accordingly, the effects of a submicron scale variation in DNA density next to the colloidal beads on the viscoelastic response are vanishingly small and can be safely neglected [27, 31]. The viscoelastic moduli are displayed in Figure 5.9 in double logarithmic representation. With increasing frequency, G'' first increases, then levels off to a certain extent depending on the concentration of DNA, and eventually increases again. Concurrently, G' monotonously increases and eventually levels off at a constant high frequency plateau value G. For a concentration exceeding 0.5 g/L of DNA, G' becomes larger than G'' in an intermediate frequency range. The crossing of G' and G'' and the development of an elastic plateau modulus are caused by the formation of entanglements [55, 27]. It should be

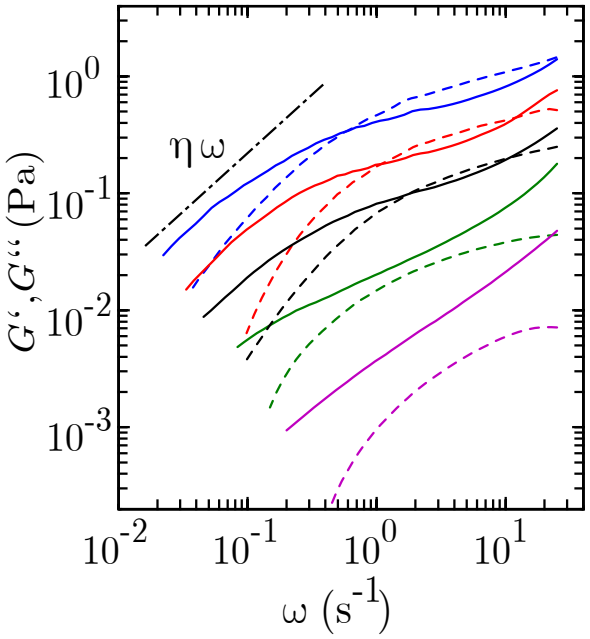

Figure 5.9: Elastic storage modulus G'(dashed) and the viscous loss modulus G'' (solid) versus frequency, ω. The DNA concentrations shown are 0.2 g/L (magenta), 0.4 g/L (green), 0.7 g/L (black), 1.0 g/L (red) and 1.4 g/L (blue).

noted that these entanglements are temporary and continuously disappear and reappear by the reptation dynamics of the DNA molecules [16, 17, 18]. Furthermore, the critical concentration for the formation of entanglements, *i.e.* the entanglement concentration, is about ten times the overlap concentration from the dilute to the semi-dilute regime.

The formation of entanglements can also be inferred from the concentration scaling of the transport properties $\Delta\eta$, G and τ.

The low shear viscosity, η, is obtained from the behavior of $G'' = \eta\omega$ in the diffusive limit at low frequencies. The viscosity increments, $\Delta\eta = \eta - \eta_s$

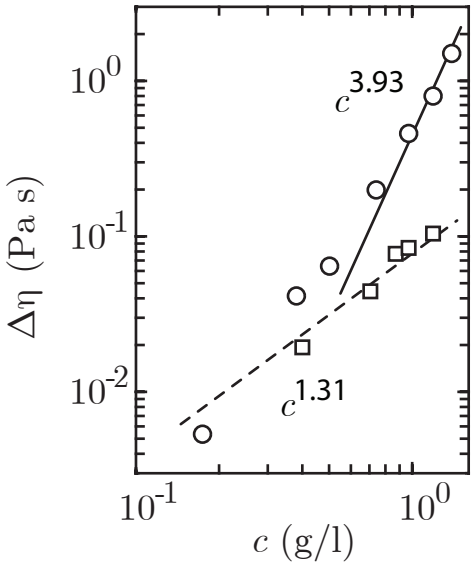

Figure 5.10: Low shear viscosity increment $\Delta\eta$ versus DNA concentration c. The circles and the squares represent the viscosity increment for DNA solutions without topoisomerase II and that after the full relaxation of entanglements with topoisomerase II.

with respect to the viscosity of the buffer $\eta_s = 0.0007$ Pa s are shown in Figure 5.10 . It can be seen that the viscosity increment increases by two orders of magnitude if the DNA concentration is increased from 0.2 to 1.4 g/L. For concentrations exceeding 0.5 g/L, it follows a power law $\Delta\eta \propto c^{3.93}$ for entangled polyelectrolyte with screened electrostatics as seen in equation 2.15 [18, 61]. All scaling exponents have been derived with a Flory exponent $\nu = 0.588$ [16].

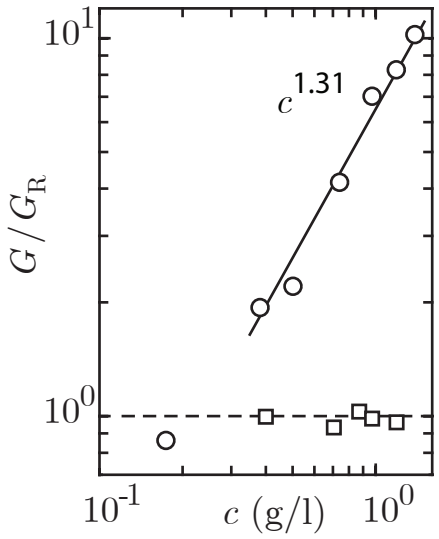

Figure 5.11: High frequency elasticity modulus divided by the Rouse modulus $G/G_{\rm R}$ versus the DNA concentration, c. The circles and the squares represent the G/G_R for DNA solutions without topoisomerase II and that after the full relaxation of entanglements with topoisomerase II.

As discussed earlier, the elasticity modulus is given by the density of the dynamical units times the thermal energy k_BT [16, 18, 17]. In the absence of entanglements, the dynamical units are the individual DNA molecules. The elasticity modulus G, is then given by the Rouse modulus, $G_R = \rho k_B T$ with DNA density ρ. Hence, for the non-entangled DNA solution, $G/G_R = 1$.

In the entangled network, the dynamical units are the DNA segments between the entanglements (entanglement strands). Let N_e be the number of entanglements. The density of entanglement strands is then given by $[N_e{+}1]\rho$. Hence, for entangled DNA solution, the elasticity modulus, $G = [N_e + 1]G_R$. So the number of entanglements, $N_e = G/G_R - 1$. The

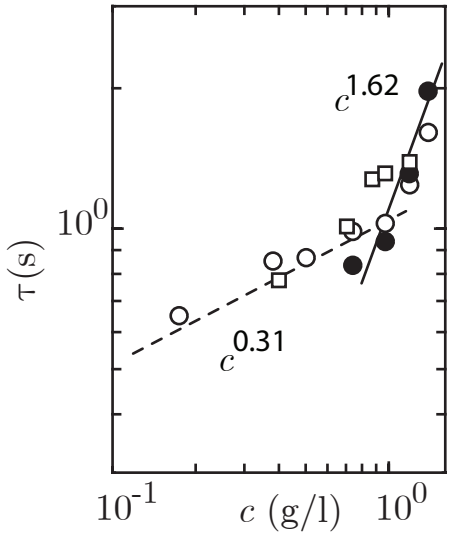

Figure 5.12: Relaxation time τ versus the DNA concentration, c. The circles and the squares represents the relaxation times for DNA solutions without topoisomerase II and that after the full relaxation of entanglements with topoisomerase II. Relaxation times derived from the low shear viscosity and high frequency elasticity modulus are shown by (o) and relaxation times obtained from the cross over frequency are shown by (•).

results for G/G_R is shown in Figure 5.11. The experimental values can be considered under limits, because G' might increase a bit for even higher frequencies outside our window of observation. At the lowest concentration of 0.2 g/L of DNA, G/G_R is around unity, which is in agreement with non-entangled dynamics. At higher concentrations, it follows the scaling law for an entangled, salted polyelectrolyte $G/G_{\mathrm{R}} \propto c^{1.31}$ and for a concentration of 1.4 g/L there are about 12 entanglements per chain.

The longest, global relaxation time τ pertaining to the motion of the DNA molecule can be derived from the low shear viscosity and the high

frequency elasticity modulus according to $\Delta\eta = \pi^2/12\ G\tau$ [17]. For entangled solutions, τ can also be obtained from the lowest crossover frequency $\omega_c = \tau^{-1}$. Relaxation times derived from the low shear viscosity and high frequency elasticity modulus as well as from the cross over are shown in Figure 5.12. It can be seen that the values of τ obtained with both procedures agree within experimental accuracy. The relaxation time increases from 0.6 s for non-entangled DNA to around 2 s for the sample with the highest concentration of DNA. With increasing concentration, τ first follows the scaling law for Rouse dynamics of a non-entangled and salted polyelectrolyte $\tau \propto c^{0.31}$. With the onset of entanglements, the relaxation time follows for higher concentrations of DNA, follows a reptation dynamics with $\tau \propto c^{1.62}$.

In the relevant experimental conditions, the model system exhibits the transition from the non-entangled to the moderately entangled regime with around 12 entanglements per DNA molecule at the highest DNA concentration of 1.4 g/L. The entanglement concentration is in the range as obtained for λ-DNA in 10 mM tris-EDTA at 296 K [27, 82]. The increased ionic strength of the reaction buffer and the elevated temperature of 310 K result in a shift in entanglement concentration of DNA from 0.3 to 0.5 g/L, but no qualitative change in viscoelastic behavior. In the entangled regime, the concentration scaling of the transport properties also agrees with previously reported results. In the next section, it is demonstrated that the entanglements can be relaxed by topoisomerase II in conjunction with the

consumption of ATP. In particular, it will be shown that Rouse dynamics with $G/G_{\mathrm{R}} = 1$ can be realized for relatively dense solutions of DNA.

5.2.2 Relaxation of entanglements

In this section, the effect of topoisomerase II on the viscoelastic properties of our model system in the presence of ATP is discussed. As seen from the previous section, the entanglement concentration is about 0.5 g/L. Topoisomerase II is added to initially entangled solutions and the trajectories of the probe beads as a function of the time evolved after the addition of the enzyme were monitored. For most samples, 4 units (80 ng) of topoisomerase II per μg of DNA was added, which corresponds with around 8 topoisomerase dimers per DNA molecule. The number of dimers is hence of the same order of magnitude as the number of entanglements per molecule.

Furthermore, it was necessary to maintain the temperature of the assays at 310 K, because at ambient temperature no effect of the enzyme on the viscoelastic behavior was observed. The trajectories of the beads were binned into time intervals of various durations. It was observed that the time scale of the change in viscoelasticity (minutes) is much longer than the one pertaining to the loss of correlation in the velocity of the beads (seconds). Within each interval, the system is in quasi-equilibrium with Gaussian distributions in the displacements of the beads. Accordingly, for

each interval $\langle \Delta x^2(t) \rangle$ and, subsequently, G' and G'' were obtained as described in chapter 2 [27].

Relaxation with different DNA concentrations

Topoisomerase II was added to solutions of different DNA concentrations. The ATP concentration was fixed at 1 mM as it was the concentration in the standard reaction buffer. The topoisomerase II concentration was 4 units/μg of DNA. For DNA concentrations less than 1.0 g/L, full and fast relaxation of entanglements was observed with an ATP concentration of 1 mM. But for DNA concentrations of 1.0 and 1.2 g/L it was necessary to increase the ATP concentration to 2.5 and 4.0 mM, respectively to observe full and fast relaxation. The time evolution of G' and G'' pertaining to a solution of 0.4 g/L and 0.7 g/L of DNA is shown in Figure 5.13.

The solution of 0.4 g/L is not entangled. It can be seen that topoisomerase II has very little effect at this DNA concentration. The solution of 0.7 g/L of DNA is just in the entanglement regime as shown by the crossing of G' and G'' in the intermediate frequency range. With increasing time, both G' and G'' decrease until they no longer cross each other. It can be seen that the topoisomerase immediately relaxes the entanglements and transfers the solution from a physical elastic gel to a viscous fluid.

Figure 5.14 show the time dependence of G/G_R after the addition to

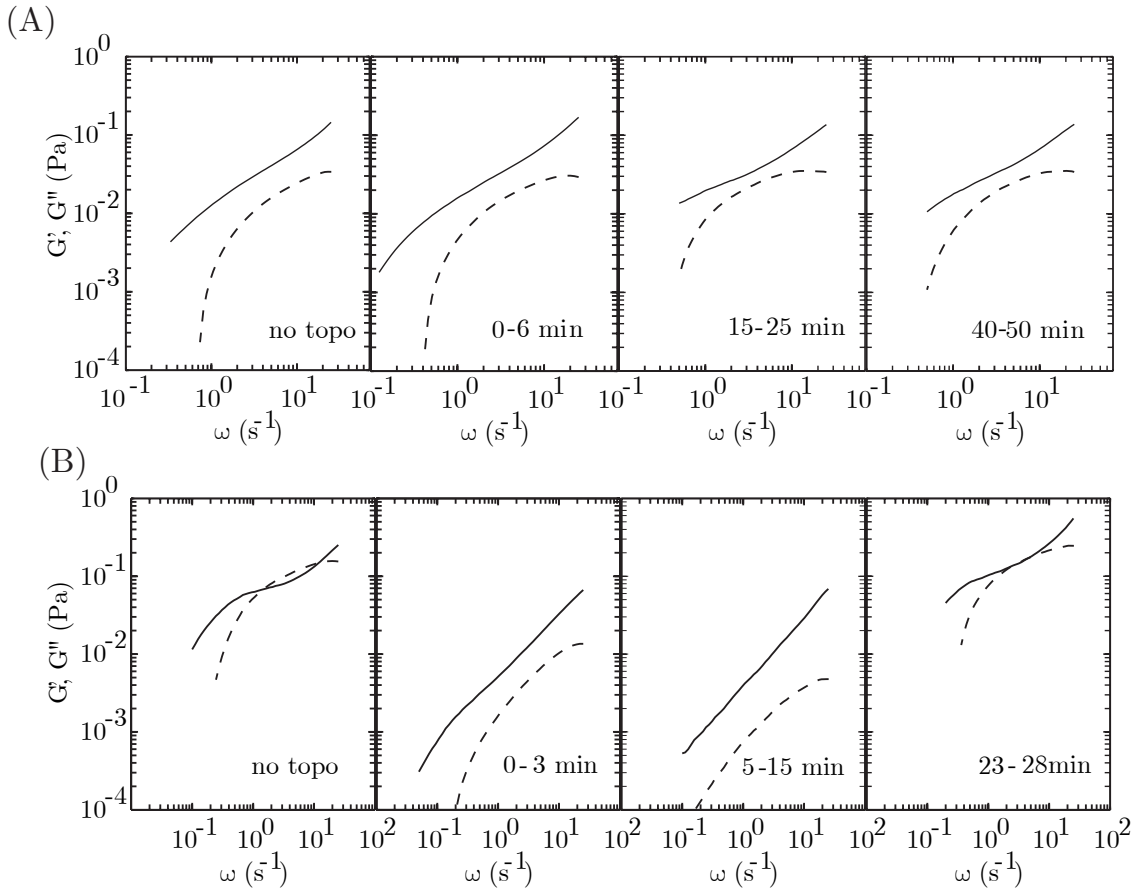

Figure 5.13: The evolution of elastic storage G'(dashed curves) and the viscous loss G'' (solid curves) moduli after the addition of the topoisomerase II (4 units/μg) to a solution of 0.4 g/L (panel A)and 0.7 g/L (panel B) of DNA with an ATP concentration of 1mM.

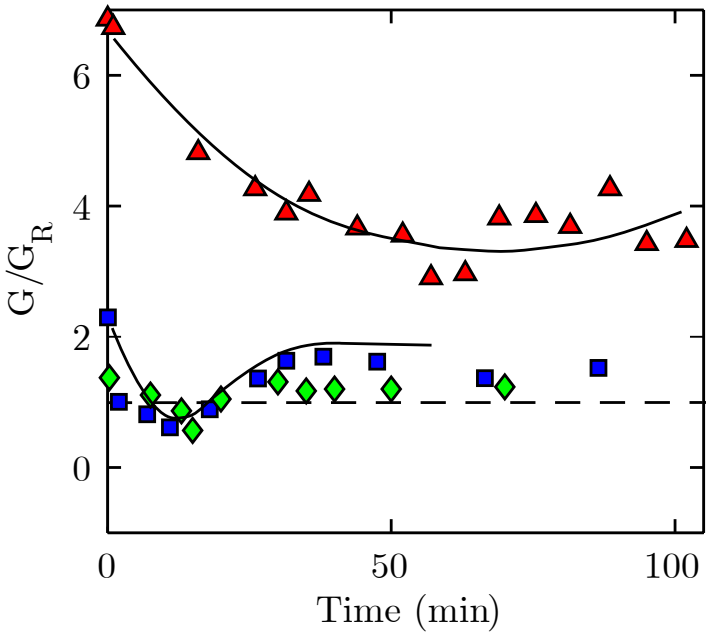

Figure 5.14: High frequency elasticity modulus divided by the Rouse modulus G/G_{R} versus time t after the addition of topoisomerase II (4 units/μg) to a solution of 1.0 g/L of DNA ($\triangle$), 0.7 g/L ($\square$) and 0.4 g/L($\diamond$) in 1mM ATP

topoisomerase II. For a DNA concentration 0.4 g/L, G/G_R remains almost constant as G/G_R=1 for a non-entangled solution with Rouse behavior. For a concentration of 0.7 g/L of DNA, G/G_R immediately drops from 2 to 1 after the addition of topoisomerase II. A solution of 1 g/L DNA is moderately entangled with about 6 entanglements per molecule. With 1 mM ATP it can be seen that the entanglements are only partially relaxed. For all other higher concentrations of DNA, partial relaxation was observed (with 1 mM ATP). Complete relaxation of entanglements with an ATP concentration of 1 mM and a topoisomerase II concentration of 4 units/μg

of DNA was observed only in the case of DNA concentrations less than 1 g/L. For higher DNA concentrations the ATP concentration needs to be increased.

Relaxation with different concentrations of ATP

To study the dependence of the relaxation of entanglements on the concentration of ATP, experiments were done with 1 mM, 2.5 mM, and 4 mM ATP. The DNA concentration was fixed at 1.0 g/L and the topoisomerase II was fixed at 4 units/μg of DNA. The time evolution of G' and G'' pertaining to a solution of 1.0 g/L of DNA with 2.5 mM ATP after the addition of 4 units of topoisomerase II per μg of DNA is shown in Figure 5.15. The solution is initially moderately entangled with about 6 entanglements per molecule. With increasing time, both G' and G'' decrease until they no longer cross each other. This shows that the entanglements are relaxed and that the solution is transformed from an elastic physical gel to a viscous fluid. The time required to reach the fully relaxed state depends on the relative concentrations of ATP and topoisomerase II. For very long times, G' and G'' increase again and eventually the original, entangled state is recovered.

Relaxation of entanglements is most conveniently followed by monitoring the high frequency plateau value of the elastic storage modulus G. For a solution of 1.0 g/L of DNA, the time dependencies of G/G_{R} after the ad-

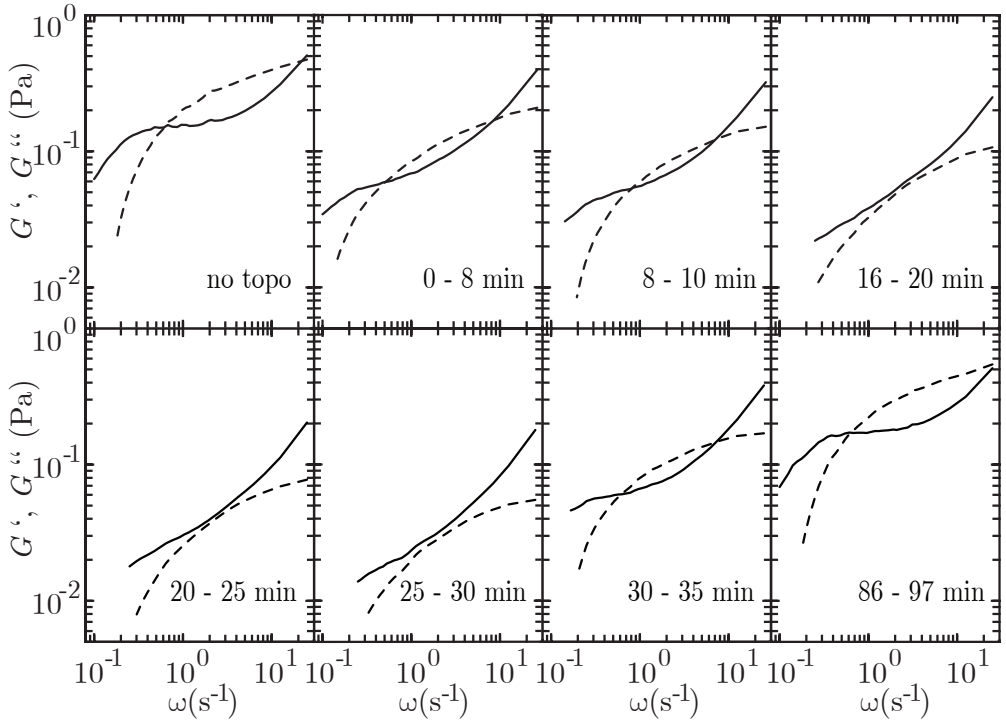

Figure 5.15: The evolution of elastic storage G' (dashed curves) and the viscous loss G'' (solid curves) moduli after the addition of the topoisomerase II (4 units/μg) to the entangled solution of 1 g/L of DNA with an ATP concentration of 2.5 mM.

dition of 4 units of topoisomerase II per μg of DNA (8 dimers per molecule) in the absence of ATP as well as in the presence of various concentrations of ATP are displayed in Figure 5.16. The initial number of entanglements per molecule is about 6. In the absence of ATP there is clearly no activity of the enzyme and G/G_{R} remains constant. With an initial ATP concentration of 1.0 mM, G/G_{R} decreases, but only 3 out of 6 entanglements per

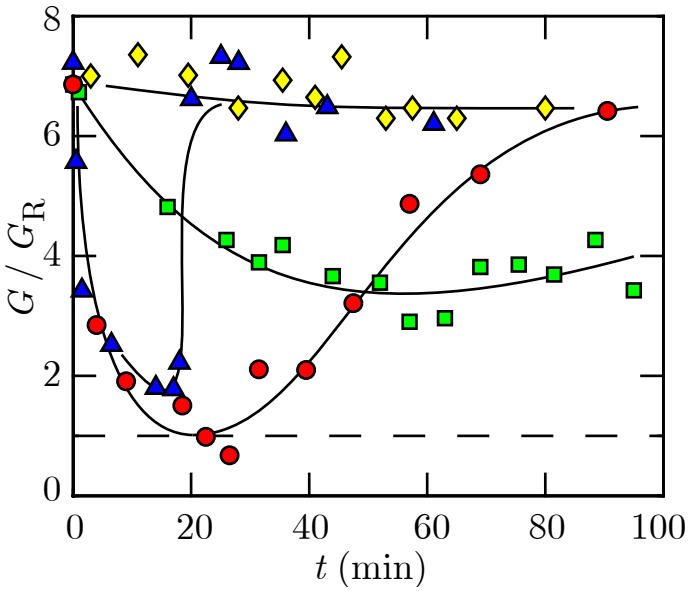

Figure 5.16: High frequency elasticity modulus divided by the Rouse modulus G/G_{R} versus time t after the addition of topoisomerase II (4 units/μg) to a solution of 1.0 g/L of DNA without ATP ($\diamond$) or with ATP concentrations of 1.0 ($\square$), 2.5 ($\bigcirc$), or 4.0 ($\triangle$) mM.

molecule are relaxed. If the initial ATP concentration is increased to 2.5 mM, G/G_{R} reduces to unity with full relaxation of entanglements within 20 minutes. However, for longer times G/G_{R} increases again and eventually approaches the original value as observed before the addition of topoisomerase II. With an ATP concentration of 4.0 mM, almost all entanglements are relaxed within a similar time span followed by a faster recovery of the original, entangled state.

Relaxation with different concentrations of topoisomerase II

In order to verify the effect of the concentration of topoisomerase II, experiments were also performed with different topoisomerase II concentrations of 1 and 2 units per μg of DNA (2 and 4 dimers per molecule, respectively). For this purpose, the DNA concentration was fixed at 1 g/L. In such a solution there are 6 entanglements per molecule. The ATP concentration is 2.5 mM. From the behavior of G/G_{R} shown in Figure 5.17, it follows that about 2 and 4 entanglements are relaxed with 1 and 2 units of topoisomerase II per μg of DNA, respectively.

After the addition of the enzyme, there are two dynamical processes which occur simultaneously. The first process is the reptation dynamics of the DNA molecules. The characteristic time scale is the molecular relaxation time τ. This means that a total number of entanglements per molecule N_{e} is renewed during the time τ (τ is also called the entanglement renewal time). The second process is the removal of entanglements by topoisomerase II, characterized by a disentanglement time τ_{d}. The disentanglement time τ_{d} includes the time for a protein dimer to find an entanglement, to bind ATP, to perform the actual double strand passage reaction, and to disengage from the DNA molecule. Let there be N_{p} dimers per molecule. Within time τ, the total number of disentanglements N_{d} executed by the enzyme

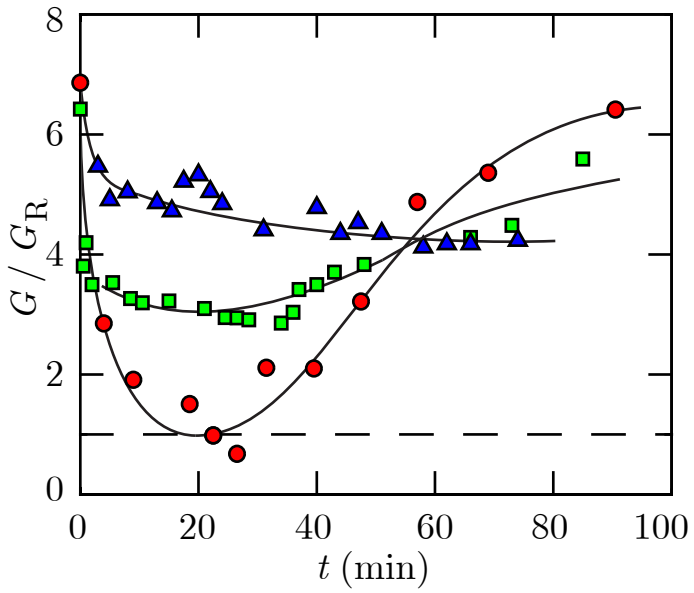

Figure 5.17: High frequency elasticity modulus divided by the Rouse modulus $G/G_{\rm R}$ versus time t after the addition of 1 (△), 2 (□), or 4 (◯) units of topoisomerase II per μg of DNA to a solution of 1.0 g/L of DNA and 2.5 mM ATP. For both panels, the solid curves are guides to the eyes and the dashed lines demarcate $G/G_{\rm R} = 1$ (the non-entangled state).

is then given by $N_{\rm d} = N_{\rm p}\,\tau/\tau_{\rm d}$. Note that $N_{\rm d}$ changes over the duration of our experiment, because, among other issues, ATP is consumed. We can discern 3 cases:

(*i*) $N_{\rm d}/N_{\rm e} \geq 1$, all ($N_{\rm e}$) entanglements are relaxed. The enzyme removes an entanglement at the moment it appears by reptation.

(*ii*) $0.1 < N_{\rm d}/N_{\rm e} < 1$, the number of entanglements which are removed by the enzyme is on the order of the number of entanglements which appear by reptation. A partial relaxation of entanglements is observed.

(*iii*) $N_{\rm d}/N_{\rm e} < 0.1$, few or no entanglements are removed by the enzyme.

For full conversion of the solution from an elastic physical gel to a viscous fluid, all entanglements need to be relaxed within time τ (case i).

For a DNA solution of 1 g /L, $\tau \approx 1$ s and $N_e \approx 6$. Two key observations are made. First, with an initial concentration of 1 mM ATP and 8 protein dimers per molecule ($N_p \approx 8$), it is observed that 3 out of 6 entanglements are relaxed ($N_d \approx 3$), so that $\tau_d \approx 3$ s. The disentanglement by the enzyme is too slow to relax all entanglements within time τ. Second, with an initial concentration of 2.5 mM ATP, all entanglements are relaxed with 8 dimers per molecule. However partial relaxation of entanglements is observed in the cases of 2 and 4 dimers per molecule. For these subcritical topoisomerase concentrations, the number of disentanglements is approximately the same as the number of dimers per molecule, *i.e.* $N_d \approx N_p$. These results indicate that $\tau_d \approx \tau$, so that $\tau_d \approx 1$ s. In this situation, a single dimer relaxes around 1 entanglement within the molecular relaxation time τ of 1 s. The disentanglement time is clearly dependent on the concentration of ATP, which shows that binding of ATP is the rate limiting step in the present experimental conditions. The value of $\tau_d \approx 1$ s is in the range of previously reported values for the double strand passage time $0.1 - 1$ s in the context of supercoiling [25].

For longer times, the initial entangled state is recovered. It is our contention that this recovery is due to consumption and eventually run out of ATP. An interesting question is whether there is enough ATP to sustain

the reaction for the duration of the experiment (100 min). As an example, consider the situation with an initial concentration of 1 mM ATP and 8 dimers per DNA molecule. Here, only partial relaxation of entanglements, is observed. The number of disentanglements $N_{\mathrm{d}} \approx 3$ and each disentanglement requires the hydrolysis of 2 ATP molecules. Accordingly, per DNA molecule 6 ATP molecules are consumed during the molecular relaxation time τ of 1 s. For a concentration of 1 g/L of DNA, the reaction can proceed for 90 minutes. This duration is in reasonable agreement with the observation. It should be noted however that N_{d} is not constant, its value is less for shorter reaction times. Furthermore, the efficiency of the enzyme is not 100%; there can be closures of the protein dimer without transport event. The estimation of the maximal duration is hence an approximation. For higher concentrations of ATP, the reaction can run for similar durations. However a faster recovery of the initial entangled state is observed with increasing concentration of ATP. This observation can be rationalized in terms of the efficiency of ATP consumption. For the removal of supercoils by yeast topoisomerase II, it has been reported that the passage reaction becomes more efficient at low concentration of ATP [47, 88]. At high concentration of ATP, passage is fast due to rapid binding of ATP. However, more ATP is wasted by closures without capture and transport of a second DNA segment. The higher passage rate in conjunction with a less ATP efficient transport mechanism result in rapid relaxation of entanglements,

but also quicker run out of ATP.

In the present range of DNA concentrations, all entanglements can be relaxed with 4 units (80 ng) of topoisomerase II per μg of DNA (8 dimers per molecule) and a sufficiently high concentration of ATP. The values of the transport properties $\Delta\eta$, G, and τ pertaining to the fully relaxed state as a function of the concentration of DNA have been derived. The results are also displayed in Figure 5.10, 5.11 and 5.12. The low shear viscosity increments $\Delta\eta$ are significantly reduced with respect to the values in the absence of topoisomerase II. Furthermore, they follow the scaling law $\Delta\eta \propto c^{1.31}$ for a salted polyelectrolyte in the non-entangled regime [16, 18]. The ratio G/G_{R} remains close to unity, because the entanglements are fully relaxed and the molecules move as single units. Any significant changes in the molecular relaxation time τ is not observed, but they follow the relatively weak concentration dependence for Rouse dynamics $\tau \propto c^{0.31}$. In the present range of DNA concentrations, the main effect of topoisomerase II on the viscoelasticity is hence through a reduction in G rather than τ. In order to observe significant effects on τ, the experiments need to be extended to higher concentrations of DNA and/or DNAs of larger molecular weight. The concentration scaling of the transport properties is in agreement with Rouse dynamics in the condition of full relaxation of entanglements by topoisomerase II.

5.2.3 Conclusions

In consequence of the double strand passage facilitated by topoisomerase II, semi-dilute entangled solutions of DNA are transformed from elastic physical gels to viscous fluids. This transformation has been inferred from a change in the relative frequency dependencies of the viscoelastic moduli as well as the concentration scaling of the derived transport properties. The main effect of topoisomerase II on the viscoelasticity is through the reduction in high frequency plateau value of the elastic storage modulus rather than a change in global, longest relaxation time of the DNA molecules. In the case of semidilute non-entangled solutions, there is no significant effect on the viscoelastic response. An important feature is that the change in flow properties requires the dissipation of energy through the hydrolysis of ATP. For full relaxation of the entanglements, the initial concentration of ATP has to be sufficiently high. This shows that binding of ATP to the enzyme is the rate limiting step. At a too high concentration of ATP, the transport mechanism becomes less efficient in terms of consumption of ATP due to closures of the protein dimer without capture and transport of a second segment. Furthermore, for full conversion to a viscous fluid, we observed that the number of dimers has to be the same or exceed the number of entanglements per molecule. This implies that each entanglement is relaxed by a single dimer with a disentanglement time of around 1 s and within the 1 s

time scale for renewal of the entanglements by reptation. The temperature of the assays needs to be maintained at 310 K; at ambient temperature no disentanglement by the enzyme has been observed.

5.3 Effect of the topoisomerase II targeting inhibitor on the viscoelastic properties of DNA

Another aspect of study is the effect of topoisomerase II inhibitors. DNA Topoisomerase II are targets of many anti cancer drugs because they impede the division of cancerous cells. This can be due to the blocking of the double strand passage reaction and/or the formation of cross-linking protein clamps between different DNA segments. Different inhibitor acts at different stages of the catalytic cycle, stabilizing either the covalently bonded or non-covalently bonded DNA-topoisomerase complex. However, the mechanism of action of enzymes on the topoisomerase II is still not clearly understood and is a widely researched topic.

Adenylyl-imidodiphosphate (AMP-PNP), a $\beta,\gamma-$imido analog of ATP, is a generic topoisomerase inhibitor. The activity of AMP-PNP on the relaxation of the entanglements is investigated. It binds to topoisomerase II in the same fashion as ATP, but it cannot be hydrolyzed. Triggered by the binding of AMP-PNP, the protein dimer closes, cannot be re-opened, and is converted to an annular form. The cross-sectional diameter of the hole of the closed dimer is sufficiently large for a DNA molecule to thread through [75, 7, 28].

Since the double strand passage activity is suppressed, we expect that entanglements are no longer relaxed. Furthermore, a cross-linking protein

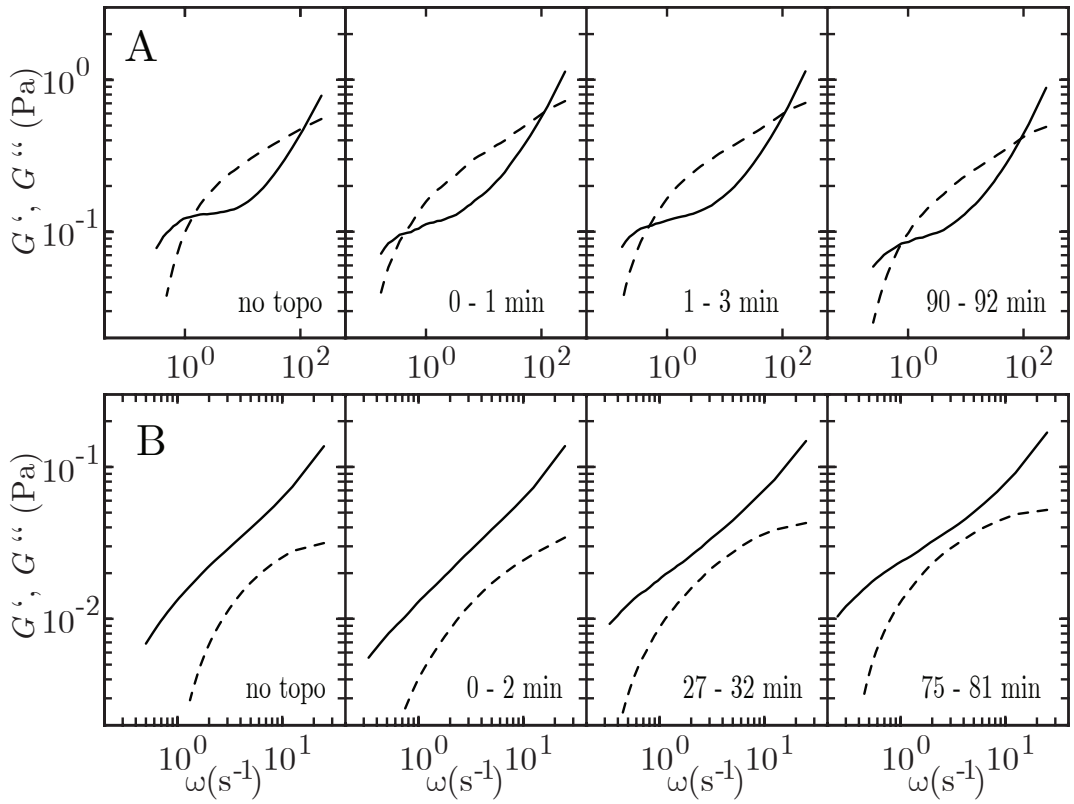

Figure 5.18: (A) Time evolution of the elastic storage G' (dashed curves) and viscous loss G'' (solid curves) moduli after the addition of topoisomerase II (4 units/μg) to a solution of 1.0 g/L of DNA with an AMP-PNP concentration of 2.5 mM.(B) As in panel A, but for a non-entangled solution of 0.4 g/L of DNA.

clamp between two DNA segments is formed, if a second segment has been captured before closure. Both the inhibition of the double strand passage reaction and the formation of cross-linking clamps are expected to affect the viscoelasticity.

5.3.1 Inhibition of topoisomerase II with AMP-PNP

In the inhibition experiments, 4 units of topoisomerase II per μg of DNA (about 8 dimers per DNA molecule) were added to solutions of various DNA, ATP, and AMP-PNP concentrations. All assays were kept at 310 K. The non-entangled and entangled solutions of 0.4 and 1.0 g/L of DNA, respectively, was first investigated with an initial AMP-PNP concentration of 2.5 mM. These samples do not contain ATP. Note that the experimental conditions are the same as those in the previous section, besides the 100% replacement of ATP by AMP-PNP. The time evolutions of G' and G'' after the addition of the enzyme are displayed in Figure 5.18. There is no qualitative change in the behavior of G' and G''. In particular, we do not observe a transition to an elastic gel with fixed cross-links as characterized by parallel frequency scaling of G' and G'' and $G' > G''$ for all frequencies [45]. The initially non-entangled DNA solution of 0.4 g/L remains a viscous fluid with $G' < G''$. In the case of the entangled solution of 1.0 g/L of DNA, fluid-like behavior is observed at low frequencies and corresponding long times.

The effects of the inhibitor on the elasticity modulus are most conveniently probed by monitoring G. High frequency elasticity modulus divided by the Rouse modulus G/G_R versus time, t, after the addition of topoisomerase II is shown in Figure 5.19. In a solution of 0.4 g/L, G/G_R is almost

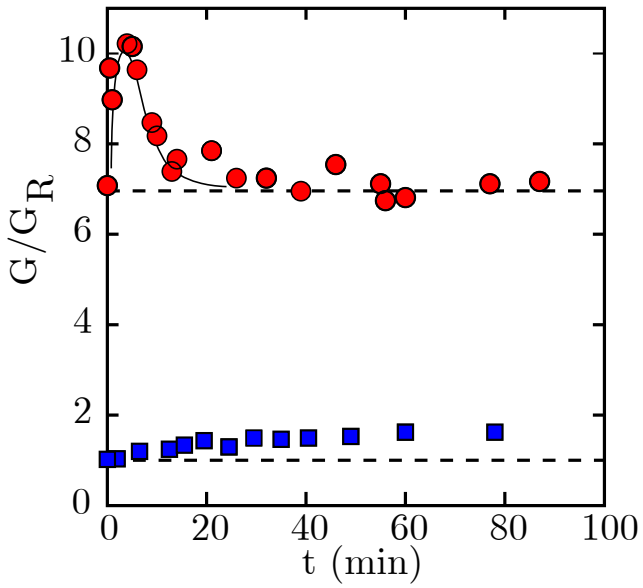

Figure 5.19: High frequency elasticity modulus divided by the Rouse modulus G/G_R versus time, t, after the addition of topoisomerase II (4 units/μg) to a solution of 1.0 g/L of DNA (o) and 0.4 g/L (□) in 2.5 mM AMP-PNP

a constant and remains close to unity. In the case of 1.0 g/L of DNA, G/G_R immediately increases from 7 to about 10 after the addition of topoisomerase II. The elasticity modulus relaxes back to the equilibrium value within a short time. To further investigate the effect of AMP-PNP, experiments where also done with different concentrations of ATP and AMP-PNP.

With a total replacement of ATP by AMP-PNP, the protein can close and form a clamp only once. In the case of 2.5 mM AMP-PNP, G/G_{R} is seen to increase followed by a decrease towards the original, entangled state. The initial increase implies that the number of constraints per molecule are

enhanced rather than reduced, albeit for a short time on the order of a few minutes after the addition of the enzyme. The temporary increase in G/G_{R} can be rationalized in terms of cross-linking protein clamps. The clamps act as dynamic constraints, similar to entanglements. However, the captured DNA segment can thread through the hole of the clamp, will eventually be released, and the probability for re-capturing of another DNA molecule by a closed clamp is small (but not impossible, see Ref. [75]). The constraints formed by the protein clamps are thus short-lived with a lifetime on the order of the DNA relaxation time and they are not (or inefficiently) renewed by reptation. As a result of clamp release by the threading motion of the linear DNA molecules, there is no transition to an elastic gel with fixed cross-links and the original, entangled state is recovered for longer times.

5.3.2 Inhibition of topoisomerase II with different ATP to AMP-PNP ratios

For a series of entangled solutions of 1.0 g/L of DNA, the initial concentration of AMP-PNP was increased from 0 to 2.5 mM with a fixed 2.5 mM *total* concentration of ATP and AMP-PNP. The results are displayed in Figure 5.20. In the presence of a mixture of ATP and AMP-PNP, G/G_{R} is seen to decrease immediately after the addition of the enzyme followed

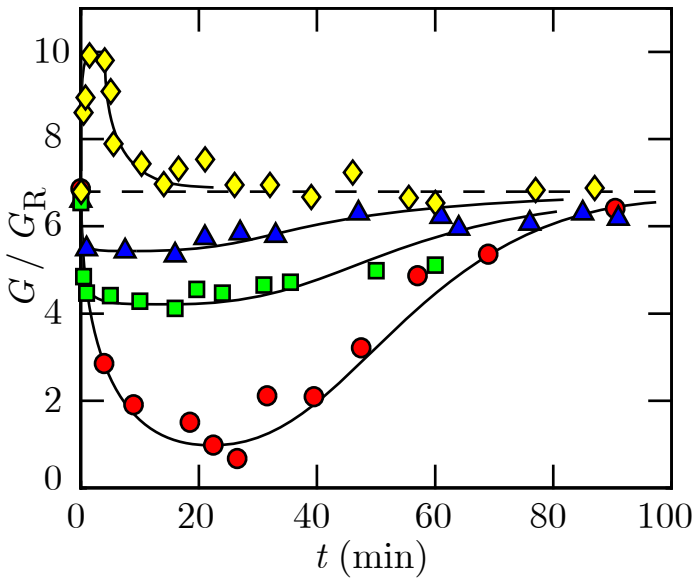

Figure 5.20: High frequency elasticity modulus divided by the Rouse modulus G/G_R versus time, t, after the addition of topoisomerase II (4 units/μg) to a solution of 1.0 g/L of DNA with ATP/AMP-PNP concentrations of 0/2.5 (◊), 1.25/1.25 (△), 2.3/0.2 (□), and 2.5/0 (o) mM. The dashed line demarcates the initial value of G/G_R.

by a slow recovery to the original, entangled state. With a small amount of inhibitor, some, but not all entanglements are relaxed. For instance, in the case of initial concentrations of 0.2 mM AMP-PNP and 2.3 mM ATP, G/G_{R} drops from around 7 to 4, which corresponds with the relaxation of 3 out of 6 entanglements in the previous experiments. With equal concentrations of ATP and AMP-PNP (1.25 mM each), only 2 out of 6 entanglements are relaxed. It should be noted that in the presence of ATP each dimer can catalyze a number of transport events before it is transformed to an annular form by binding of AMP-PNP. The double strand passage reaction gets

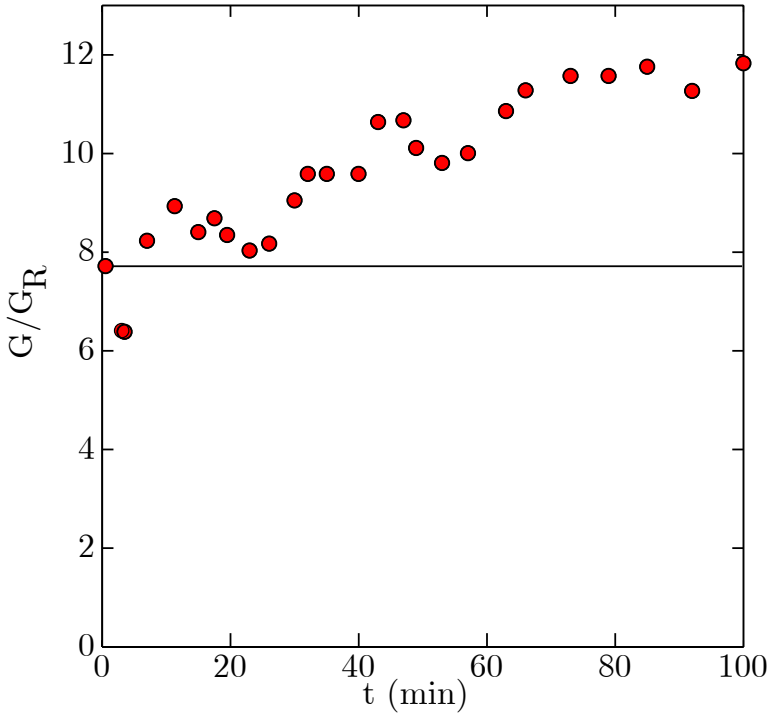

Figure 5.21: High frequency elasticity modulus divided by the Rouse modulus G/G_R versus time, t, after the addition of topoisomerase II (4 units/μg) to a solution of 1.0 g/L of DNA with 2.5 mM ATP and 1 mM ICRF-193. The line demarcates the initial value of G/G_R.

hence progressively blocked, so that increasingly fewer entanglements are relaxed.

5.3.3 Inhibition of topoisomerase II with ICRF- 193

In the experiments with ICRF-193, a DNA solution of 1 g/L was prepared with an ATP concentration of 2.5 mM and an ICRF-193 concentration of 1 mM. 4 units of topoisomerase II per micro gram of DNA were added to the solution and the experiment was performed at 310 K. The high frequency

elasticity modulus divided by the Rouse modulus, G/G_R, versus time, t, after the addition of topoisomerase II is shown in Figure 5.21.

The G/G_R value gradually increases from an initial value of 8 to about 12 after 70 minutes of the reaction time. It is evident from this observation that ICRF-193 inhibits the activity of topoisomerase II and results in an increase in number of constraints per molecule. ICRF-193 has been shown to bind to a closed clamp complex to inhibit ATP hydrolysis but still allows hydrolysis at a much lower rate [99, 100]. Studies have also shown that ICRF-193 acts as a topoisomerase II poison [101]. The actual mechanism of action of ICRF-193 remains unclear and further studies with different inhibitors are required to interpret the observed data.

5.3.4 Conclusions

In mixtures of AMP-PNP and ATP, the double strand passage reaction gets blocked and progressively fewer entanglements are relaxed. A significant fraction of cross-linking protein clamps is formed in the condition of a total replacement of ATP by AMP-PNP. The resulting constraints are however dynamic and short-lived, due to the threading motion of the linear DNA molecule through the hole of the clamp and the fact that they are not (or inefficiently) renewed by reptation. Accordingly, we do not observe a transition to an elastic gel with fixed cross-links. The non-entangled

solutions remain viscous fluids and for the entangled solutions fluid-like behavior is observed at low frequencies and corresponding longer times. For linear DNA, the main effect of the inhibitor is the blocking of the double strand passage reaction, so that entanglements are no longer relaxed. The formation of cross-linking clamps between DNA segments is of secondary importance. This situation might be different for closed circular DNA, because a captured circle cannot be released from the clamp by threading motion [29].

Chapter 6

Conclusions

Particle tracking microrheology is used to study the viscoelastic properties of phage $\lambda-$DNA through the entanglement transition. Particle tracking microrheology is found to be very useful and effective in studying the dynamics of DNA as it uses minute samples of no more than 15 μL and does not involve excessive shearing of the sample. The mean square displacement of the particle executing Brownian motion is obtained. The generalized Stokes-Einstein relation is used to derive the viscous loss modulus and the elastic storage modulus from the mean square displacements. With increasing frequency, the viscous loss modulus first increases, then levels off, and eventually increases again. Concurrently, the elastic storage modulus monotonously increases and eventually levels off to a constant high frequency plateau value. Once the DNA molecules become entangled at about ten times the overlap concentration, the elastic storage modulus becomes

larger than the viscous loss modulus in an intermediate frequency range. The number of entanglements per chain is obtained from the plateau value of the elasticity modulus. A range of concentrations from the non-entangled, semidilute to the moderately entangled regime with about seven entanglements per chain have been studied. The longest, global relaxation time pertaining to the motion of the DNA molecules is obtained from the low shear viscosity as well as from the lowest crossover frequency of the viscous loss and elastic storage moduli. In the entangled regime, both relaxation times agree and can be identified with the entanglement disengagement time or tube renewal time. The concentration dependencies of the low shear viscosity, the number of entanglements per chain, and the relaxation time agree with the relevant scaling laws for reptation dynamics of entangled polyelectrolytes with screened electrostatic interactions. The high frequency dispersion in the viscous loss modulus is relatively insensitive to the DNA concentration and is related to the Rouse dynamics of the DNA molecule inside the tube formed by the entanglements.

In consequence of the double strand passage facilitated by topoisomerase II, semi-dilute entangled solutions of DNA are transformed from elastic physical gels to viscous fluids. This transformation has been inferred from a change in the relative frequency dependencies of the viscoelastic moduli as well as the concentration scaling of the derived transport properties. The main effect of topoisomerase II on the viscoelasticity is through the reduc-

tion in high frequency plateau value of the elastic storage modulus rather than a change in global, longest relaxation time of the DNA molecules. In the case of semi-dilute non-entangled solutions, there is no significant effect on the viscoelastic response. An important feature is that the change in flow properties requires the dissipation of energy through the hydrolysis of ATP. For full relaxation of the entanglements, the initial concentration of ATP has to be sufficiently high. This shows that binding of ATP to the enzyme is the rate limiting step. At a too high concentration of ATP, the transport mechanism becomes less efficient in terms of consumption of ATP due to closures of the protein dimer without capture and transport of a second segment. Furthermore, for full conversion to a viscous fluid, we observed that the number of dimers has to be the same or exceed the number of entanglements per molecule. This implies that each entanglement is relaxed by a single dimer with a disentanglement time of around 1 s and within the 1 s time scale for renewal of the entanglements by reptation. The temperature of the assays needs to be maintained at 310 K; at ambient temperature no disentanglement by the enzyme has been observed.

A second aspect of this study is the effect of the generic topoisomerase II inhibitor AMP-PNP. In mixtures of AMP-PNP and ATP, the double strand passage reaction gets blocked and progressively fewer entanglements are relaxed. A significant fraction of cross-linking protein clamps is formed in the condition of a total replacement of ATP by AMP-PNP. The result-

ing constraints are however dynamic and short-lived, due to the threading motion of the linear DNA molecule through the hole of the clamp and the fact that they are not (or inefficiently) renewed by reptation. Accordingly, we do not observe a transition to an elastic gel with fixed cross-links. The non-entangled solutions remain viscous fluids and for the entangled solutions fluid-like behavior is observed at low frequencies and corresponding longer times. For linear DNA, the main effect of the inhibitor is the blocking of the double strand passage reaction, so that entanglements are no longer relaxed. The formation of cross-linking clamps between DNA segments is of secondary importance. This situation might be different for closed circular DNA, because a captured circle cannot be released from the clamp by threading motion [76].

Topoisomerases are mainly known for their ability to change the topological state of closed circular or looped DNA [8]. It is shown that topoisomerase II can also disentangle linear, non-supercoiled molecules with a concurrent change in the properties of the flow. A conclusive evidence that the disentanglement is powered by the hydrolysis of ATP and, conversely,that it is inhibited by binding of AMP-PNP is presented. This was made possible through microrheology. As in the case of simplification of the topology of closed circular DNA,topoisomerase II disentangles and does not tangle linear DNA. In order to explain disentangling, it has been proposed that the enzyme acts at a hooked juxtaposition of two DNA strands [29].

Human topoisomerase II α relaxes positively supercoiled plasmids faster than negatively supercoiled molecules [58]. This selectivity is likely due to differences in processivity associated with protein binding, as observed for bacterial topoisomerase IV [62, 19] . Chiral discrimination may also result in faster removal of entanglements, if there is a preferred crossing angle of less than 90^o. This could be investigated with topoisomerase that have no preference for positive supercoiling (e.g. human topoisomerase IIβ).

The enzyme may find the randomly distributed entanglements by diffusion, possibly directed along the contour of the DNA molecule. Alternatively, an entanglement may slide along the contour by reptation until it is captured by a sharp bend induced by a DNA bound topoisomerase [91]. Disentanglement is subsequently accomplished by the catalyzed double strand passage reaction. An important feature of the latter model is that unidirectional double strand passage follows from the specific orientation of the enzyme with respect to the bend. Furthermore, the sliding mechanism requires the preexistence of entanglements, which naturally explains the disentangling activity of the enzyme.

The results in this work are of interest from a polymer physics point of view, because we can realize the formerly hypothetical Rouse dynamics for initially entangled dense polymer chains. From a biological point of view, we have demonstrated that high concentrations are not necessarily problematic for transport of the genetic material, as long as the topological

constraints are efficiently relaxed by topoisomerase.

6.1 Scope for future research

6.1.1 Effect of topoisomerase II in closed circular and supercoiled DNA

Topoisomerase II catalyzes the passage of a double stranded DNA through another strand by introducing a transient break in one of the strands. Effective relaxation of entanglements in the case of linear DNA have been observed and discussed in this thesis. The formation of permanent crosslinks was however not observed with the replacement of ATP with AMP-PNP. The formation of permanent crosslinks can be investigated by using circular DNA.

6.1.2 Viscoelastic properties of the genome in cells

The concentration of DNA inside a living cell depends on the stages of its life. The concentration is high during mitosis. The segregation of daughter chromosomes during the anaphase stage happens after the entanglements are relaxed by the topoisomerase II. The failure of topoisomerase II to relax the entanglements leads to cell death. The anti-cancer drugs are found to inhibit the activity of topoisomerase II to prevent the cell from dividing

and causing cell death. The dynamics of the genome inside a cell during different stages of its life cycle can be probed by using the video particle tracking. Also the effect of different anti-cancer drugs on the viscoelasticity of DNA can be investigated.

6.1.3 Effect of topoisomerase II poisons

Topoisomerase poisons target topoisomerase II and stabilize the DNA - topoisomerase II complex at different stages of the catalytic cycle. In particular, the class of anti-cancer drugs called topoisomerase II poisons, act by stabilizing the noncovalent complex. This means that the DNA strands are broken and not sealed back. The viscoelastic properties are expected to change during such a situation. The dynamics of DNA treated with topoisomerase II poison can be studied both *in vitro* and *in vivo*.

These studies can be done by investigating the self diffusion of DNA with a fluorescence microscope. The conformation of tangled DNA and the relaxation of entanglements can also be investigated with Monte Carlo, Molecular and Brownian dynamics computer simulations.

Bibliography

[1] Alberts B, Johnson A, Lewis J, Raff M, Roberts K, Walter P. Molecular Biology of the Cell. (4th ed.). Garland (2002). [cited at p. 4]

[2] Clausen-Schaumann H, Rief M, Tolksdorf C, Gaub H . Mechanical stability of single DNA molecules. *Biophys. J.* 78 (4): 1997-2007 (2000). [cited at p. 2]

[3] M. Mandelkern, J. Elias, D. Eden, D. Crothers. The dimensions of DNA in solution. *J Mol Biol.* 152 (1): 153-161 (1981). [cited at p. 2]

[4] H. Lodish, A. Berk, P. Matsudaira, C.A. Kaiser , M. Krieger ,M. P. Scott , S. L. Zipurksy , J. Darnell. Molecular Cell Biology (5th ed.). WH Freeman: New York (2004). [cited at p. 4]

[5] Cooper GM . The cell: a molecular approach (2nd ed.). Washington, D.C: ASM Press (2000). [cited at p. 4]

[6] J. C. Watson,and F. H. C. Crick. Genetic implications of the structure of deoxyribonucleic acid. *Nature*. 171: 964-967 (1953). [cited at p. 5, 40]

[7] James C Wang. Moving one DNA helix through another by type II DNA topoisomerase: the story of a simple molecular machine. *Quarterly Review of Biophysics*. 31: 107-144 (1998). [cited at p. 5, 40, 46, 116]

[8] J. C. Wang. Untangling the Double Helix: DNA Entanglement and the Action of the DNA Topoisomerases, Cold Spring Harbor Laboratory Press, Woodbury, NY (2009). [cited at p. 6, 128]

[9] A. J Schoeffler, J. M Berger. Recent advances in understanding the structure- function relationships in the type II topoisomerase mechanism. *Biochemical society* 33: 1465-1470 (2005). [cited at p. 6, 45]

[10] Sikorav J-L, Jannink G. Kinetics of chromosome condensation in the presence of topoisomerases: A phantom chain model. *Biophys J* 66: 827-837 (1994). [cited at p. 6, 40, 48, 93]

[11] Duplantier, B., G. Jannink, and J.-L. Sikorav. Anaphase chromatid motion: Involvement of type II DNA topoisomerases. *Biophys. J.* 69:1596-1605 (1995). [cited at p. 6, 93]

[12] John L Nitiss. DNA topoisomerase II and its growing repertoire of biological function.*Cancer* 9: 327-337 (2009). [cited at p. 6, 60, 93]

[13] J.C. Wang. Interaction between DNA and an *Escherichia coli* protein. *J. molec. Biol.* 55: 523-533 (1971). [cited at p. 6, 43]

[14] L. F. Liu. DNA Topoisomerases and Their Applications in Pharmacology. Boca Raton: Academic Press (1994b). [cited at p. 7, 42]

[15] A. Kathleen McClendon, Neil Osheroff. DNA topoisomerase II, genotoxicity, and cancer, *Mutation Research* 623: 8397 (2007). [cited at p. 8]

[16] P.G. de Gennes. Scaling Concepts in Polymer Physics. Cornell University Press, Ithaca. NY. (1979). [cited at p. 16, 87, 97, 98, 99, 113]

[17] Doi and Edwards Scaling concepts in polymer physics. Cornell University Press, Ithaca, NY. (1979). [cited at p. 87, 89, 97, 99, 101]

[18] J.R. C. van der Maarel, Introduction to Biopolymer Physics. World Scientific, Singapore, (2008). [cited at p. 83, 87, 89, 97, 98, 99, 113]

[19] D.E. Adams, E.M. Shekhetman, E.L. Zechiedrich, M.B. Schmid, N.R. Cozzarelli. The role of topoisomerase IV in partitioning bacterial replicons and the structure of catenated intermediates in DNA replication. *Cell.* 71: 277-288 (1992). [cited at p. 129]

[20] Allan Y. Chen and Leroy F. Liu. DNA topoisomerases: Essential enzymes and lethal targets. *Annu. Rev. Pharmacol. Toxicol.* 34: 191-218 (1994) [cited at p. 42]

[21] Annette K Larsen, Alexander E Escargueil, Andrzej Skladanowski. Catalytic topoisomerase II inhibitors in cancer therapy. *Pharmacology and Therapeutics.* 99: 167-181 (2003) [cited at p. 51]

[22] Bajer, A., and J. Mole-Bajer. Spindle dynamics and chromosome movements. *Int. Rev. Cytol.* 3(Suppl.):1-271 (1972). [cited at p. 40]

[23] Bajer, A. Observations of dicentrics in living cells. *Chromosoma* 14:18-30 (1963). [cited at p. 40]

[24] R. Bandyopadhyay and A. K. Sood. Rheology of the semi dilute solution of the calf thymus DNA. *Pramana, Journal of Physics.* 58:685-694 (2007). [cited at p. 27]

[25] Baird, C. L., T. T. Harkins, S. K. Morris, and J. E. Lindsley. Topoisomerase II drives DNA transport by hydrolyzing one ATP. *Proc. Natl. Acad. Sci. U.S.A.* 96:13685-13690. (1999). [cited at p. 111]

[26] C. G. Baumann, S. B. Smith, V. A. Bloom field and C. Bustamante. Ionic effects on the elasticity of single DNA molecules. *Proc. Natl. Acad. Sci.* 94:6185 (1997). [cited at p. 17]

[27] Xiaoying Zhu, Binu Kundukad and Johan R. C van der Maarel. Viscoelasticity of entangled λ-phage DNA solutions. *Journal of chemical physics.* 129:185103 (2008). [cited at p. 95, 96, 101, 103]

[28] James M. Berger, Steven J Gamblin, Stephen C Harrison, James C Wang. Structure and Mechanism of DNA Topoisomerase II. *Nature.* 379:225-232 (1996). [cited at p. 45, 46, 116]

[29] Buck, G. R., and E. L. Zechiedrich. DNA disentangling by type-2 topoisomerases. *J. Mol. Biol.* 340:933-939 2004. [cited at p. 49, 124, 128]

[30] James J. Champoux. DNA Topoisomerases: Structure, Function and Mechanism. *Annu. Rev. Biochem.*70:369-413 (2001). [cited at p. 45, 46]

[31] Chen, D. T., E. R. Weeks, J. C. Crocker, M. F. Islam, R. Verma, J. Gruber, A. J. Levine, T. C. Lubensky, and A. G. Yodh. Rheological microscopy: Local mechanical properties from microrheology. *Phys. Rev. Lett.* 90:108301 (2003). [cited at p. 90, 96]

[32] Dulbecco, R. and Vogt, M. Evidence for a ring structure of polyoma virus DNA. *Proc. natn. Acad. Sci.* 50:730-739 (1963). [cited at p. 40]

[33] Weil, R. and Vinograd, J. The cyclic coil helix and cyclic forms of polyoma viral DNA. *Proc. natn. Acad. Sci.* 50, 730-739 (1963). [cited at p. 40]

[34] Kavenoff, R., Klotz, L. C. and Zimm, B.H. On the nature of chromosome-sized DNA molecules. *Cold Spring Harbor Symp. Quant. Biol.* 38:1-8 (1974). [cited at p. 40]

[35] Bivash R. Dasgupta. Estimation of viscoelastic moduli of complex fluids using the generalized Stokes-Einstein's equation. *Rheol Acta.* 39:371-378 (2000). [cited at p. 24]

[36] S.L. Davies, J. Bergh, A.L. Harris, I.D. Hickson. Response to ICRF-159 in cell lines resistant to cleavable complex forming topoisomerase II inhibitors. *Br. J. Cancer.* 75, 816-821 (1997). [cited at p. 53]

[37] Dong KC, Berger JM. Structural basis for gate-DNA recognition and bending by type IIA topoisomerases. *Nature* 450:12011205 (2007). [cited at p. 49]

[38] Albert Einstein and R Furth. Albert Einstein Investigation on the theory of Brownian motion.Dover, New York, (1956). [cited at p. 28]

[39] C.l. Fattman, W.P. Allan, B.B. Hashino, J.C. Yalowich. Collateral sensitivity to the bisdioxopiperazine dexrazoxane (ICRF-187) in etoposide (VP-16)-resistant human leukemia K562 cells. *Biochem. Pharmacol.* 52: 635-642 (1996). [cited at p. 53]

[40] Y. Heo and R. G. Larson. The scaling of zero shear viscosities of semidilute polymer solutions with concentration. *Journal of Rheology* 49: 1117-1128 (2005). [cited at p. 26]

[41] Hopfield JJ. Kinetic proofreading: a new mechanism for reducing errors in biosynthetic processes requiring high specificity. Proc. Natl. Acad. Sci. USA 71: 41354139 (1974). [cited at p. 49]

[42] T. Hu, H. Sage and T. S. Hsieh. ATPase domain of eukaryotic DNAtopoisomerase II Inhibition of ATPase activity by the anti-cancer

drugbisdioxopiperazine and ATP/ADP-induced dimerization. *J Biol Chem.* 277: 59445951 (2002). [cited at p. 53]

[43] Gerard Jannink, Bertrand Duplantier, and Jean-Louis Sikorav. Forces on chromosomal DNA during Anaphase *Biophys. J.* 71: 451-465 (1996). [cited at p. 40]

[44] D. Jary, J. L. Sikorav and D. Lairiez. Nonlinear viscoelasticity of entangled dna solutions *Europhysics Letters* 46: 251 (1999). [cited at p. 27, 84, 85, 86]

[45] Larson, R. G. The Structure and Rheology of Complex Fluids. Oxford Univ Press, Oxford (1998). [cited at p. 53, 118]

[46] A. J. Levine and T. C. Lubensky. Twopoint microrheology and the electrostatic analogy. *Phys. Rev. E* 65, 011501 (2001). [cited at p. 90]

[47] J. E. Lindsley , and J. C. Wang. On the coupling between ATP usage and DNA transport by yeast DNA topoisomerase II. *J. Biol. Chem.* 268: 8096-8104 (1993). [cited at p. 48, 112]

[48] L. F. Liu , T. C. Rowe, L. Yang, K.M. Tewey and G.L. Chen. Cleavage of DNA by mammalian DNA topoisomerase II. *J. biol. Chem.* 258, 15365-15370 (1983). [cited at p. 46]

[49] L. F. Liu. DNA topoisomerase poisons as antitumor drugs. *Annu. Rev. Biochem.* 58: 351-75 (1989). [cited at p. 51]

[50] L. F. Liu, C. C. Liu, B. M. Alberts. T4 DNA topoisomerase. A new ATP dependent enzyme essential for the initiation of T4 bacteriophage DNA replication. *Nature* 281: 456-61 (1979). [cited at p. 42]

[51] T. G. Mason and D. A. Weitz. Optical Measurements of frequency-dependent linear viscoelastic moduli of complex fluids. *Physical Review Letters* 74: 1250-53 (1995). [cited at p. 24, 31]

[52] T. G. Mason, Hu Gang and D. A. Weitz. Diffusing-wave-spectroscopy measurements of viscoelasticity of complex fluids. *Journal of optical society of America* 14: 139-149 (1997). [cited at p. 24]

[53] Mason, T. G., A. Dhople, and D. Wirtz. Concentrated DNA rheology and microrheology. *Mat. Res. Soc. Symp. Proc.* 463: 153-158 (1997). [cited at p. 23, 24]

[54] T. G. Mason, K. Ganesan, J. H. van Zanten, D. Wirtz, and S. C. Kuo, Particle Tracking Microrheology of Complex Fluids. *Physical Review Letters* 79: 3282-3285 (1997). [cited at p. 22]

[55] T. G. Mason, A. Dhople and D. Wirtz. Linear viscoelastic moduli of concentrated DNA solutions. *Macromolecules*. 31: 3600-3603 (1998). [cited at p. 27, 85, 96]

[56] T. G. Mason, Estimation of viscoelastic moduli of complex fluids using the generalized Stokes-Einsteins equation. *Rheol. Acta.* 39: 371-378 (2000). [cited at p. 96]

[57] D. Mazia. Mitosis and the physiology of cell division. *In The Cell.* (ed.J. Brachet and A. E. Mirsky, editors. Academic Press, New York. 1961). [cited at p. 40]

[58] A. K. McClendon, A. C. Rodriguez, and N. Osheroff. . Human topoisomerase IIα rapidly relaxes positively supercoiled DNA. Implications for enzyme action ahead of replication forks. *J. Biol. Chem.* 280: 39337-39345 (2005). [cited at p. 129]

[59] F.C. MacKintosha, C.F. Schmidt. Microrheology. *Current Opinion in Colloid and Interface Science* 4: 300-307 (1999). [cited at p. 22]

[60] A. Morrison and N. R. Cozzarelli. Site-specific cleavage of DNA by E. coli DNA gyrase. *Cell* 17: 175-184 (1979). [cited at p. 46]

[61] R. Musti, J. L. Sikorav, D. Lairiez, G. Jannink, and M. Adam. Viscoelastic properties of entangled DNA solution. *C. R. Acad. Sci., SerIIb:Mec.Phys. Chim. Astron* 320: 599-605 (1995). [cited at p. 26, 83, 85, 87, 89, 98]

[62] K. C. Neuman, G. Charvin, D. Bensimon, and V. Croquette. Mechanisms of chiral discrimination by topoisomerase IV. *Proc. Natl. Acad. Sci.*106: 6986-6991 (2009). [cited at p. 129]

[63] J. Ninio. Kinetic amplification of enzyme discrimination. *Biochimie* 57: 587595 (1975). [cited at p. 49]

[64] Kerson Huang. Introduction to statistical physics. Taylor and Francis Group USA second edition (2010). [cited at p. 29]

[65] A. Kathleen McClendona, Neil Osheroff. DNA topoisomerase II, genotoxicity and cancer. *Mutation Research* 623: 8397 (2007). [cited at p. 47]

[66] John M. Fortune and Neil Osheroff. Topoisomerase II as a Target for Anticancer Drugs: When Enzymes Stop Being Nice. *Progress in Nucleic Acid Research and Molecular Biology* 64: 221-253 (2000). [cited at p. 48, 51]

[67] Neil Osheroff. Role of the Divalent Cation in Topoisomerase I1 Mediated Reactions. *Biochemistry* 26: 6402-6406 (1987). [cited at p. 48]

[68] N. Osheroff, E.L. Zechiedrich. Calcium-promoted DNA cleavage by eukaryotic topoisomerase II: trapping the covalent enzymeDNA complex in an active form. *Biochemistry.* 26: 43034309 (1987). [cited at p. 48]

[69] N. Osheroff. Eukaryotic topoisomerase II. Characterization of enzyme turnover. *J. Biol. Chem.* 261: 99449950 (1986). [cited at p. 48]

[70] Michelle Saburin, Neil Osheroff. Sensitivity of human type II topoisomerases to DNA damage: stimulation of enzyme mediated DNA cleavage by a basic, oxidized and alkylated lesions. *Nucleic Acids Research* 28: No.9 1947-1954 (2000) [cited at p. 61]

[71] J. E. Deweese, Alex B. Burgin, Neil Osheroff. Human topoisomerase II α uses a two metal ion mechanism for DNA cleavage. *Nucleic acid research* 36: 4883-4893 (2008). [cited at p. 60]

[72] $http://nobelprize.org/nobel_prizes/physics/laureates/1926/perrin-lecture.html$ [cited at p. 28]

[73] D. Perrin, B. van Hille and B. T. Hill. Differential sensitivities of recombinant human topoisomerase IIa and b to various classes of topoisomeraseII-interacting agents. *Biochem Pharmacol* 56: 503 507 (1998). [cited at p. 53]

[74] Federick Reif. Fundamentals of Statistical and Thermal Physics. (McGraw Hill International)(1985). [cited at p. 29]

[75] J. Roca and J. C. Wang. The capture of a DNA double helix by an ATP-dependent protein clamp: A key step in DNA transport by type II DNA topoisomerases. *Cell* 71: 833-840 (1992). [cited at p. 52, 116, 120]

[76] J.Roca and J. C.Wang. DNA transport by a type II DNA topoisomerase: Evidence in favor of a two-gate mechanism. *Cell* 77: 609-616 (1994). [cited at p. 53, 128]

[77] J. Roca, J. M. Berger and J. C. Wang. On the simultaneous binding of Eukaryotic DNA topoisomerase II to a pair of Double stranded DNA helices. *Journal of Biological chemistry*, 268: 14250-14255 (1993). [cited at p. 52]

[78] V. V. Rybenkov ,C. Ullsperger ,A. V. Vologodskii , N. R. Cozzarelli. Simplification of DNA topology below equilibrium values by type II topoisomerases. *Science* 277: 690693 (1997). [cited at p. 48]

[79] M. Sander and T. Hsieh. Double strand DNA cleavage by type II DNA topoisomerase from Drosophila melanogaster. *J. biol. Chem.* 258: 8421-8428 (1983). [cited at p. 46]

[80] Patrick Schultz, Stephane Olland, Pierre Oudet and Ronald Hancock. Structure and Conformational change of DNA topoisomerase II visualized by elctron microscopy. *Proc. Natl. Acad. Sci* 93: 5936-5940 (1996). [cited at p. 60]

[81] Sikorav J-L, Jannink G. Dynamics of entangled DNA molecules in the presence of topoisomerases. *C R Acad Sci Paris, Series IIb* 316: 751-757 (1993). [cited at p. 93]

[82] D. E. Smith, T.T Perkins and S. Chu. Self-Diffusion of an entangled DNA molecule by reptation. *Physical review letter* 75: 4146 (1995). [cited at p. 26, 85, 101]

[83] E.S.Sobel and J.A Harpst. Effect of Na^+ ions on the persistence length and the excluded volume of T7 bacteriophage DNA. *Biopolymers* 31: 1559 (1991). [cited at p. 17]

[84] $http://www.physik.uni-augsburg.de/theo1/hanggi/History/Sutherland-1902.pdf$ [cited at p. 29]

[85] $http://www.physik.uni-augsburg.de/theo1/hanggi/History/Phil_Mag.pdf$ [cited at p. 29]

[86] Tadashi Uemura, Hiroyuki Ohkura, Yasuhisa Adachi, Katuhiko Morino, Kazuhiro Shiozaki, and Mitsuhiro Yanagida. DNA Topoisomerase II Is Required for Condensation and Separation of Mitotic Chromosomes in S. pombe.*Cell*, 54: 917-925 (1987). [cited at p. 4]

[87] R. E. Teixaira, A. K. Dambal, D. H. Richer, E.S.G.Shaqfeh and S. Chu. The individualistic dynamics of entangled DNA in solution. *Macromolecules* 40: 2461-2476 (2007) [cited at p. 87]

[88] Timothy R. Hammonds, Antony Maxwell. The DNA dependence of the ATPase activity of human DNA topoisomerase IIα. *Journal of biological chemistry* 272: 32696-32703 (1997). [cited at p. 112]

[89] Toshiwo Andoh, Ryoji Ishida. Catalytic inhibitor of DNA topoisomerase II. *Biochimica et Biophysica Acta*. 1400: 155-171 (1998). [cited at p. 51]

[90] R. Verma, J. C. Crocker, T. C. Lubensky and A. G. Yodh. Entropic colloidal interactions in concentrated DNA solutions. *Phys. Rev. Lett.* 81: 4004-4007 (1998). [cited at p. 90, 96]

[91] A. V. Vologodskii, W. Zhang, V. V. Rybenkov, A. A. Podtelezhnikov, D. Subramanian, J. D. Griffith, and N. R. Cozzarelli.. Mechanism of topology simplificationby type II DNA topoisomerases. *Proc. Natl. Acad. Sci.* 98: 3045-3049 (2001). [cited at p. 49, 129]

[92] J.C. Wang and L.F. Liu. DNA topoisomerases: enzymes that catalyze the concerted breaking and rejoining of DNA backbone bonds. In Molecular Genetics, New York: Academic Press (1979). [cited at p. 41]

[93] James C. Wang. DNA Topoisomerases. *Annu. Rev. Biochem.* 65: 635-692(1996). [cited at p. 42, 43]

[94] Paul M. Watt and D. Hickson. Structure and function of type II DNA topoisomerases. *Biochemical Journal*. 303: 681-695 (1994). [cited at p. 52]

[95] T A Waigh. Microrheology of complex fluids. *Rep. Prog. Phys.* 68: 685742, (2005). [cited at p. 22]

[96] Yanagida, M. and Sternglanz, R. Genetics of DNA topoisomerases. In DNA Topology and its Biological Effects. Cold Spring Harbor Laboratory Press (1990). [cited at p. 40]

[97] Yan J, Magnasco MO, Marko JF. A kinetic proofreading mechanism for disentanglement of DNA by topoisomerases. *Nature* 401: 932-935 (1999). [cited at p. 49]

[98] Zhirong Liu, Richard W.Deibler, Hue Sun Chan and Lynn Zechiedrich. The why and how of DNA unlinking. *Nucleic acids Research*37: 661-671 (2009). [cited at p. 49, 50]

[99] Morris S. K., Baird C. L., and Lindsley J. E. Steady-state and Rapid Kinetic Analysis of Topoisomerase II Trapped as the Closed-Clamp Intermediate by ICRF-193. *J. Biol. Chem.* 275:2613-2618 (2000). [cited at p. 123]

[100] Tao Hu, Harvey Sage and Tao-shih Hsieh. ATPase Domain of Eukaryotic DNA Topoisomerase II Inhibition of ATPase activity by the anti-cancer drug bisdioxopiperazine and ATP/ ADP- induced dimerization. *The Journal of Biological Chemistry* 277: 5944-5951 (2002). [cited at p. 123]

[101] Huang KC, Gao H, Yamasaki EF, Grabowski DR, Liu S, Shen LL, Chan KK, Ganapathi R, Snapka RM. Topoisomerase II poisoning by

ICRF-193. *Journal of Biological Chemistry* 276(48):44488-94. (2001).

[cited at p. 123]

[102] *http : //www.labconco.com/productlit/appnotes/concentration.asp*

[cited at p. 64]

[103] *http : //www.harvardapparatus.com* [cited at p. 64]

[104] *http : //www.sigmaaldrich.com/catalog* [cited at p. 61]

[105] *http : //users.physik.fu−berlin.de/ kleinert/files/eins$_b$rownian.pdf*

[cited at p. 29]

[106] *http : //www.nshtvn.org/ebook/molbio/Current%20Protocols/CPMB/mba03d.pdf*

[cited at p. 67]

[107] *http : //library.thinkquest.org/20465/DNArep.html* [cited at p. 4]

Appendices

Appendix A

Appendix

A.1 Mean square displacement as an integral over the velocity correlation function

Let us consider the velocity correlation function, $\langle v(t')v(t'')\rangle$.

The velocity correlation function is stationary, so we can write, $\langle v(t')\, v(t'')\rangle = \langle v(t'-t'')v(0)\rangle$. It is also symmetric, so we can write,

$$\langle v(t')\, v(t'')\rangle = \langle v(t''-t')v(0)\rangle$$

So the velocity correlation function can be written as a function of t' and t''

$$\langle v(t')\, v(t'')\rangle = f(t'-t'') = f(t''-t') \tag{A.1}$$

Therefore equation 2.43 can be written as,

$$\langle \Delta x^2(t) \rangle = \int_{t'=0}^{t} dt' \int_{t''=0}^{t} dt'' f(t'' - t') \tag{A.2}$$

Substituting, τ for $t'' - t'$,

$$\langle \Delta x^2(t) \rangle = \int_{t'=0}^{t} dt' \int_{\tau=-t'}^{t-t'} d\tau f(\tau) \tag{A.3}$$

By partial integration, we can write the above equation as the sum of two quantities,

$$\langle \Delta x^2(t) \rangle = t' \int_{\tau=-t'}^{t-t'} d\tau f(\tau) \Big|_{t'=0}^{t} - \int_{t'=0}^{t} dt' \quad t' \frac{d}{dt'} \left[\int_{\tau=-t'}^{t-t'} d\tau f(\tau) \right] \tag{A.4}$$

The first term in equation A.4 can be written as

$$t' \int_{\tau=-t'}^{t-t'} d\tau f(\tau) \Big|_{t'=0}^{t} = t \int_{0}^{t} d\tau f(\tau) \tag{A.5}$$

By substituting $t' = -x$ and $dt' = -dx$, the second term in equation A.4 can be written as

$$\begin{aligned} -\int_{t'=0}^{t} dt' \quad t' \frac{d}{dt'} \left[\int_{\tau=-t'}^{t-t'} d\tau f(\tau) \right] &= \int_{x=0}^{-t} dx \quad x \frac{d}{dx} \left[\int_{\tau=x}^{t+x} d\tau f(\tau) \right] \\ &= \int_{x=0}^{-t} x \left[f(t+x) - f(x) \right] dx \\ &= \int_{x=0}^{-t} dx \quad x f(t+x) - \int_{x=0}^{-t} x f(x) dx \end{aligned} \tag{A.6}$$

Substituting $(t + x) = \tau$, $dx = d\tau$, in the first term and $x = -\tau$ and $dx = -d\tau$ in the second term of the above equation, we get,

$$-\int_{t'=0}^{t} dt' t' \frac{d}{dt'} \left[\int_{\tau=-t'}^{t-t'} d\tau f(\tau) \right] = -2 \int_{0}^{t} \tau f(\tau) d\tau + 2t \int_{0}^{t} d\tau f(\tau) \tag{A.7}$$

Substituting A.7 and A.5 in equation A.4, we get,

$$\begin{aligned}\langle \Delta x^2(t) \rangle &= 2t \int_0^t d\tau f(\tau) - 2 \int_0^t d\tau \quad \tau f(\tau) \\ &= 2t \int_0^t d\tau \left[1 - \frac{\tau}{t}\right] f(\tau) \end{aligned} \tag{A.8}$$

where, $f(\tau) = f(t'' - t') = \langle v(\tau) v(0) \rangle$

Therefore, we can write,

$$\langle \Delta x^2 \rangle = 2t \int_0^t d\tau \left[1 - \frac{\tau}{t}\right] \langle v(\tau) v(0) \rangle \tag{A.9}$$

For long times, $t \gg \tau$, the mean square displacement is expressed as an integral over the velocity correlation function.

A.2 Relation between the one sided Fourier transform of the mean square displacement and the velocity correlation function

Let us define $G(\tau) = \langle v(\tau)v(0)\rangle$, such that

$$f(t) = 2t \int_0^t d\tau \, (1 - \tau/t) \, G(\tau) \tag{A.10}$$

The one sided Fourier transform of mean square displacement is expressed as,

$$\int_0^\infty e^{-i\omega t} \langle \Delta x^2(t)\rangle dt = \langle \Delta \tilde{x}^2(\omega)\rangle \tag{A.11}$$

Replacing $\langle \Delta x^2(t)\rangle$ with $f(t)$, we get,

$$\langle \Delta \tilde{x}^2(\omega)\rangle = \int_0^\infty e^{-i\omega t} f(t) dt \tag{A.12}$$

$$= \frac{1}{-i\omega} \int_0^\infty f(t) \, d(e^{-i\omega t}) \tag{A.13}$$

Calculations are done with a frequency $\omega - i0^+$, *i*.e., ω has a small negative imaginary part, to insure convergence to 0 of boundary terms such as $e^{-i\omega t}$, when integrating by parts at t$\rightarrow +\infty$. Partial integration of the above equation gives,

$$\langle \Delta \tilde{x}^2(\omega)\rangle = \frac{1}{i\omega} \int_{t=0}^\infty e^{-i\omega t} \frac{\partial f}{\partial t} \, dt \tag{A.14}$$

$$\langle \Delta \tilde{x}^2(\omega)\rangle = \frac{-1}{(i\omega)^2} \int_{t=0}^\infty \frac{\partial f}{\partial t} \quad d(e^{-i\omega t}) \tag{A.15}$$

Again, taking the partial derivative of the above equation, we get two terms one which is a first derivative of f and the other a second derivative of f.

$$\langle \Delta\tilde{x}^2(\omega)\rangle = \frac{-1}{(i\omega)^2}\frac{\partial f}{\partial t}\, e^{-i\omega t}\Big|_0^\infty + \frac{1}{(i\omega)^2}\int_0^\infty e^{-i\omega t}\,\frac{\partial^2 f}{\partial t^2}dt \tag{A.16}$$

To find the first and the second derivative of f, let us consider,

$$f = 2t\int_0^t G(\tau)\,d\tau - 2\int_0^t \tau\, G(\tau)\,d\tau \tag{A.17}$$

Taking the first derivative of f, and using $\frac{\partial}{\partial t}\int_0^t G(\tau)d\tau = G(t)$ and $\frac{\partial}{\partial t}\int_0^t \tau G(\tau)d\tau = tG(t)$

$$\frac{\partial f}{\partial t} = 2\int_0^t G(\tau)d\tau + 2tG(t) - 2tG(t) \tag{A.18}$$

$$= 2\int_0^t G(\tau)d\tau \tag{A.19}$$

But, $\frac{\partial f}{\partial t}$ =0 at t=0. Therefore, the mean square displacement should only contain the second derivative of f. So equation A.16 can be written as,

$$\langle \Delta\tilde{x}^2(\omega)\rangle = \frac{1}{(i\omega)^2}\int_0^\infty e^{-i\omega t}\frac{\partial^2 f}{\partial t^2}\,dt \tag{A.20}$$

The second derivative of f is given by

$$\frac{\partial^2 f}{\partial t^2} = 2\,\frac{\partial}{\partial t}\int_0^t G(\tau)\,d\tau = 2G(t) \tag{A.21}$$

Substituting this in the above equation,

$$\begin{aligned}\langle \Delta\tilde{x}^2(\omega)\rangle &= \frac{1}{(i\omega)^2}\int_0^\infty e^{-i\omega t}2\,G(t)dt \\ &= \frac{2}{(i\omega)^2}\int_0^\infty e^{-i\omega t}\langle v(t)\,v(0)\rangle dt \\ &= \frac{2}{(i\omega)^2}\int_0^\infty e^{-i\omega t}\langle v(0)\,v(t)\rangle dt \end{aligned}\tag{A.22}$$

From the definition of one sided Fourier transform of velocity, we can then write,

$$\langle \Delta\tilde{x}^2(\omega)\rangle = \frac{2}{(i\omega)^2}\langle v(0)\ \tilde{v}(\omega)\rangle \tag{A.23}$$